QUANTITATIVE MOSSBAUER SPECTRA AND CHEMISTRY OF IRON

by

Earle R. Whipple

B. Sc., Univ. of British Columbia (1968)

Submitted in partial fulfillment

of the requirements for the

Degree of Doctor of

Philosophy

at the

Massachusetts Institute of Technology

August 8, 1973, i.e. Feb. 1974

Signature of Author.....
Dept. of Earth and Planetary Sciences

Certified by.....
Thesis Supervisor

.....
Thesis Supervisor

Accepted by.....

ABSTRACT

Ratios of ferrous to ferric iron in several natural minerals have been measured by Mossbauer Spectra and chemical analyses, and the results compared. To assure reliability of the comparison, the chemical method and the Mossbauer Spectrometer were both investigated. Technological improvements in the spectrometer are highly desirable.

In the garnet mineral system, the spectral line strength (recoil-free fraction) of ferric iron is 29% greater than that of ferrous iron. Very small amounts of titanium have no effect on garnet spectra, but high-titanium garnets show anomalously low ferrous iron content in their spectra, which appears to be very difficult to explain theoretically. In low-titanium garnets, the titanium is quadrivalent and all manganese is divalent.

In the amphibole system, the results are similar. Titanium is quadrivalent but large amounts of titanium produce no anomalous spectra. Manganese is probably divalent.

In the titanaugites (pyroxenes) the recoil-free fractions of ferrous and ferric iron are approximately the same. Titanium is quadrivalent. In the pyroxenoid mineral babingtonite, the recoil-free fractions are nearly equal if all the manganese is divalent. The equality of the recoil-free fractions in the titanaugites is difficult to explain because much of the ferric iron is in tetrahedral coordination, which should have a high value for the recoil-free fraction, compared to octahedral coordination.

In micas, the ferric recoil-free fraction appears to be the greater. Evidence exists for considerable trivalent manganese

in one phlogopite studied.

Considerable effort was expended in finding the chemical variables in the chemical ferrous iron determination which lead to non-statistical errors; the same was done for the total iron determination.

The appendix to the thesis contains applications of theory to the quantitative use of Mossbauer Spectra, and a computer program to correct the non-linear amplitudes and areas of Mossbauer Spectra.

ACKNOWLEDGEMENTS

The author wishes to thank his advisor Prof. R.G. Burns for the use of the Mossbauer spectrometer, for instruction in the art of fitting spectra by computer, and for support, and his advisor Assoc. Prof. Fred Frey who read the chemical section of this work.

He is also indebted to Prof. Burns, Dr. Irene Leung of Lehman College, N. Y., Dr. Clifford Frondel of Harvard, the Natural History Museums of Bern and Vienna, and to Assist. Prof. John Dickey of MIT for many of the mineral specimens.

Many instructive discussions were had with Dr. David Wones, who suggested the charge transfer problem, Prof. Burns, James Besancon, Frank Huggins, and Rateb Abu-Eid of MIT, with Prof. R. V. Pound of Harvard, and with my old friend and former chief, Dr. John B. Goodenough of the Lincoln Laboratory.

Invaluable aid in the format problems of the computer program was given by Carl Johnson and Rudolph Hon of MIT.

Thanks go to Mrs. Gerda Schrauwen for the typing and tables in the manuscript.

INDEX

A. Analytical Chemistry

1. Ferrous Iron Determination, Discussion (P.8)
2. Effect of Accidental Catalysis (P.13)
3. Apparatus and Reagents (P.14)
4. Procedure for Ferrous Iron (P.17)
5. Corrections Applied (for air) (P.18)
6. More Discussion (P.18)
7. Study of the Oxygen Side-Reaction in Minerals (P.20)
8. Some Results from the Ferrous Iron Determination (P.21)
9. Difficulties with Minerals of High Mg Content (P.25)
10. Total Iron by Silver Reductor (P.28)
11. Apparatus and Reagents (P.28)
12. Procedure for Total Iron (P.30)
13. Discussion (P.31)
14. Total Iron by Electron Microprobe (P.33)
    (A) Table 5 of Microprobe Analyses (P.34)
    (B) Microprobe Analyses of Titanaugites CPX3 and 4, Tables 6 and 7 (P.37-38)
    (C) Table 8 of Mineral Formulae (P.39)
15. Errors in Analytical Chemistry (P.42)

B. Preparation of the Mineral Samples (P.44)

C. Computer Plots of the Mossbauer Spectra (P.55)
   (except GN5, P.71 and BAB1, P.192)

D. Mossbauer Spectroscopy

1. Investigation of the Mossbauer Spectrometer (P. 65)

2. Special Problems in Computer Fitting of Mossbauer Spectra (P. 73)
Including:

(a) Baseline curvature, channel (baseline) drift variations (Tables 8a, 8b), including mirror runs, sundry runs, values of X^2, R

(b) Chi-squared criterion of best fit, Law's case (ref. 64); problems with crossite CR1

(c) Site multiplicity in pyroxenes; CPX4, ferrous and ferric iron

(d) Electronic relaxation

(e) Resolution problems

3. Fitting of the Mossbauer Spectra and Site Occupancy of Iron (P. 86)

(A) Table 9 of Site Occupancy (P. 114)

4. Results and Discussion (P. 117)

(A) Table 10 of Mossbauer vs. Chemical Results (P. 128)

(B) Table 11 of Results at 77° K and 295° K (P. 132)

(C) Jakob's Titanian Micas (P. 133)

5. Charge Transfer in Titanian Garnets (P. 134)

E. Appendix of Mossbauer Spectroscopy (P. 139)

(A) Index to Appendix (P. 7)

F. References (P. 195)

INDEX TO APPENDIX

1. Introduction (P. 140)

2. Two Mossbauer Absorption Models (P. 141)

3. Symbols (P. 143)

4. Absorption Equation; Layer Model (P.145)

5. Absorption Equation; Cylinder Model (P.150)

   (a) Unsound quantitative character of two-mineral Mossbauer absorbers

6. Total Area of a Doublet, and Relative Recoil-Free Fractions,

   (P. 153)

7. Variation of ψ with Temperature; Ideal (isotropic monatomic) case (P. 156)

   (a) Determination of ferrous-ferric ratio from temperature data, table.

8. The Crystal-Shape Effect (P. 164)

   (a) Table of transmittance and non-resonant absorbances (P. 168)

9. The Sine Function, Stone's Program (Correlated with Distance Variation of the Source) (P. 170)

10. Program Mosscorr; to correct the non-linear amplitudes of Mossbauer spectra.

    (a) The absorption amplitude (P.173)

    (b) Use of Program Mosscorr (P.180)

    (c) An experimental test of Program Mosscorr (P. 185)

    (d) The computer program (P. 187)

11. The Sign of the Quadrupole Splitting (P. 191)

ANALYTICAL CHEMISTRY

"Ferrous Iron" Determination (Reducing Power)

For decades, the ferrous iron determination has posed difficulties in the analysis of minerals and rocks. Three of these difficulties are lack of silicate standards for ferrous iron, the presence of sulfides in whole rocks which contribute reducing values not due to ferrous iron, and procedures which demand excellent analytical technique.

Two aims of this investigation are to provide a ferrous iron procedure which does not demand the experience of a talented analytical chemist, and to investigate the chemical variables of the procedure. The latter will also indicate some of the inherent weaknesses of older ferrous iron procedures. One of these chemical variables has not been previously reported, to the author's knowledge. A silicate standard for ferrous iron is still lacking, but investigation of the chemical variables is more important than such a standard, and exposes effects which a standard alone probably would not expose.

The best of the old standard procedures for the determination of ferrous iron is probably that of Pratt (ref. 5) who dissolved his sample in boiling HF in a covered vessel and prevented oxidation of ferrous iron by atmospheric oxygen by a protective atmosphere of carbon dioxide and steam. Because of the high temperature used, and the difficulty of excluding all atmospheric oxygen, results for ferrous iron are often low. Pratt's procedure also requires platinum ware, which is expensive.

Improvements in the ferrous iron determination have been made by inclusion of an oxidizing agent, such as pentavalent vanadium, in the HF solution which oxidizes the ferrous iron as soon as it is set free from the

mineral. The best known of these procedures is that of Wilson (ref. 5). On the basis of the author's experience with vanadium solutions in the ferrous iron determination in synthetic oxides (ref.11,13,15) it was decided to study Wilson's procedure.

Pratt dissolves his sample in boiling HF, dissolves the residue of CaF_2 and MgF_2 in boric acid, and titrates the ferrous iron in solution directly with an oxidizing agent. Wilson dissolves the sample at room temperature in about 20 hours (overnight) and protects the solution from oxidation by atmospheric oxygen using pentavalent vanadium as an oxidizing agent in the reaction

$$VO_2^+ + 2H^+ + Fe^{+2} \rightarrow VO^{+2} + H_2O + Fe^{+3} \quad .$$

The reduced form of the vanadium is more stable to oxidation than ferrous iron; the amount of the reduced vanadium is the measure of the ferrous iron content. This is measured by adding an equal amount of ferrous iron (in solution) to the samples and the blanks, which reduces all the VO_2^+ (V^{+5}) in the blanks and samples. The samples then contain more reducing agent than the blanks, and these are titrated by potassium dichromate. The ferrous iron content is the difference between the sample and blanks.

In experiments using solid ferrous ammonium sulfate (analyzed by ceric sulfate titration, standardized by arsenic trioxide) as a standard, it was quickly found that complete recoveries of ferrous iron (ref. 16) could not be obtained. Moreover, it was found that four different phenomena gave rise to low recoveries. Only one of these (#2), was previously unsuspected. They were

1. Slow oxidation of quadrivalent vanadium on standing in the HF solution in air.

2. Oxidation of either V^{+4} or Fe^{+2} via a side-reaction with oxygen, a kinetic effect occurring as the oxidation-reduction reactions proceed.

3. Coprecipitation or adsorption of ferrous iron in CaF_2 or MgF_2 precipitates formed from the minerals (especially MgF_2), despite the presence of the oxidizing agent (V^{+5}) (ref. 12).

4. Incomplete solution of the mineral, as with some calcium-bearing garnets. This can be overcome by weighing the mineral residue. Manganese-bearing garnets (GN5 and 7) leave no undissolved garnet.

Slow oxidation on standing in HF, the first phenomenon, occurs when the V^{+5} reagent used is about 1M in H_2SO_4, the concentration used by Wilson as quoted by Maxwell (ref. 5). When the H_2SO_4 concentration was raised to 5M, oxidation was greatly slowed, agreeing with the mass-action in the equation

$$2VO^{+2} + 9HF + \frac{1}{2}O_2 \rightarrow V_2O_2F_9^{-3} + 7H^+ + H_2O$$

or more simply

$$2VO^{+2} + H_2O + \frac{1}{2}O_2 \rightarrow 2VO_2^+ + 2H^+ \quad .$$

The V^{+5} species is written as such because of some complexation by fluoride, which is shown by the disappearance of the yellow color of VO_2^+ on the addition of much HF. V^{+4} forms fluoride complexes, but V^{+4} forms the least stable complexes of vanadium (ref. 10 , p. 971-2). The actual species of the complexes are in doubt.

Table 1 shows the increase in recovery of Fe^{+2} (ferrous ammonium sulfate) with increased H_2SO_4 concentration, from about 98% (with 1M H_2SO_4)

to about 99% (with 5M H_2SO_4) on 20 hours' standing. One percent of the loss is due to the side-reaction, #2. On 140 hours' standing (5M H_2SO_4) losses are about 0.3%—0.6%, and appear to increase in percentage with greater amounts of Fe^{+2} (i.e., V^{+4} produced). The lower amount of Fe^{+2}, 7 mg (or less), is the usual amount used in the determination, and so a loss of 0.3% is closer to the truth.

In these experiments, no liquid was allowed to touch the solid salt, ferrous ammonium sulfate, until the addition of the HF excepting for one case in Table 1 (same result). Several variations in the procedure were made, as seen by the table, but the result depended mainly on the H_2SO_4 concentration. One case used a V^{+5} reagent of NH_4VO_3. Each value in the table is the average of 2 or 3 samples, and the errors include the blanks.

The side-reaction, phenomenon two, is a kinetic reaction in which a little Fe^{+2} or V^{+4} is oxidized by dissolved oxygen as the oxidation-reduction reactions proceed. This reaction occurs only when ferrous iron in a solid material is attacked by V^{+5} in solution. Table 1 shows that this phenomenon is not dependent on the presence of HF, an interesting point. When ferrous ammonium sulfate is first dissolved in 1M H_2SO_4, and titrated with ceric sulfate, no loss occurs since the Fe^{+2} is in solution, not the solid state, when the oxidation-reduction reactions occur. Also, Reuter and Siewart (ref.14) state that V^{+5} in solution can be determined quantitatively by Fe^{+2} titration. Table 1 shows that elimination of oxygen, using a nitrogen atmosphere (purging with N_2 four hours before allowing the solid salt to react) gives quantitative recovery of the Fe^{+2}. In air, the loss is about 1 percent.

Table 1

Recovery of Ferrous Iron (from ferrous ammonium sulfate)

mg Fe^{+2} (as Fe amm. sulf.)	Time of standing (hr)	H_2SO_4 in V^{+5} reagent	HF (cc, 48%)	H_3BO_3 (cc)	Source of loss #	Atmos.	Recovery of Fe^{+2}(%) (incl. blanks)
9.4	20	1M	8	105	1, 2	air	98.0±0.5
9.3*	20	1M	8	105	1, 2	air	97.9±0.2
9.4	20	1M	8	105	1, 2	air	98.1±0.3
7.4	140	5M	8	105	1, 2	air	98.7±0.2
9.4	140	5M	8	105	1, 2	air	98.4±0.1
8.9	2	1M	8	105	2	air	99.0±0.4
9.3	20	5M	8	105	1, 2	air	98.9±0.4
9.3	20	5M	6	80	1, 2	air	98.9±0.5
9.3	20	5M	8	105	1, 2	air	98.7±0.6
9.4††	2	5M	8	105	2	air	99.0±0.5
9.2	2	5M	none	none	2	air	98.9±0.4
9.0†	2	5M	none	none	2	air	99.1±0.2
9.3	2	5M	none	none	2	air	99.1±0.2
4.6	2	5M	none	none	2	air	98.5±0.1
9.3**	2	5M	none	none	2	N_2	99.6±0.2
9.2**	2	5M	none	none	2	N_2	99.5±0.2
9.4	2	5M	none	none	-	N_2	100.0±0.2

†V^{+5} reagent contained 0.5M $NH_4Fe^{+3}(SO_4)_2$.

††Dissolved salt in V^{+5} reagent, <u>before</u> adding HF.

*Used NH_4VO_3.

**Imperfect N_2 box technique.

1. Slow oxidation.
2. Side-reaction with oxygen.

Effect of Accidental Catalysis

It is to be emphasized that the $V^{+5} - V^{+4}$ oxidation-reduction couple, used to conserve the reducing power of the sample from air, has a Gibbs free energy in reaction with atmospheric oxygen, and depends upon kinetic factors to avoid reoxidation of quadrivalent vanadium on standing in air. During the work, a dramatic case of catalysis was encountered in which all quadrivalent vanadium in the solution was oxidized during twenty hours' standing! The loss was traced to influence of the plastic box in which the polypropylene beakers were covered, which was not even in contact with the solutions! Quite possibly, the catalyst was an organic plasticizer in the plastic of the box. The box was the same make as that successfully used for the regular ferrous-iron determinations. To guard against failures of this type, recovery studies with analyzed ferrous ammonium sulfate should be made with the identical pieces of equipment to be used in the analysis.

Effect of Polypropylene Beakers

Table 1 also indicates that the polypropylene beakers are not reactive to the V^{+5} reagent. When the V^{+5} reagent is 5M in H_2SO_4, if the samples stood 20 hours, the average recovery is 98.9%; if 2 hours, then the recovery is 99.0% on the average (for 9.7 mg Fe^{+2}). Since the blank always contains much more V^{+5}, because it is not reduced, the beakers can be contributing very little to the reduction of the reagent on 20 hours standing.

FERROUS IRON DETERMINATION

Apparatus and Reagents

Polypropylene Beakers – 250 cc, "Tri-pour"

There was some evidence that polyethylene is a little reactive to pentavalent vanadium.

NH_4VO_3, Purified

To 2 liters of water, add 80 cc conc. NH_3 (1.18 moles). Heat and add 110 gm (0.6 moles) V_2O_5 plus as much more as the solution will dissolve near boiling (yellow solution).

Filter through clean sintered glass, and add excess NH_3 (30 cc) while hot, put in refrigerator to crystallize.

Dry over NaOH with a little ammonium sulfate in the NaOH to produce ammonia, which prevents the salt turning yellow.

Burette

Registered, 5 cc graduated in 0.01 cc units. Estimate to 0.001 cc.

V^{+5} Reagent (in 5M H_2SO_4) (0.05 N V^{+5})

To 5.9 gm of the purified NH_4VO_3 (0.05 moles) and 7 gm NaOH (0.175 moles), add 300 cc H_2O and boil off all the NH_3. Add 400 cc H_2O and 285 cc conc. H_2SO_4 slowly. Dilute to more than 1 liter, and boil thoroughly to eliminate reducing agents. Add a pinch of $NaHSO_3$ to produce a little V^{+4}, to mitigate the oxidation potential of the solution, and dilute to one liter. Pipette 4 cc

4:4:2 Reagent

400 cc H_2O, 400 cc conc. H_2SO_4 and 200 cc 85% H_3PO_4.

Pipette 5 cc just before endpoint. The phosphate readjusts the potential of the Fe^{+2}-Fe^{+3} oxidation-reduction couple by complexing ferric iron.

Indicator

0.02% (W/V) sodium diphenylamine p-sulfonic acid. Pipette 1 cc.

Saturated boric acid

Add 55-60 gm H_3BO_3 to 1 liter H_2O. Heat and let crystallize. Store in a warm place to maintain high concentration. Use 105 cc.

0.04 N $K_2Cr_2O_7$

Weigh accurately 0.4 gm primary standard $K_2Cr_2O_7$, and dilute to 200 cc in a volumetric flask.

48% HF, anal. reag.

Use 8 cc. Do not exceed this amount. A little less, rather than more, is preferable.

0.047 N Fe^{+2}

Dissolve 3.7 gm ferrous ammonium sulfate hexahydrate in 200 cc 1M H_2SO_4. Pipette 5 cc.

Nitrogen box (if desired)

Use with 10 cc Teflon beakers (for samples only) which contain the HF separate from the sample. These are placed within the Tripour beakers, and after purging several hours with clean N_2, they are overturned to mix with the vanadium reagent and the sample.

The nitrogen box should have a tight-fitting lid with stoppered holes, through which a stirring rod can be inserted to overturn the beakers containing the HF. It should have an inlet for the N_2, and be enclosed in a large plastic bag (to help exclude air) which is crimped over the N_2 inlet tube. The bag must be opened to overturn the beakers.

Box (for use in air)

Essentially the same as the N_2 box. Some plastic boxes contain catalysts in their walls which catalyze the oxidation of V^{+4} by oxygen. See section on "Effect of Accidental Catalysis."

To Clean Nitrogen

Bubble N_2 slowly through conc. H_2SO_4 containing $K_2Cr_2O_7$ (cleaning solution), via two towers with a thimble-shaped sintered glass tip, and a final tower of water. Flow must be slow, because reagent foams. This is very effective treatment.

Both N_2 and CO_2 contain reducing agents which reduce the V^{+5} reagent. This is probably due to the oils in the pumps used to compress these gases. Firing these gases over copper oxide at high temperature was ineffective.

Water-pump nitrogen is probably purer, and better to start with than the nitrogen grade used here.

To weigh mineral residues

$Al(NO_3)_3$, reagent

Approx. 10% (W/V) aluminum nitrate hydrate in 1M H_2SO_4. Filter through paper.

Decant the solution (diluted to 250 cc) twice from the residue by narrow bore suction tube. Add 10-20 cc of the aluminum nitrate reagent to the residue and let stand overnight. Insoluble fluorides remaining are dissolved by complexation of fluoride by aluminum. Decant twice more.

Filter on sintered glass, wash with 6N HCl, then water, then with acetone. Dry at 110°C $\frac{1}{2}$ hour, let cool $\frac{1}{2}$ hour and weigh.

Procedure

To samples and two blanks, pipette in 4 cc of the V^{+5} reagent, allowing the pipette, which must be very clean, to drain thoroughly (5-6 minutes). Add 8 cc of 48% HF carefully down the side of the beakers (if using N_2, put the HF in 10 cc Teflon beakers, but this is not necessary for the blanks) and swirl gently to spread sample powder.

Let stand for the desired time in a closed box and add 105 cc of saturated H_3BO_3. Stir magnetically until precipitates are broken up and dissolved; use the stirrer to scour the bottom. (If there is much more Mg than Ca in the sample, let the boric acid solutions stand overnight to dissolve the MgF_2, which is not easily seen in suspension; see separate section.)

Let the H_3BO_3 solutions cool from the reaction with HF, and pipette in 5 cc of the 0.047 N Fe^{+2} (as above). Stir. At the last moment, just as titration begins, not before, pipette in 1 cc of the indicator and titrate slowly with the 0.04 N $K_2Cr_2O_7$, until the violet color of the oxidized indicator just barely disappears, near the endpoint. This gives warning of the endpoint.

Then add 5 cc of the 4:4:2 reagent (phosphate) and titrate about 0.005 cc at a time to the point where gray turns to violet, the final endpoint.

If a N_2 atmosphere is desired, purge the fluids and box five hours with the slow flow of gas; then overturn the Teflon beakers of HF, which keep the HF separate from the V^{+5} reagent and the sample, with a stirring rod. During the purging and after, enclose the box in a large plastic bag, crimping the bag over the gas delivery tube (see apparatus and reagents).

Corrections Applied (for air)

For 20 hours' standing (overnight), multiply the result by 1.003, to correct for the side-reaction (#2). Slow oxidation of V^{+4} is nil in 20 hours.

For 140 hours (6 days), multiply the result by 1.006, which corrects for slow oxidation by 1.003 (#1) and the side-reaction (#2) by 1.003 (see Table 2). For lesser standing time, use 1.001 for every 2 days to correct for the slow oxidation.

Do not apply a correction for time elapsed after addition of boric acid.

Discussion

Sample should contain 7 mg or less of ferrous iron. If it contains much Mg and little Ca, after breaking up and dissolving the CaF_2 and MgF_2, let it stand overnight to dissolve the remainder of the MgF_2, which is not easily seen in suspension. (This is very important, see separate section). If the mineral is very resistant to attack, the undissolved mineral must be weighed, and the weight deducted (see section on apparatus and reagents). Some garnets and enstatites require this. Garnets must be 200 mesh; for others see section on preparation of the mineral samples.

Garnets require 6 days' treatment; pyroxenes are best with this time also. Hornblendes require only overnight treatment. Much manganese in a garnet greatly facilitates solution. Phlogopites, like enstatite, often require

an additional night's standing with H_3BO_3 to dissolve the large amount of MgF_2, after thorough breaking up and stirring of the MgF_2 precipitate.

STUDY OF THE OXYGEN SIDE-REACTION IN MINERALS

The oxygen side-reaction (#2) accounts for a loss of 1 percent of the titre in thesolid soluble salt, ferrous ammonium sulfate (see Table [1] and its discussion). Conducting the determination in nitrogen (purging 4 hours before reaction) eliminates this loss.

The side-reaction causes a lesser loss in minerals, but this is much more difficult to demonstrate, because one must show the true ferrous iron content of the mineral before the losses can be proven.

Before the excellent cleaning of the nitrogen by $K_2Cr_2O_7 - H_2SO_4$ cleaning solution was found, Cu O in boats at red-heat was tried, but was found ineffective. It was effective only when spread on the bottom of the tube, which always ruined the tube.

The impure nitrogen (or CO_2) reduces V^{+5} on standing and lowers the recovery of Fe^{+2}. Note that <u>either</u> an oxidizing (air) <u>or</u> reducing atmosphere will cause <u>losses</u> of Fe^{+2} in the determination, because both environments tend to bring the blanks and samples to the <u>same value</u>, either oxidized <u>or</u> reduced.

The true ferrous iron content of HB1 and Hbde Conc. #613 (HB1 plus 4% anthophyllite) could be determined because the rate of reduction of the blank in impure N_2 can be seen by comparison with a blank done in air. The blank contains little V^{+4} and cannot be affected by oxygen. The average rate of reduction of the blank was found to be 0.010 cc/20 hr of 0.04 N $K_2Cr_2O_7$ (equivalent to 4×10^{-7} moles of Fe^{+2}), whereas the net titration is about 3.0 cc of 0.04 N $K_2Cr_2O_7$ ($1,300 \times 10^{-7}$ moles of Fe^{+2}). Since about 13/20

of the V^{+5} of the blank is reduced by the sample of mineral, the sample and blank are different in rate of reduction by this factor. The correction factor to be applied to find the true Fe^{+2} content is therefore 1.002.

The results of this study are in Table 2 . From runs done in air, and in pure and impure N_2 (weights of Fe^{+2} a little more than 7 mg) the correction factor for the oxygen side-reaction is 1.004—1.005. (Slow oxidation is nil with the 20 hours standing used in the tables, for less than 7 mg.) This value is for amphiboles and the values for other minerals may be a little different, but the long times of standing for other minerals make the study lengthy.

The mechanism of the side-reaction with oxygen cannot be explained at present, but the relative size of the effect in solid ferrous ammonium sulfate and the amphibole can be attempted. With the soluble salt, the reaction with the vanadium reagent is so rapid that the V^{+5} concentration in the vicinity of the soluble salt crystal is greatly depleted during the reaction, and the ratio of O_2/V^{+5} rises to where the oxygen side-reaction becomes relatively important. In the slowly-soluble amphibole, the V^{+5} can be replenished by diffusion in the vicinity of the crystal. Since other minerals also dissolve slowly, the side-reaction should be similarly low for them also.

Probably, it is best to undercorrect the values rather than overcorrect, so a correction factor of 1.003 has been applied for the side reaction in practice.

Some Results from the Ferrous Iron Determination

Besides the studies of the chemical variables of the procedure, outlined above, some other results are important in studying the worth of the method.

Table 2 . Side-Reaction Correction in Air

Analyses of hastingsite HB1 (sample soluble, no residue) and Hb concentrate 613 (impure HB1). Errors in blanks not given.

Wt. Fe^{+2} (mg)	Time of standing (hr)	Atmos.†	Mineral	% Fe^{+2} (wt)	Corr. factor	% Fe^{+2} (wt) (corr.)	% Fe^{+2} (ave.) (corr.)
7.5	20	imp. N_2	HB1	8.624	1.002	8.641	8.631
7.6	20	imp. N_2		8.603	1.002*	8.620	
7.2	20	air	HB1	8.591	1.004	8.626	8.626
7.0	20	air		8.590	1.004	8.625	
7.1	20	pure N_2	HB1	8.642	none	8.642	8.625
7.2	20	pure N_2		8.608	none	8.608	
6.8	20	imp. N_2	Hb Conc. 613	8.782	1.0020	8.800	8.795
7.6	20	imp. N_2		8.788	1.0020*	8.806	
6.9	20	imp. CO_2	Hb Conc. 613	8.766	1.002	8.784	
7.1	20	imp. CO_2		8.773	1.002*	8.791	
7.0	20	air	Hb Conc. 613	8.743	1.005	8.787	8.798
7.3	20	air		8.766	1.005	8.810	

*Factor derived from impure gas data.

†imp. N_2 is furnace-cleaned N_2, not pure.

Table 3

Det'n of Ferrous Iron in Air and Pure N_2

Mineral	Time (hr, air)	Corr. factor	mg Fe^{+2}	No. samples	Value in air (Fe^{+2}%)	Time (hr, N_2)	Corr. factor	mg Fe^{+2}	No. samples	% value in N_2(Fe^{+2}%)
DTS1, DUNITE	90	1.005	5-6	2	5.78† (±0.4%)					
GN7, ANDRADITE	140	1.006	5.2	2	1.920 (±0.1%)	140	none	6.7	2	1.911† (±0.3%)
HB1 HASTINGSITE	20	1.003	7.0	2	8.617† (±0.1%)	20	none	7.0	2	8.625† (±0.3%)
CR1 CROSSITE	20	1.003	5.5-6	2	13.50 (±0.5%)	20	none	6.9	2	13.53 (±0.5%)
OPX1 ENSTATITE						140	none	7.1	3	5.952† (±0.4%)
CPX4 TITANAUGITE	140	1.006	6.7	2	4.379 (±0.3%)	140	none	5.6	1	4.366† (±0.3%)

†Stood in H_3BO_3 1 day.

Table 4

Analyses of orthopyroxene OPX1; high Mg content. Errors in air are due to oxidation on standing, the side reaction (both corrected) and coprecipitation by MgF_2.

Wt. Fe^{+2} (mg)	Time of standing (hr)	Atmos.	% sample undissolved	% Fe^{+2} (wt.)††	Corr. factor	% Fe^{+2} (wt.) (corr.)
7.8	140	air	not detn'd	5.733	1.006	5.767
7.6	140	air	not detn'd	5.861	1.006	5.896
4.0	140	air	not detn'd	5.807	1.006	5.842
4.0	140	air	not detn'd	5.865	1.006	5.900
6.7	140	air	0.5	5.837	1.006	5.872
6.6	140	air	0.0	5.767	1.006	5.802
6.8	140	clean N_2	0.1	5.870	none	5.870
6.6	140	clean N_2	0.1	5.771	none	5.771
7.2†	140	clean N_2	0.0	5.944	none	5.944†
7.1†	140	clean N_2	0.0	5.951	none	5.951†
7.0†	140	clean N_2	0.1	5.962	none	5.962†

†MgF_2 dissolved by standing overnight in H_3BO_3.

††Corrected for undissolved sample.

In two of the minerals, GNIA (almandine) and OPX1 (enstatite) almost all the iron was present in the ferrous state. In GNIA, 99.1% of the total iron was ferrous, and in OPX1, 98.5%. Such recoveries could not be obtained without a good method.

Another aspect of the method is shown by the analysis of the rock standard DTS1. The accepted value for the FeO content is 8.00%, which is probably by Pratt's procedure in boiling hydrofluoric acid. By the present method, at room temperature, the FeO content was 7.440% (error, ±1 in 250). Several milligrams of chromite remained undissolved, which was far more than enough to account for the difference. It appears that the value 7.44% FeO represents the silicate content of FeO of the rock, and that Pratt's method (boiling) is capable of attacking a little of the chromite.

It is known that Wilson's procedure (essentially the same as the present one) is less sensitive to pyrrhotite as impurity than Pratt's (ref. 16). Pyrite is about the same in both procedures.

Table 3 lists some mineral analyses done in air and in pure N_2 (purified by cleaning solution).

Difficulties with Minerals of High Mg Content

Extremely bad precision was found with an orthopyroxene, OPX1 (100 + mesh) in which the values for ferrous iron varied up to about 2.3 percent of the total content, even on six days' standing.

Values on three days' standing were, on the average, two percent less than on six days' standing, due to undissolved orthopyroxene (values not tabulated).

The incompleteness and slowness of attack is due to the gelatinous and coating nature of the magnesium fluoride produced. The gelatinous precipitate is colored blue, due to quadrivalent vanadium which either is adsorbed or cannot diffuse out.

The bad precision and low results is due to coprecipitation of ferrous iron in the magnesium fluoride (see Table 4). One hour of stirring after addition of boric acid, even when the precipitate is well broken up, is not sufficient to dissolve all of it. It must also stand overnight to dissolve (before excess ferrous iron is pipetted in). When this is done, results are high and precise, as seen in Table 4 .

OPX1, from Webster, N.C., has been previously analyzed (not the same sample) and found to have about 90% of its iron in the reduced form (ref. 3 , p. 16, Anal. #2). This result conflicts with the new value, and also with results for orthopyroxenes (from 37 localities) found by Virgo and Hafner by Mössbauer spectroscopy (ref. 78). On page 206 of their work, they state that orthopyroxenes contain less than 1% of their iron in the ferric state.

In the presence of aluminum, the magnesium precipitate has the composition

$$MgAlF_5 \cdot xH_2O \text{ (ref. 12)}$$

with substitution of Fe^{+2} and Fe^{+3}, which is apparently more insoluble than MgF_2. In OPX1, this is not possible because it contains almost no aluminum. For sake of simplicity, the precipitate will be referred to as magnesium fluoride.

When an equivalent amount of calcium is present in the mineral, as in clinopyroxenes, the precipitate is granular rather than gelatinous. No undissolved clinopyroxene (0.4 gms of CPX1, 200 + mesh) was found by weighing even on only three days' standing. Precision was good, despite the low net titration volume (1 cc; 0.8 gms of CPX1). This indicates that this precipitate has different characteristics than that of the orthopyroxene. The MgF_2 coprecipitated with the CaF_2 is the last to dissolve, but is easier to dissolve than that of the orthopyroxene OPX1.

If much granular CaF_2 is formed, as with a mineral very low in iron and high in calcium content, as CPX1, it is best to break up the cake of CaF_2 with a plastic stirring rod after about 1 day's standing, washing the rod with a few drops of water. MgF_2 alone is gelatinous and it is probably best not to do this, because it may stick to the stirring rod.

MgF_2 formed from attack of phlogopites is not gelatinous, and may be broken up effectively.

TOTAL Fe BY SILVER REDUCTOR

The silver reductor is well chronicled in the literature and is considered by some to be the best method of determining iron in rocks, in the presence of such metals as Ti, V, and Cr (ref. 5, Maxwell, p. 212). Metals interfering with the total iron by the silver reductor are Cu, Mo, U and Pt (Pt, ref. 8). V^{+5} is reduced to V^{+4}, but V^{+4} is not reoxidized by the titrant (Ce^{+4}) with the indicator ferroin when the solution is 5M in H_2SO_4.

A detailed discussion of the silver reductor will be omitted here, but the procedure will be described, and certain useful tactics discussed which give increased accuracy to the method.

Aluminum chloride is used in this procedure for complexing fluoride, and has been shown to be more effective for this than boric acid (ref. 7,9).

Apparatus and Reagents

Silver Reductor

An old 100 cc burette of 1.5 cm diameter with a pyrex wool plug and filled with 10-11 cm of silver powder. Store the reductor under the Fe-1.0M HCl reagent, filling the burette to near the top. The plug is slowly eaten away by the AlF_6^{-3} solutions in the procedure, and must be replaced from time to time. Glass is not etched.

Prepare the silver by reduction of $AgNO_3$ by sodium formate and boiling to coagulate the powder.

HF-HCl Reagent

Equal volumes of 48% (30M) HF and 6M HCl. Use 4 cc.

Fe-0.1M HCl Reagent

100 mg ferrous ammonium sulfate in 1 liter of 0.1M HCl. Pipette 10 cc.

Fe-1.0M HCl Reagent

100 mg ferrous ammonium sulfate in 1 liter of 1.0M HCl. Store reductor under a deep column of this solution.

2M $AlCl_3$ in 0.1N HCl

500 gm of $AlCl_3 \cdot 6H_2O$ and 8 cc 12M HCl, dilute to 1 liter. Filter through pyrex wool. Pipette 10 cc. (Contains more Fe as impurities than the Fe-0.1M HCl reagent.)

0.00125N ferroin – Pipette 2-0.3 cc portions.

10M H_2SO_4

Equal volumes of 18M H_2SO_4 and water. Refrigerate to avoid heating the solution to be titrated. Use 160 cc. (No H_3PO_4 used because it does not complex ferric iron at this high acid concentration.) This avoids oxidation of V^{+4} at the endpoint, and sharpens the endpoint.

1M HCl (saturated with CO_2)

This decreases the oxygen content of the wash solutions, but does not eliminate all oxygen since the reducing column is exposed to air. The receiver, however, is flushed with flowing CO_2 to minimize oxidation of ferrous iron.

Beakers (marked with volume scale)

50 cc Nalgene. Tight-fitting tops can be cut from the bottoms of old plastic bottles.

Titration Thief

Bend the top of an old, 10 cc pipette, attach a short length of rubber tubing with a screw clamp, and withdraw part of the solution before beginning the titration, after the second wash.

Procedure

Dissolve an amount of mineral containing 9mg Fe (for 4 cc titration; less if desired) but not more than about 0.3 gram of silicate mineral in 4 cc of the HF-HCl reagent on a steam bath in a plastic beaker, well covered, for several hours. Include two blanks.

Pipette 10 cc of both the $AlCl_3$ and Fe-0.1N HCl reagents into the unknowns and blanks, dilute to 30-35 cc, and heat on steam bath until all the CaF_2 and MgF_2 precipitates are dissolved by complexation of F^- by Al^{+3}. (MgF_2 is resistant.)

Pass this solution through the silver reductor in 15-20 minutes into a CO_2-filled 500 cc three-necked flask which includes a 10 cc "titration thief." Wash with 4-30 cc portions of CO_2-saturated 1M HCl, passing the first portion throughin15-20 minutes; the last three can be put through faster. Add 0.3 cc of the ferroin to the flask and after the first two washes withdraw 5-10 cc of solution into the titration-thief, and titrate with 0.04N ceric sulfate until an endpoint is reached, then release some liquid from the "thief" and restore the color. After the last wash, add 0.3 cc more ferroin, and 160 cc of the cold 10M H_2SO_4 (to prevent oxidation of V^{+4}). Rinse the thief and complete the titration.

Do the blanks the same way, using the same times of passage through the reductor (this is very important). The "thief" is not used and the titration can be completed in one stage.

Store the reductor under a deep column of the Fe-1.0M HCl reagent. If this is not done, the first sample will be low due to peroxide formation, despite washing. Wash the reductor with 5-30 cc portions of CO_2-saturated 1M HCl, passed through quickly, except the last wash, immediately before use.

Discussion

Diphenylamine-sulfonic acid cannot be used as an indicator because it consumes much titrant (increasing the titre by about 2% for 15mg Fe) without being compensated fully in the blank in the HCl medium. It is much more stable in H_2SO_4.

When iron is not present in the HCl solutions, hydrogen peroxide is produced in the reductor during the later washings, which is minimized by saturating the solutions with CO_2, probably by the reaction

$$2Ag + O_2 + 2H^+ + 2Cl^- \rightarrow 2AgCl + H_2O_2 \quad ,$$

and oxidizes a little ferrous iron in the receiver. When iron is included in the blank also, the oxidation of ferrous iron by peroxide in the unknowns and blanks is almost exactly balanced (when the blanks are passed through the reductor at the same rate!) and an increase in accuracy results over that obtained when no iron is in the blank.

Trial runs with 15 mg of 99.9% iron wire (no 10M H_2SO_4) showed 99.7-100.1% recovery, with an average of 99.8% (5 values). A correction factor of 1.002 was therefore applied. In practice, the procedure was scaled down to 9 mg or less of iron.

Regeneration of the column was done with chromous chloride solution.

During the solution of the sample, if no HF were consumed, the resulting 30 cc of solution would be 2.46 M in both H^+ and Cl^-. Most silicates consume about 1.5 times their weight in HF (including the insoluable fluorides produced) and neutralize about three-quarters of the H^+ content of the HF used. Some HF undoubtedly escapes by evaporation, and these two losses reduce the H^+ concentration below the above value. One half of the Al^{+3} introduced is not complexed by F^- (if no losses of HF occur) and this should complex some of the Cl^- in the solution and reduce its effective concentration also. The most used concentration of HCl for this procedure in the literature is 1M.

Complete solution of the CaF_2 and MgF_2 precipitates by the $AlCl_3$ reagent is necessary, because these co-precipitate iron seriously, and must be completely eliminated. In difficult cases (as MgF_2 in the analysis of phlogopite) an air oven at 60°-70° for 1 day was handy, and less trouble than the steam bath.

In a few cases, so much sample was needed for an adequate-sized titration, that the normal amount of HF (4 cc 1:1 48% HF-6M HCl, i.e. 2 cc 48% HF) was not enough. For the 0.4 gm of CPX1 (diopside), an extra 0.5 cc of 48% HF was added to the samples and the blanks, and the blanks (only!) allowed to evaporate to a low volume to eliminate the excess of HF. If this was not done, silica gel formed in the unknowns. The extra HF added must not be enough to overshoot the capacity of the $AlCl_3$ reagent in the unknowns. With 0.8 grams of CPX1, insoluble precipitates formed which could not be dealt with.

When much unknown is present (as above) the unknown, after short treatment, must be broken up with a stirring rod to facilitate attack by the HF. If not, silica gel will remain after addition of the $AlCl_3$ reagent.

It is best not to evaporate the sample solutions, because ferric chloride can be lost by sublimation when the solutions concentrate. The beakers are therefore tightly covered.

Silica gel (insoluble in $AlCl_3$) is sometimes encountered. This can occur even when the sample weights are small.

The 0.04N ceric sulfate was standardized by primary standard arsenic trioxide, dissolved in 10 cc cold 1M NaOH and immediately acidified by 100 cc of 1M H_2SO_4 on solution of the trioxide. For the iron determination, a 5 cc semi-micro buret of 0.01 cc intervals was employed, the same as for the ferrous-iron determination (which employs $K_2Cr_2O_7$).

Total Iron by Electron Microprobe

Despite the heterogeneity of many of the minerals, total iron by the electron microprobe compared with the chemical method by silver reductor gave nearly identical results on the average. In 13 minerals (GN2 and CPX1 not averaged) with 45 microprobe analyses, the chemical analyses gave 1.007 times the microprobe values on the average.

All the microprobe values for one mineral were averaged, and then compared by ratio with the chemical value for that mineral. The ratios for all 13 minerals were then averaged. The biggest difference was for the very heterogeneous M3 which had only 3 grains, each analyzed twice (6 in all) by the microprobe. If the results for M3 are neglected, the chemical values gave 1.003 times the microprobe values.

The hourglass-zoned titanaugite CPX4, which in all but one case gave unworkable gels in the solutions of the total iron determination, gave the same answer, 6.09% iron, by both methods using nine microprobe analyses.

The microprobe iron standard was the forsterite P140.

Table 5

Electron-Microprobe Analyses†

(% by weight)

	GN1A	GN2A-B *	GN5	GN6	GN7
Na_2O	0.47	0.05	0.05	0.43	0.00
MgO	4.48	0.06	0.43	0.46	0.00
Al_2O_3	21.32	19.97	18.91	3.79	10.68
SiO_2	36.77	37.80	35.51	33.46	35.38
K_2O	0.00	0.00	0.00	0.00	0.00
CaO	0.60	34.38	2.55	32.29	21.05
TiO_2	0.13	0.15	0.00	2.73	0.18
Cr_2O_3	0.02	0.00	0.01	0.02	0.01
MnO	2.00	0.22	31.46	0.84	10.72
FeO	33.87	4.79	5.86	21.00	15.74
ZnO	-	-	0.25	-	0.49
$O(Fe^{+3})$	0.03	0.40	0.23	2.25	1.49
Total	99.69	97.82	95.25	97.27	95.75

† For GN3 and 4, see Howie (ref. 54).

* GN2A and GN2B are two fractions of this garnet, separated magnetically. The above composition is intermediate between them.

Table 5 (cont.)

Electron-Microprobe Analyses

	OPX1	CPX1	CPX2	CPX3	CPX4	BAB1
Na_2O	0.22	0.23	3.25	1.15	0.77	0.58
MgO	33.01	18.20	8.83	10.19	12.81	0.70
Al_2O_3	1.02	0.28	2.85	11.38	7.73	0.78
SiO_2	55.16	54.19	50.00	38.87	47.38	50.63
K_2O	0.00	0.01	0.00	0.01	0.00	0.00
CaO	0.34	23.76	22.58	22.59	22.44	18.31
TiO_2	0.02	0.06	0.17	3.96	2.97	0.00
Cr_2O_3	0.43	0.01	0.02	0.01	0.05	0.05
MnO	0.17	0.03	0.19	0.13	0.10	0.77
FeO	7.86	0.41	13.39	7.81	7.84	21.70
H_2O	-	-	-	-	-	~2.060*
$O(Fe^{+3})$	0.01	0.01	0.11	0.67	0.25	1.28
Total	98.26	97.19	101.38	96.76	102.34	96.84

* Water content is a rough estimate.

Table 5 (cont.)

Electron-Microprobe Analyses

	CR1†	HB†1	HB2	HB3	M2	M3
Na_2O	6.27	1.79	3.14	3.37	0.27	0.21
MgO	3.93	12.07	9.30	13.57	6.90	27.90
Al_2O_3	4.51	14.85	13.41	14.55	13.09	10.93
SiO_2	52.16	43.82	40.03	41.09	35.67	43.64
K_2O	0.09	0.12	1.98	2.09	9.10	10.20
CaO	1.19	10.20	10.36	10.40	0.00	0.00
TiO_2	0.04	0.68	5.04	4.79	3.16	0.14
Cr_2O_3	-	-	0.00	0.04	0.00	0.01
MnO	0.51	0.27	0.22	0.11	1.31	1.02
FeO	18.19	11.15	17.19	10.04	26.54	4.50
Fe_2O_3	10.53	3.32				
H_2O	2.25	1.94	~1.0*	~1.0*	~4.0*	~4.0*
$O(Fe^{+3})$	-	-	0.47	0.29	0.33	0.26
Total	99.82	100.31	102.14	101.49	100.37	102.81

† By J. H. Scoon, chemical.

* Water contents are rough estimates.

Table 6

Microprobe Analyses of Titanaugite CPX3

(basis, 6 oxygens)

CPX3 is hourglass-zoned. Correlation of zones with analyses is unknown.

	#1	#2	#3	#4	#5	#6
Na	0.107	.057	.117	.110	.073	.084
Mg	0.651	.585	.579	.573	.629	.648
Al	0.487	.574	.535	.547	.521	.483
Si	1.606	1.510	1.544	1.490	1.579	1.596
Ca	0.881	.977	.953	1.004	.926	.944
Ti	0.116	.128	.116	.137	.106	.101
Fe(+2)	0.224	.262	.271	.281	.245	.235

Table 7

Microprobe Analyses of Titanaugite CPX4

(basis, 6 oxygens)

CPX4 is hourglass-zoned. Correlation of zones with analyses is unknown.

	#1	#2	#3	#4	#5	#6	#7	#8	#9
Na	0.047	.064	.070	.053	.042	.051	.050	.042	.064
Mg	0.763	.693	.690	.637	.730	.672	.679	.717	.714
Al	0.313	.308	.389	.409	.285	.404	.317	.292	.292
Si	1.761	1.750	1.680	1.676	1.806	1.663	1.747	1.775	1.782
Ca	0.861	.889	.880	.901	.851	.896	.896	.889	.871
Ti	0.061	.087	.093	.104	.059	.105	.087	.073	.064
Fe(+2)	0.230	.243	.250	.246	.230	.251	.243	.225	.241

Table 8

Formulae

	GN1A	GN2A-B *	GN5	GN6	GN7
Na	0.073	0.008	0.008	0.071	0.000
Mg	0.535	0.005	0.055	0.057	0.000
Al	2.018	1.840	1.903	0.382	1.074
Si	2.954	2.954	3.032	2.867	3.019
K	0.000	0.000	0.000	0.000	0.000
Ca	0.049	2.880	0.233	2.965	1.924
Ti	0.007	0.008	0.000	0.176	0.012
Cr	0.001	0.000	0.001	0.001	0.001
Mn	0.134	0.013	2.276	0.060	0.775
Fe^{+2}	2.275	0.125	0.264	0.081	0.174
Fe^{+3}		0.186	0.154	1.423	0.949
Zn	-	-	0.016	-	0.031
O	12	12	12	12	12

* GN2A and GN2B are two fractions of this garnet, separated magnetically. The above formula is intermediate between them.

Table 8 (cont.)

Formulae

	OPX1	CPX1	CPX2	CPX3	CPX4	BAB1
Na	0.014	0.015	0.239	0.088	0.054	0.219
Mg	1.745	1.002	0.501	0.602	0.696	0.201
Al	0.042	0.012	0.127	0.531	0.332	0.179
Si	1.956	2.004	1.904	1.541	1.729	9.950
K	0.000	0.000	0.000	0.000	0.000	0.000
Ca	0.012	0.940	0.920	0.959	0.877	3.853
Ti	0.000	0.001	0.004	0.118	0.082	0.000
Cr	0.011	0.000	0.001	0.000	0.002	0.006
Mn	0.004	0.000	0.005	0.003	0.002	0.127
Fe^{+2}	0.232	0.012	0.392	0.059	0.172	1.706
Fe^{+3}			0.034	0.200	0.067	1.859
O	6	6	6	6	6	29

Table 8 (cont.)

Formulae

	CR1	HB1	HB2	HB 3	M2	M3
Na	1.83	0.52	0.900	0.938	0.039	0.026
Mg	0.88	2.60	2.053	2.914	0.813	2.860
Al	0.90	2.53	2.340	2.469	1.222	0.886
Si	7.84	6.33	5.933	5.920	2.822	3.001
K	0.01	0.02	0.374	0.380	0.917	0.894
Ca	0.19	1.58	1.644	1.603	0.000	0.000
Ti	0.01	0.07	0.561	0.516	0.188	0.006
Cr	-	-	0.000	0.004	0.000	0.001
Mn	0.07	0.03	0.026	0.012	0.085	0.058
Fe^{+2}	2.29	1.35	1.612	0.896	1.560	0.133
Fe^{+3}	1.20	0.36	0.519	0.313	0.196	0.125
O	23	23	23.26	23.16	11.10	11.06

ERRORS IN ANALYTICAL CHEMISTRY

The differences in Mössbauer line strength (recoil-free fraction) of ferrous and ferric iron are deduced as a ratio, and the chemical values must be expressed the same way for comparison.

Let X = fraction of Fe^{+2} in mineral; 1 - X = fraction of Fe^{+3}. Then the ratio

$$R = \frac{X}{1 - X} \quad .$$

If

n = frac. error in Fe^{+2} (pos. or neg.)

N = frac. error in total Fe (pos. or neg.)

then the error in Fe^{+3} is (N - nX) where n and N are small numbers rarely greater than 0.005 in the chemistry.

Then

$$R = \frac{X + nX}{(1 + N) - (X + nX)} = \frac{X + nX}{(1 - X) + (N - nX)} \quad .$$

The error in the ratio is

$$\frac{nX}{x} - \frac{(N - nX)}{1 - X} = \frac{n - N}{1 - X} = (n - N)(R + 1) = \text{error}$$

because a positive error in ferrous iron (nX) increases the numerator and decreases the denominator.

Maximum error occurs when n and N have opposite signs. The chemical values are usually reproducible to 0.3% (0.003), and are seldom greater than

0.5% (0.005). If the errors in the ferrous iron and total iron are maximal (0.005) and moreover are in opposite directions as well, then the error in the ratio is 0.01 (R+1) or (R+1) percent, which is a good round number to remember.

The errors in the Mössbauer spectra are much more difficult to determine, and must be approached in a different way.

Errors in the chemistry are tabulated as errors assuming that the value quoted is 100%. For example, GN2A contains 1.278% ferrous iron (±0.5%), meaning that the value 1.278% should be multiplied or divided by 1.005.

PREPARATION OF THE MINERAL SAMPLES

All samples were handpicked and/or underwent other purification (except 2 micas). Magnetic separation of impurities using the Frantz Isodynamic Separator, or the splitting of a sample by it (GN2A and GN2B) into two compositional fractions were useful. All opaque samples as well as most of the transparent ones (not micas) were passed through the Frantz, thus insuring the removal of most of the magnetite, and steel from the percussion mortar.

Heavy liquid separations were usually avoided, because of possible absorption into cracks in the minerals and their possible reducing activity which might prejudice the ferrous iron determination.

A mullite mortar was used to grind the minerals to the final size, always crushing and grinding under acetone to avoid air-oxidation during grinding. Acetone, also used to wash the final ground products, is stable to oxidizing agents. The final products were dried 15-30 minutes at 80°-130°C in air.

Chemical purification of a mineral, such as GN3, GN4, or GN6 (titanian garnets), was often effective. In these cases, short treatment with hot 6M HCl served to remove calcite and partially destroy feldspathoids, although these garnets were partially attacked by HCl. After decantation with water, short treatment with 48% HF removed remaining feldspathoids and silica gel. CaF_2 or MgF_2 was removed by decantation, followed by overnight treatment with aluminum nitrate in 1M H_2SO_4 to dissolve the remainder. Water soluble salts (aluminum sulfate?) which precipitated were removed by thorough washing with water, 1M H_2SO_4, and water again, and dried. These were put through the magnetic separator and handpicked, etc.

Usually, at least 4 grams of mineral were prepared. The final grain size preferred usually depended on the resistance of the mineral to solution in the ferrous-iron determination. All garnets were greater (finer) than 200 mesh (75 microns), since they are very resistant to HF.

When the sample was handpicked and the supply of mineral abundant, coarse grains of 35-42 mesh were employed for handpicking. Handpicking of sizes, finer than 60 mesh was seldom attempted.

Details of each mineral, its preparation, and impurities in the original material are given in this section.

Garnets

GN1A

Almandine. From Washington Camp contact metamorphic copper deposit, Arizona. MIT research collection, specimen 4623 (2593). Contained diallage, feldspar (?), clay mineral (?); wollastonite and epidote (or vesuvianite) visible in oil immersion.

Handpicked. Contains fine crystals of wollastonite and epidote (or vesuvianite). Ground, dried.

Treated 200 mesh with 48% HF 3/4 hour, then $Al(NO_3)_3$ in 1M H_2SO_4 1/2 hour. Most of epidote removed. Ferrous iron content increased by this treatment. Dried 20 min at 120°C; this is GN1A.

GN2A and 2B

Grossularite (Hessonite) from California (no site stated; Crestmore?). MIT research collection. Heterogeneous pieces. Contained diallage (?), feldspar (?), hematite, a light blue prismatic mineral (cyprine vesuvianite?) and a little quartz.

Split into two fractions magnetically. Handpicked. Oil immersion; many grains anisotropic, especially in 2A, which is common in grossular.

Picked light-colored garnet from 2B, which is darker. Both appear clean.

Final size, 200 + mesh.

GN3

Schorlomite. Magnet Cove, Arkansas (ref. 54) (Smithsonian, 80433) contained feldspar, feldspathoids. Very dirty; thin section strongly zoned.

To 35 + mesh, added boiling 6M HCl five minutes, decanted with water. 48% HF $\frac{1}{2}$ hour, then $Al(NO_3)_3$ in 1M H_2SO_4 1 day to remove CaF_2. This garnet is attacked by hot HCl, but resistant to HF.

Handpicked. Magnetic separation; contains a little feldspar, little crusty material (schorlomite?).

Final size, 200 + mesh.

GN4

Schorlomite. High Atlas Mtns., Morocco (ref. 54). (Smithsonian, 112864). Contained calcite, feldspathoids, and green pyroxene. Dirty. Thin section zoned.

Purified as GN3, with HCl, etc. Magnetic separation, very clean. Handpicked.

Final size, 200 + mesh.

GN5

Red-brown spessartite from Franklin, N. J. From MIT Dc. Geology collection, number (2258)3589. Associated with calcite, franklinite and feldspar (?).

This single euhedral crystal is porous, crumbles easily in mortar. Sieved, treated with cold dilute HNO_3. Magnetic treatment. Small crystals beautiful red-orange.

Handpicked. Ground in mullite mortar under acetone. Washed with H_2O and acetone on sintered glass. Dried 20 minutes at 110°C.

Final size, 200+mesh. Very clean.

GN6

Melanite from Oka, Quebec. In melanite carbonatite, associated with nepheline, a little pyroxene and calcite. From Gold's Figure 4, d, a boulder in woods (ref. 96). Collector, Earle R. Whipple.

Freed melanite by cold 6N HCl overnight (silica gel), then 3N HCl. Soaked in water, acetone, dried.

Crushed a large amount to 42-60 mesh (fine inclusions). Treated one hour with cold 48% HF; had to cool since acid heated. Decanted off much CaF_2, washed with water.

Removed CaF_2 with warm $Al(NO_3)_3$ reagent (after using hot 6N HCl unsuccessfully). Washed with cold 6N HCl, water, acetone, dried.

Magnetically treated, no magnetite. Very clean, no pyroxene visible. Handpicked.

Ground in mullite mortar under acetone, washed with water and acetone on sintered glass. Dried 20 minutes at 110°C.

Final size, 200+mesh.

GN7

Andradite, Franklin Furnace, N.J. Largely euhedral brown garnet in calcite, with fine dark pyroxene. Color, red, orange and a little yellow

garnet when in small grains. MIT research collection, B.X. 23. Donor, O. Christensen.

Freed from calcite with dilute HNO_3. Crushed to > 60 mesh in a porcelain mortar. Too dark to handpick.

Treated with 48% HF for 15 minutes (became hot, boiled), decanted, washed, heated with dilute $Al(NO_3)_3$ reagent, washed, dried with acetone at 80°C. 48% HF two hours more, then as above.

Removed some salts with hot 3N HCl. Washed, dried. Sieved, took 100 + mesh, put through Frantz. Very little non-magnetic material.

Sunk in CH_2I_2, yellow mineral sinks also (yellow garnet). Soaked in acetone overnight. Ground in mullite mortar with acetone to > 200 mesh, washed with acetone, dried 15 minutes at 80°C.

Free of pyroxene, > 200 mesh.

Amphiboles

HB1

Hastingsite. Nearly identical to that in "Rock-Forming Minerals" by Deer, Howie and Zussman, p. 288, number 13. Supplied by J. H. Scoon as hornblende concentrate number 613, which contained four per cent anthophyllite.

Magnetic separation, handpicked. Very pure.

Composition is a little different than in the above reference, because of magnetic separation.

HB2

Kaersutite, the outside of a single crystal with a smooth undulating face. San Carlos, Arizona. (Smithsonian, 121866) (ref. 65). Contained

chalcedony, ilmenite and perhaps magnetite and olivine.

Magnetic separation, possibly foreign minerals (ilmenite?) in fine fraction; sieved at 200 mesh, rejecting fines. Handpicked.

Final size, 100 + mesh. Some opaques (ilmenite) in oil immersion.

HB3

Kaersutite. A very large xenocryst single crystal in a melanephelinite bomb, mineral breccia member, South Head, Kakanui, N. Z. On seashore, coated with barnacles. Collector, John S. Dickey (ref. 95).

Crushed gently to > 35 mesh, boiled 2-3 minutes in 6N HCl to attack feldspathoids and hematite on cleavage surfaces. Then hot strong NaOH (not boiling) to remove silica gel; decanted with water.

Soaked in water 2 days, dried with acetone at 80°C. Crushed gently to > 100 mesh, then decanted with acetone to remove fines.

Passed through Frantz to remove magnetic and non-magnetic impurities. Very little blue-greenish mineral in the non-mag. fraction, and a little flaky graphite (?). Very little dust clings to magnet. Not handpicked.

This sample is extraordinarily pure. There are no opaque inclusions to be seen in oil immersion! The sample of Dickey's analysis (OU20237) does contain inclusions.

CR1

Crossite, iron formation, Laytonville, California.

Collection No., Cambridge 93995. Sample prepared and analyzed by J. H. Scoon, analysis number 729.

Used as prepared by Scoon. Identical to the crossite #4 in Bancroft and Burns (ref. 61). The author's analysis for ferrous iron and that of Scoon do not agree.

Orthopyroxenes

OPX1

Enstatite, from Webster, N. Carolina, (ref. 99). Contained chrome diopside, a little finely-divided chromite and a black opaque. MIT teaching collection. Brown variety.

Magnetic separation, handpicked.

Final size, 100 + mesh. Contains a little chromite; lamellar twinning. A little high birefringent material (cl-pyroxene?) in oil immersion.

Clinopyroxenes

CPX1

Diopside, Cross property, Farm Point, Quebec (a magnesium mine). MIT research collection, specimen FP5. Contains green epidote, yellow vesuvianite (?), a little hematite, a trace of chondrodite (?), carbonate and cloudy crystals (all diopside by x-ray; with fluid inclusions ?), and some orthopyroxene lamellae.

Magnetic separation, at very high amperage, removes most of the cloudy crystals. Handpicked twelve grams.

Coarse crystals slightly green.

Final size, 200 + mesh. Contains a trace of orthopyroxene lamellae, and perhaps unseen hematite.

CPX2

Diopside, large single crystal with inclusions of calcite and a pink mineral. From Orange County, N.Y., U.S.A., supplied by Clifford Frondel. Harvard No. 110038. Almost opaque green.

Crushed to 35-42, 42-60 and > 60 mesh sizes, treated with warm dilute HNO_3 to remove calcite, washed, dried.

Excellent magnetic separation from pink mineral. Sample not usable; a small amount was handpicked.

CPX3

Titanaugite, Husereau Hill, Oka, Quebec. See reference by Peacor (ref. 75). Whole rock contains nepheline, biotite, little yellow andradite, magnetite, carbonate, and a little red mineral (rutile?). Some pyrrhotite and chalcopyrite (a little as inclusions in the titanaugite). Much of titanaugite is hourglass zoned. Collected by U. Toronto.

Crushed whole rock to > 35 mesh. Hot 6N HCl for $\frac{1}{2}$ hour ($H_2S\uparrow$). Decanted.

HF (1:1) for 1 $\frac{1}{2}$ hours to strip away all sulfides in matrix. Became hot, had to cool. $Al(NO_3)_3$ reagent overnight. Hot 6N HCl $\frac{1}{2}$ hour, HF (1:1) $\frac{1}{4}$ hour, etc. Washed with hot water, dried.

Through Frantz to separate andradite (mag.) and pyrrhotite (non-mag.). Some sticks to magnet (Fe_3O_4).

Very clean, no need to handpick.

Crushed to > 100 mesh under acetone. Washed with water, acetone, dried 15 minutes at 110°C.

CPX4

Titanaugite from an essexite, Crawfordjohn, Great Britain (ref. 101). Collected by Thomas Pearce, U. Toronto. Whole rock contains plagioclase, some nepheline, a little pyrite and chalcopyrite (none observed in titanaugite) and magnetite (some as inclusions). No amphibole. Titanaugite strongly hourglass zoned.

Crushed whole rock to > 60 mesh.

Treated with boiling 6N HCl 5 minutes. Decanted with water. Dried with acetone, 80°C. Through Frantz to lessen plag content.

Ground to > 100 mesh. Through Frantz twice, discarded a small mag. fraction, then non-mag.

Sank in CH_2I_2. Soaked in acetone 3 days.

Contains a little plagioclase. Not handpicked.

Micas

M1

Phlogopite, Burgess, Ontario, Canada. From Natural History Museum, Vienna, Austria. Specimen number H. 3752. This is Jakob's mica number one (ref. 88).

Contains a little of a black mineral in the cleavages, which is soluble in HCl (ilmenite?), and a little granular mineral (apatite?).

Split the sheets with a spatula, and cut up with clean scissors. Probably no apatite present in final product.

M2

Biotite, from Derome feldspar mine, Halland, South Sweden. From Natural History Museum, Bern, Switzerland. This is from the same site and museum as Jakob's mica number 3 (ref. 88).

Opaque even in thin sheets. Color, deep olive when very thin. Contains transparent inclusions (apatite?).

Cut up with a pair of clean scissors.

M3

Red manganiferous phlogopite from Oka, Quebec. Mine dump, St. Lawrence Columbium and Metals Corp. Whole rock mostly calcite, with a little magnetite and apatite (?). Collector, Earle R. Whipple.

Some is zoned hexagonally, with alternating red and green rings. Some (esp. small crystals) entirely red. Many black inclusions (magnetite?).

Dissolved out the calcite with cold 10% HNO_3; soaked in water overnight, washed with acetone, dried at 80°C.

Hand selected inclusion-free crystals, mostly small ones, some zoned ones. Low yield, about 3%.

Sheared the mica books gently in a mullite mortar to reduce grain size; did not attempt to grind. 6 gms. The Mössbauer sample was ground under acetone to > 200 mesh.

Babingtonite

BAB1

Large crystals of babingtonite, Holyoke, Mass. (ref. 82). From the outside of a large vein, associated with quartz and light green prehnite.

Harvard No.105696 . Donated by Dr. Clifford Frondel.

Ground gently in steel mortar to > 35 mesh. Through Frantz twice to free from quartz. Some powder stuck to magnet.

Ground under acetone to > 100 mesh. Washed with water and acetone, dried 10 minutes at 80°C. 1.6 gms.

COMPUTER PLOTS

OF

MOSSBAUER SPECTRA

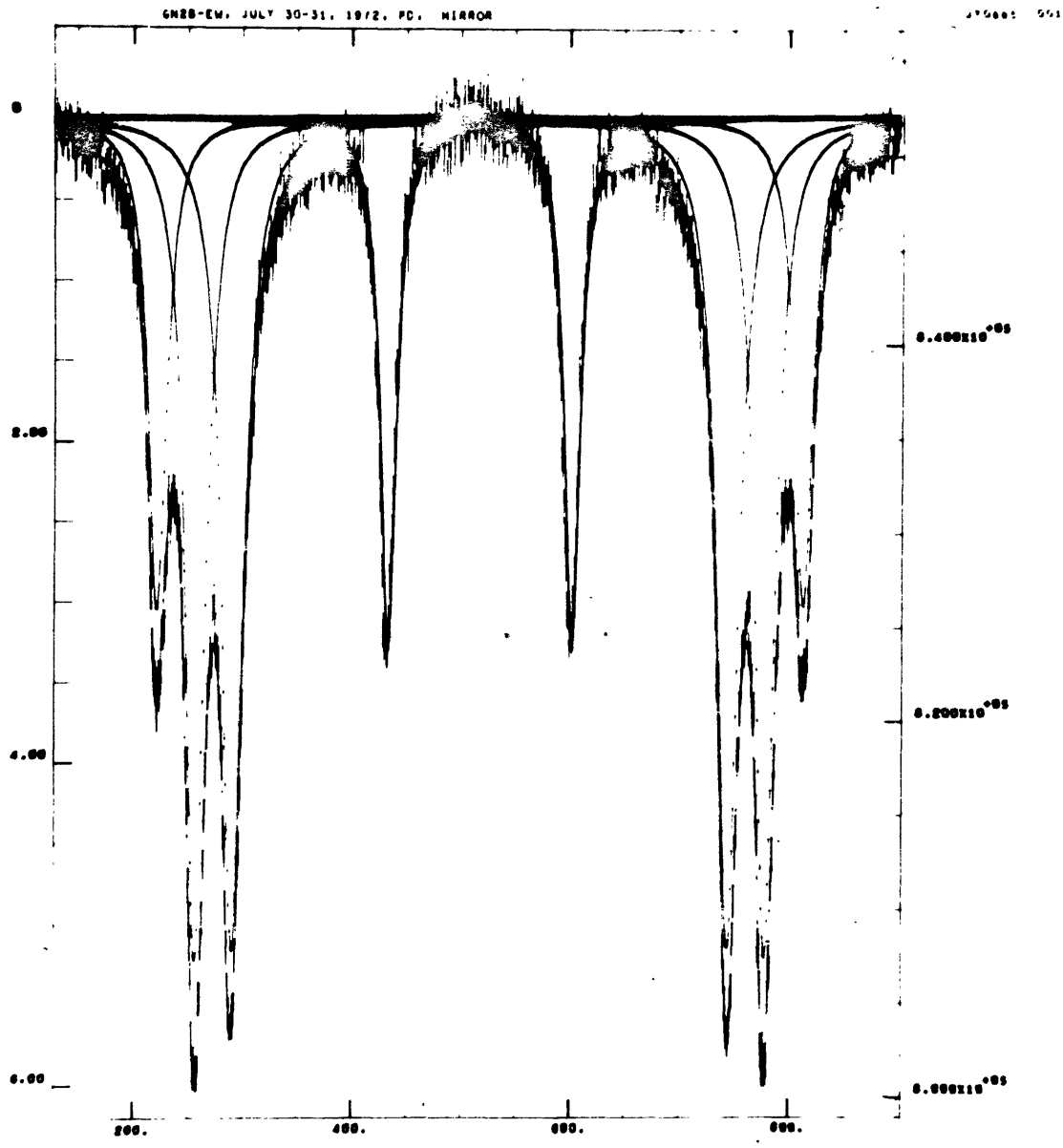

FIG. 1.

Grossular Garnet GN2B, mirror spectrum, 1024 channels.

Ferric peaks have largest amplitude.

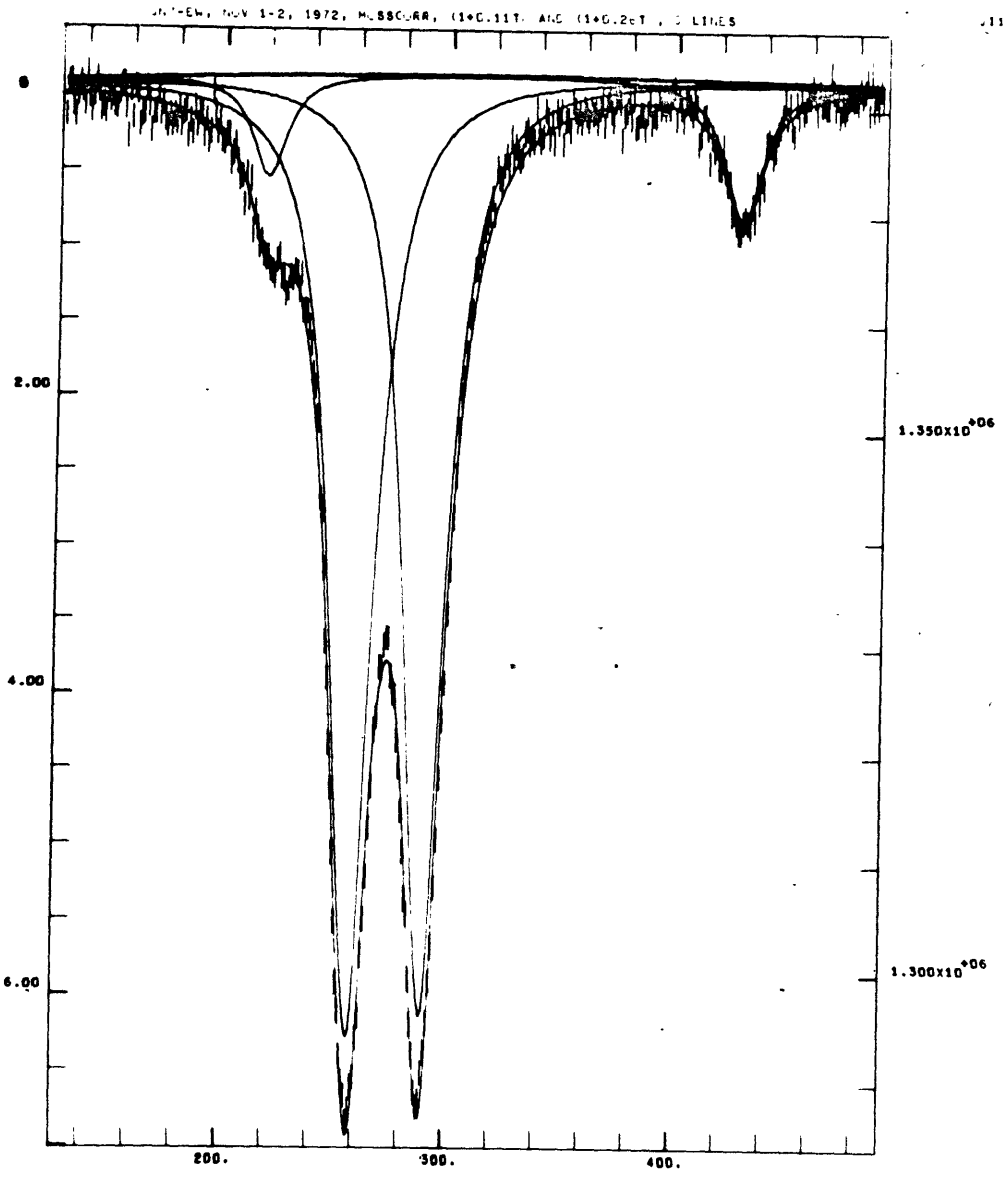

FIG. 2.

Andradite Garnet GN7, free fit, 512 channels. Corrected by Program Mosscorr.

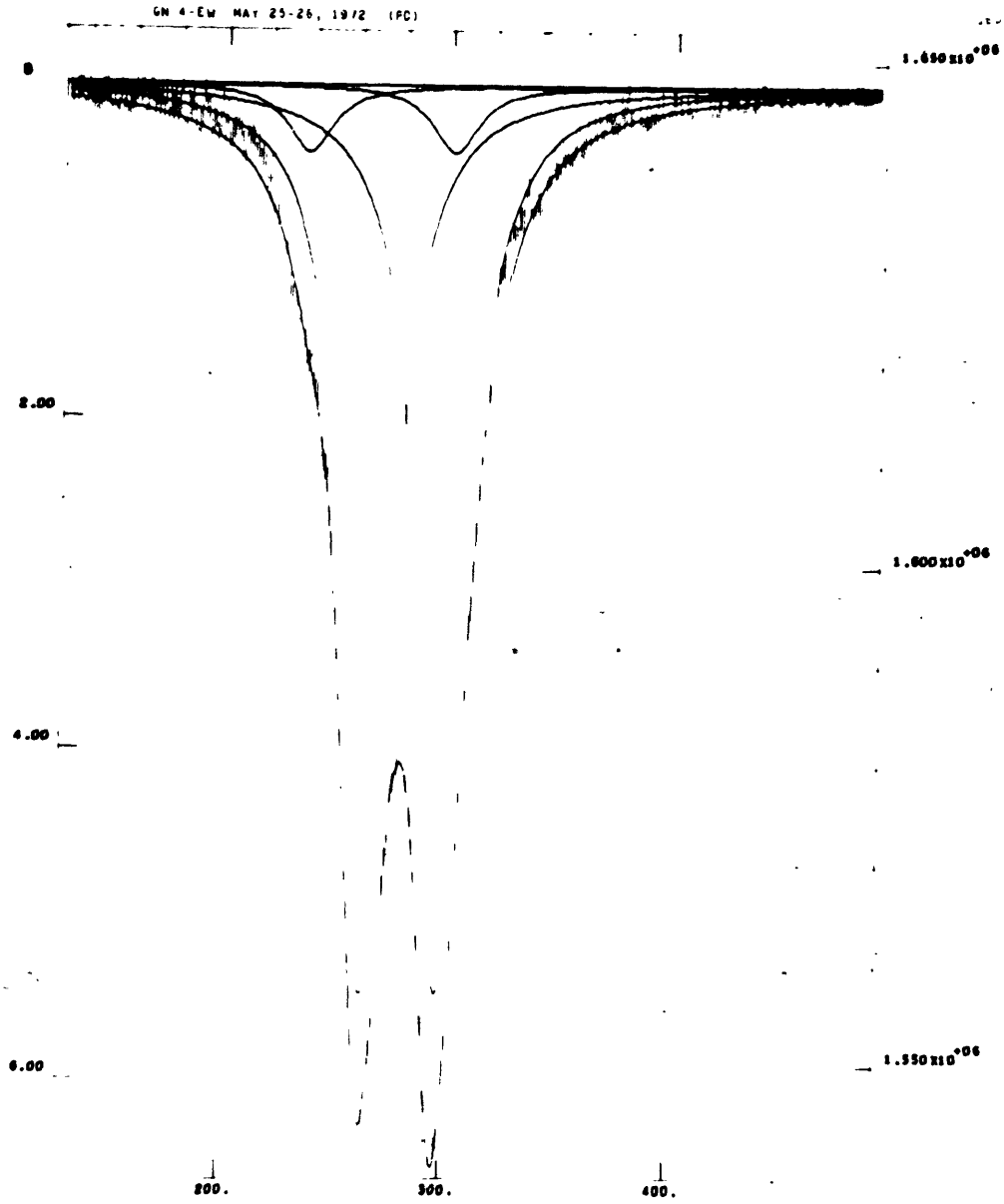

FIG. 3.

Schorlomite Garnet GN4, showing tetrahedral ferric iron (small peaks).

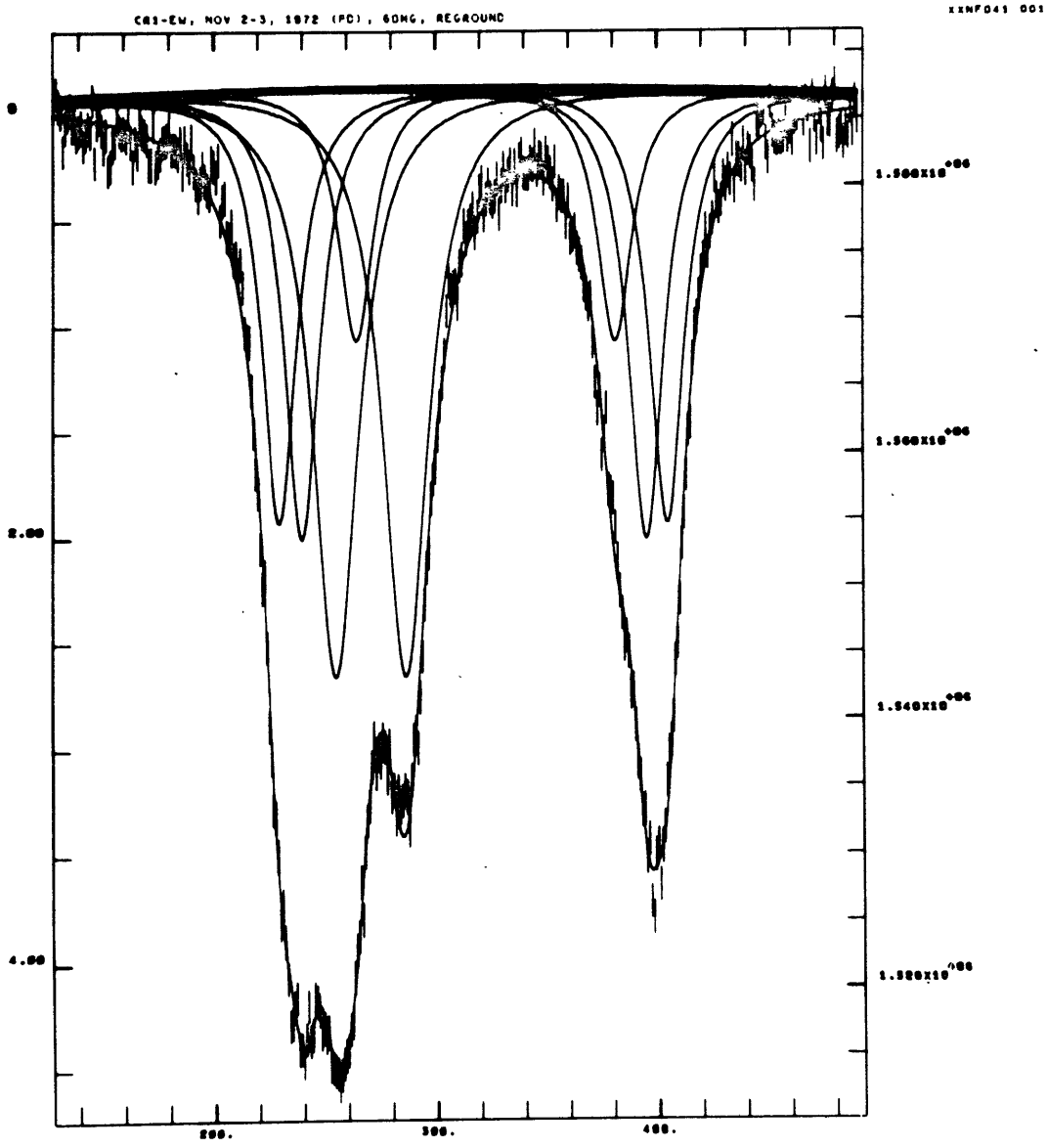

FIG. 4.

Crossite (amphibole) CR1. Ferric peaks have largest amplitude.

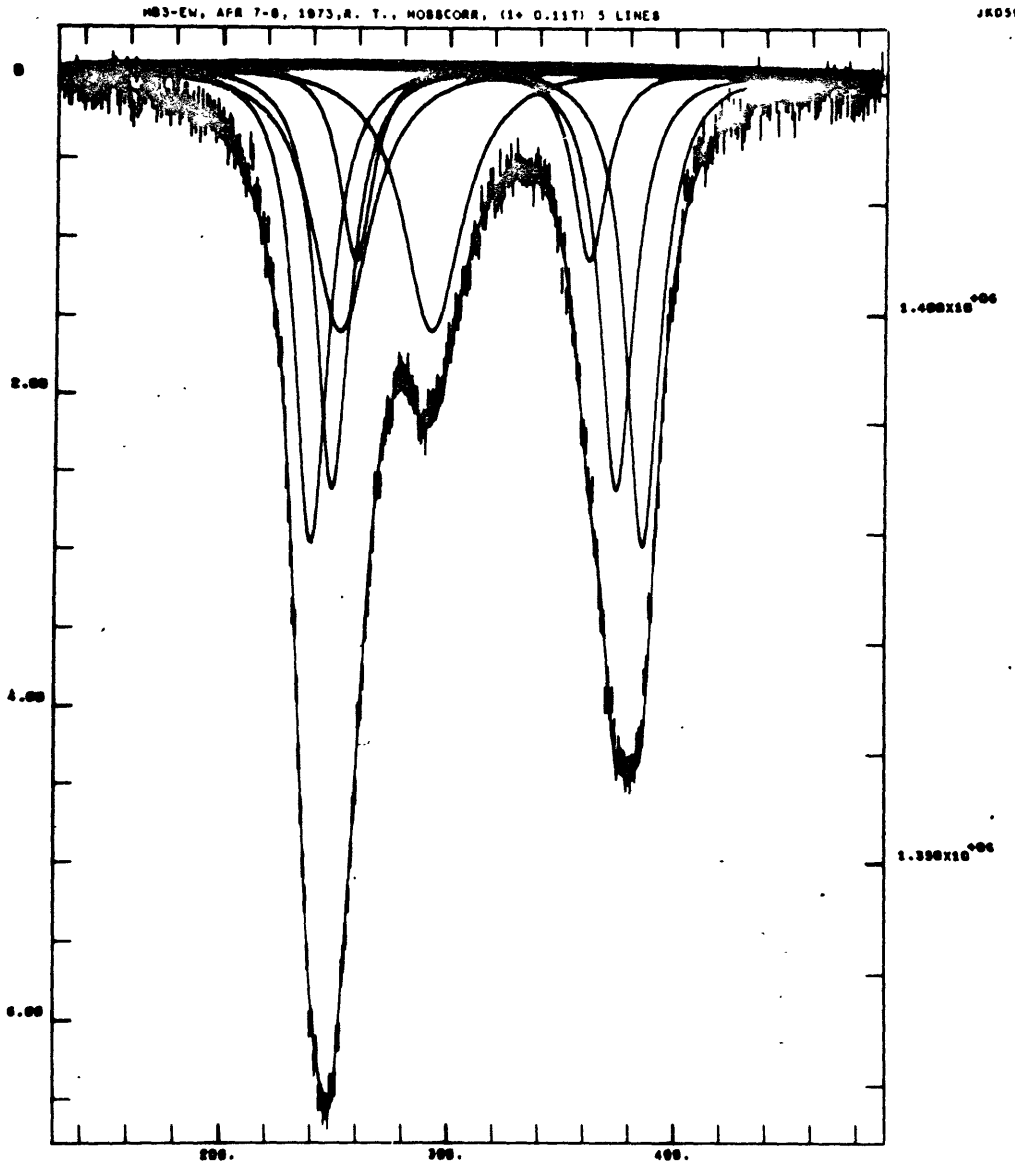

FIG. 5.

Kaersutite (amphibole) HB3. Corrected by Program Mosscorr.

Ferric peaks wide.

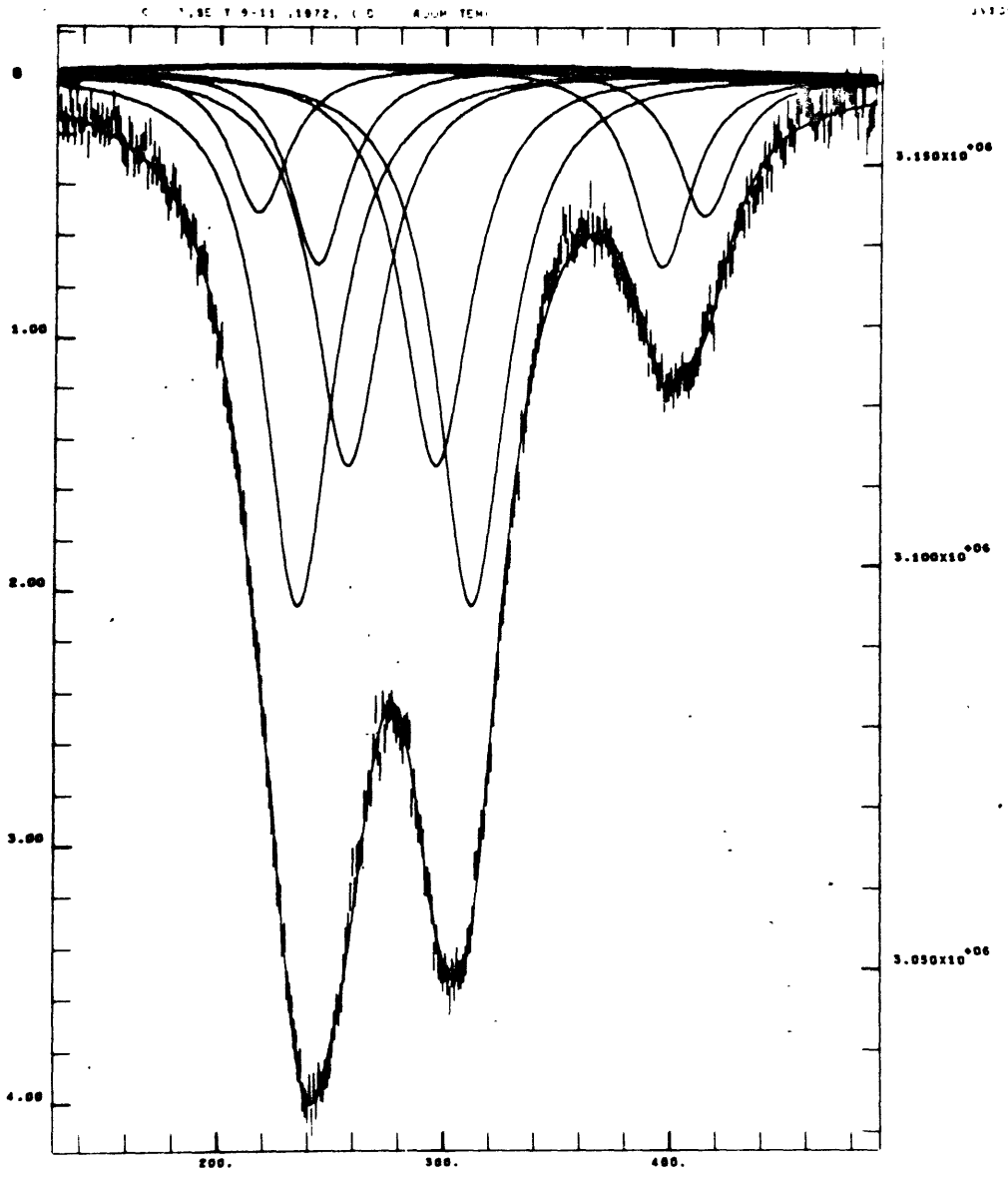

FIG. 6.

Titanaugite CPX3; four ferric peaks (largest amplitudes).

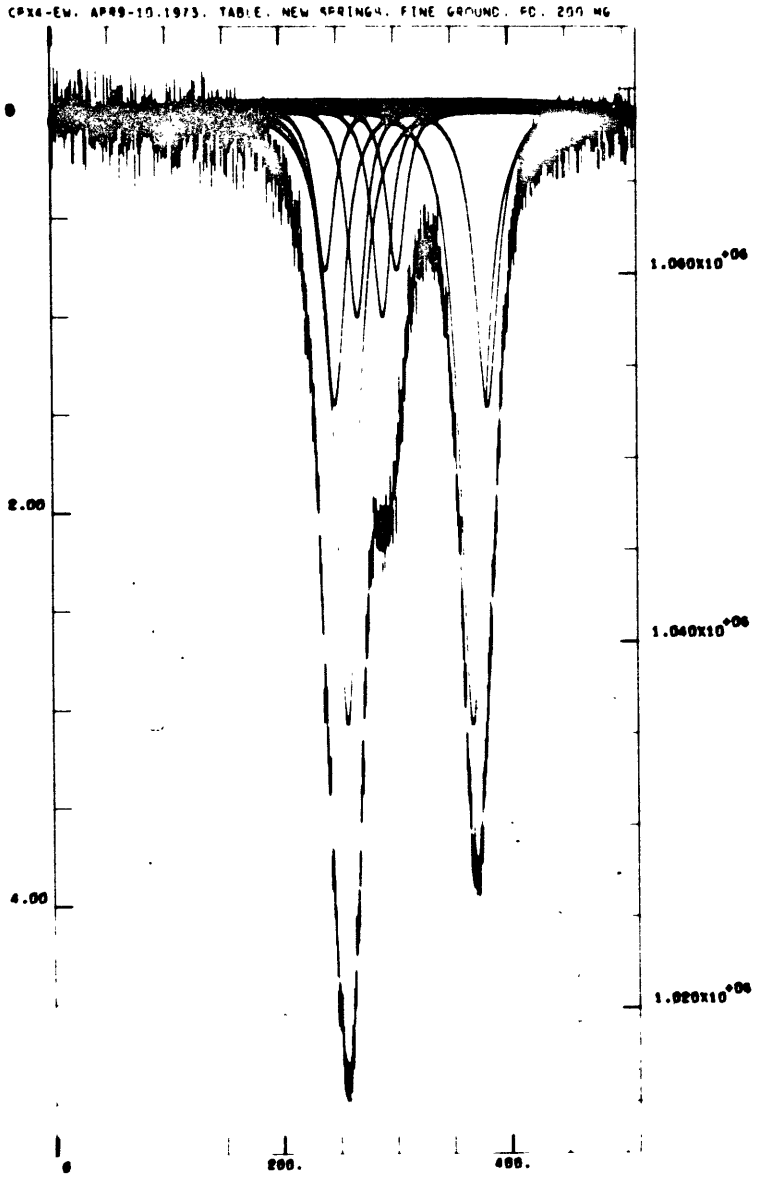

FIG. 7.

Titanaugite CPX4, showing tetrahedral ferric iron (smallest amplitude).

FIG. 8.

Biotite M2. Ferric peaks have smallest amplitude.

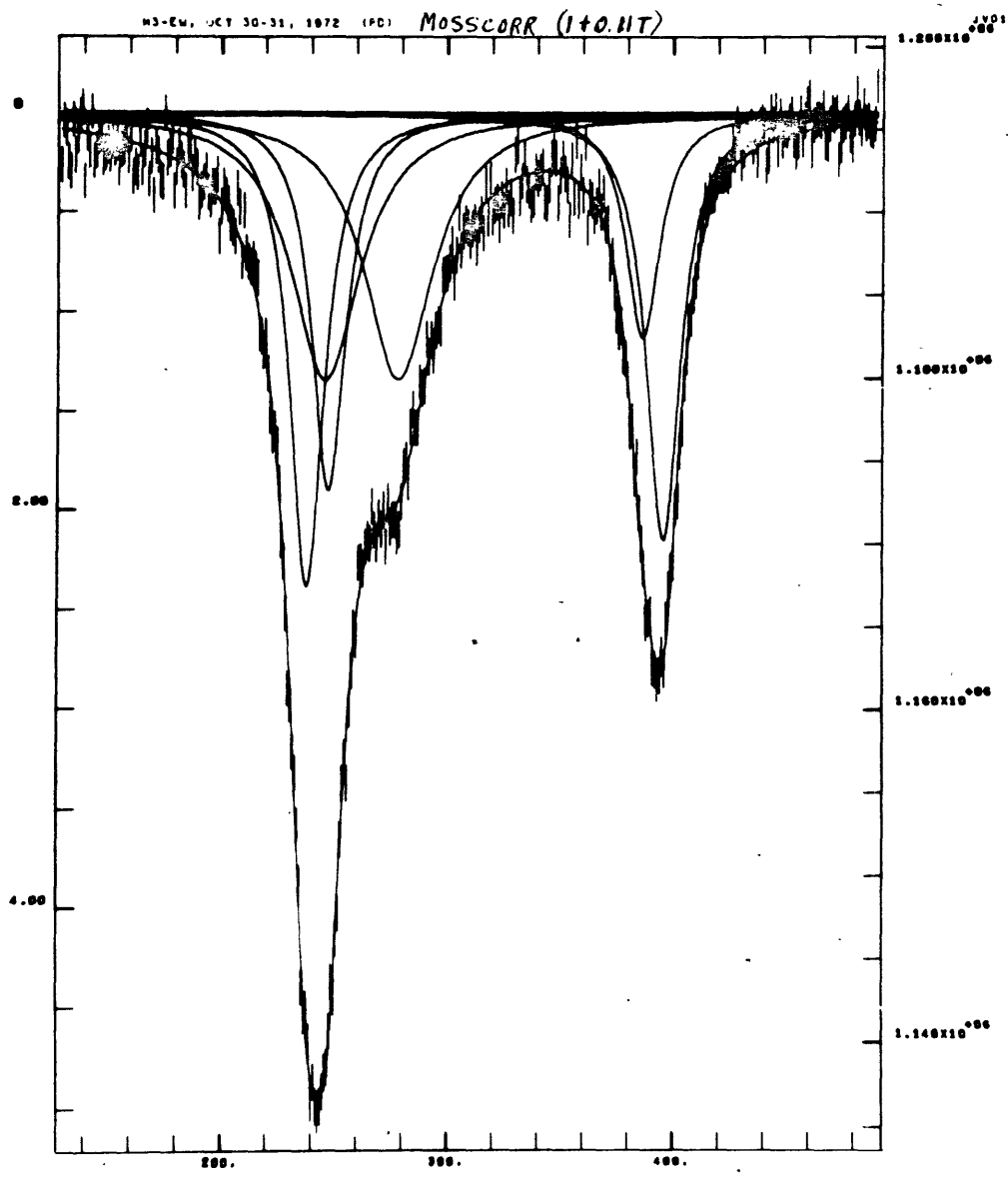

FIG. 9.

Phlogopite M3. Corrected by Program Mosscorr. Ferric peaks very wide.

INVESTIGATION OF THE MOSSBAUER SPECTROMETER

The most important point of this thesis is the quantitative comparison of results obtained from analytical chemistry with those obtained from the Mossbauer spectrometer. The chemistry has been carefully examined. The study cannot be complete without examining the spectrometer also.

The spectrometer used was an Austin Science Associates Model S3, K3, equipped with a 1024 channel multi-channel analyzer. Most spectra taken were one-half of a mirror-image spectrum, using 512 channels, and a maximum velocity of approximately 4 mm/sec. A source of Co^{57} in palladium was used, originally of 100 millicuries. The source to sample distance was always at least six inches. The sample was mounted in a round hole of 2.2 cm diameter, in sucrose, within 1 cm of the counter, with a lead shield framing the hole. The multi-channel analyzer was by Nuclear Data.

In any quantitative method, one of the necessary qualities for good performance is reproducibility, or good precision. This does not guarantee accuracy, but lack of precision destroys accuracy. It is the precision which is easiest to test on the Mossbauer spectrometer. To some degree, accuracy may be tested by observing equality or inequality of doublet peaks which should be equal in area, as the doublet peaks in a garnet which are well resolved in the spectrum.

Of the minerals used in this work, probably the three most repeated and useful for studies of precision are the garnet GN2A (grossular), hornblende HB1 (hastingsite) and CR1 (crossite). The latter two are complex spectra and show difficulties in the precision, but only the garnet, which has a simple spectrum, gives a powerful clue to the difficulties. This garnet spectrum

serves as its own internal check on the low velocity characteristics of the spectrometer, and its own quality. GN2B, GN5 and GN7 are spectra of the same type, and also provide their own internal check. This is not to say that the garnet can detect all malfunctions of the spectrometer, but at least one of them.

In the garnet, GN2A, loss of area can occur in the low velocity ferric peak. The maximum amplitude is not affected, but the width decreases markedly in the free fit. The most extreme loss observed was a run in which the low velocity ferric peak was 0.58 times as great in area as the high velocity ferric peak. In much less extreme cases, the effect is not subtle, but an easily observed fact. In the cases where this was observed, one-half of them gave the correct ferrous-ferric ratio (as judged by a spectrum, fully constrained, which had a free fit with good doublet equality) when only the high velocity ferrous and ferric peaks were used for the ratio. This shows that the low velocity (at the ferric peak) region of the spectrum is often affected, and can be strongly affected. In the extreme case, R = 0.72 whereas a good run gave R = 0.58 (baseline free) both values being for fully constrained spectra. The chemical value is R = 0.716.

This difficulty should be distinguished from a much less serious difficulty termed "area-stealing," in which area is traded between adjacent peaks in the free fit, but no total area lost. In the garnet, this commonly occurs between the two low velocity peaks. Area loss can be checked by summing the two low velocity peaks, and then the two high velocity peaks to see if the sums are equal.

It is rare to find the low velocity ferric peak greater than the high velocity ferric peak. When it does occur, it is less than five per cent greater, and sometimes partly due to "area stealing" with the adjacent ferrous peak.

Because the low velocity ferric peak is rarely greater than the high velocity one, it appears that area is generally lost, and not gained. Also, garnet spectra which give doublet equality also give the greatest amount of ferric iron. From this, one may reach the conclusion (though probably not infallible) that spectra (garnet or other) which have the maximum (or near maximum) content of ferric iron are the closest to being correct. This conclusion has been used in the present work. It applies only where a ferric line lies in the positive low velocity region.

The loss appears to be due to the spectrometer drive moving too rapidly through the positive low velocity region. The zero velocity of the drive corresponds to maximum extension of the spring. Because the channel dwell-time remains the same irrespective of the motion of the drive, the maximum amplitude remains the same. The width decreases because the drive moves too quickly. This can be mitigated by damping the springs with foam pads, and the loss may be partly due to induced vibrations in the springs. In the spectrometer, the channel number (representing velocity) is not inextricably tied to the appropriate velocity of the drive. In an optimal spectrometer design, it should be so tied.

Ferrous-ferric ratios for the hornblende HB1 ranged from R = 2.40-3.10 for fully constrained spectra, all ferrous widths equal. The value 2.40 occurred with bad statistics and can probably be discarded; a value of 2.55 was got from a copper source. A mirror run done by G. M. Bancroft gave 2.56 and 2.66 for the two sides (2.64, mirror). The ferric peak is rather small; only a shoulder shows on the low velocity envelope. The correct value (maximum ferric) is probably Bancroft's run, or another with R = 2.80. The chemical value is R = 3.41.

In the spectrum of the crossite CR1 the ferric peaks are much larger and the chemical value for R is 1.66. Values from the Mossbauer spectra ranged from 1.26 to 1.66 for 6 peak fits (as in Bancroft and Burns) and from 1.37 to 1.66 for 8 peak fits with full constraints with all ferrous widths equal. Two spectra showed signs which are symptomatic of loss of area in the low velocity region of the spectrum. One symptom is a narrowing of the ferric lines. In one run where the small M2 ferrous peak was shifted to a position on the low velocity side of both ferric peaks (see section III on amphiboles), the ferric widths were even less than the ferrous (R = 1.66), which is unusual for a mineral in which ferric iron is present on more than one site. Since both ferric peaks are bound together by constraints of width and area, a decrease in one peak will affect the other. Another symptom, not always occurring in the crossite and hornblendes, is the mentioned shifting of the small, low velocity M2 ferrous peak. This appears to coincide with the narrowing of the ferric peaks and to be another sign of trouble. It was observed also in the kaersutite HB3 when the ferric peaks narrowed. No such signs were observed in the spectra of micas and pyroxenes.

Another difficulty is loss of resolution of peaks. Figures 10 and 11 show two spectra of the spessartite GN5. The sample is identical and only the spectrometer run differs. The badly resolved spectrum gives R = 1.20 (as six peaks) and the well resolved one gives R = 1.29.

This loss of resolution may have been due to interference from the other end of the drive, which was being used concurrently for high pressure spectra.

Spectrometer difficulties were not peculiar to the instrument used here. A test of the same make of spectrometer drive in the lab of Prof. Wm. Reiff of Northeastern Univ., using GN2A in a mirror spectrum of 512 channels (256 each side), showed the low-velocity ferric peak to be 70% as wide as the high velocity peak, and 69% of its area (79% of area, corrected for area-stealing). The sine wave value was -0.109% (free fit; mirror interpretation) and chi-squared was 582. The value of R was 0.67 (mirror; R = 0.58 when corrected for area stealing; R = 0.61 with full constraints). The sum of the two high velocity peaks was 909,193 counts, the low velocity peaks 785,959 (mirror). The value of R = 0.58 seems to agree with the value in the present work, but the other values and the inequality of the high velocity and low velocity sums point to difficulties with the spectrometer. As in the present work, the low velocity region has lost area. It is uncommon for the low velocity peaks to have more area than the high velocity in a garnet spectrum, and this tendency points to non-statistical processes being responsible for the loss. Even with correction of the spectrum by Program Mosscorr (which increases the overlapped low velocity peaks), the low velocity peaks' sum was never greater than 103% of the high velocity sum. In the worst run of GN2A, the low velocity sum was 79% of the high velocity sum.

Further tests of the spectrometer function at low velocity may be done with the aid of an extraordinary andradite containing essentially no ferrous iron, donated by Dr. Clifford Frondel of Harvard (Harvard Specimen No. 98087). Lack of ferrous iron lines simplifies the test. This andradite is essentially stoichiometric in Ca, Fe^{+3} and Si composition, and should have little problem with site multiplicity. Potassium ferricyanide may also be suitable for this purpose.

Laser calibration, channel by channel, may also aid in testing the spectrometer function. In addition, there are electronic means of overcoming non-linear effects without improvement of the spectrometer drive. One such system is used by Dr. R. B. Frankel at the Magnet Lab, MIT.

A case of unequal doublet widths of the ferric lines in an andradite appears in Bancroft, et al. (ref. 17), but does not appear to be due to spectrometer difficulties. This garnet is black, a melanite from Greenland, and contains tetrahedral ferric iron. The unequal widths arise from underfitting of the spectrum to only two peaks (Roger Burns, private communication).

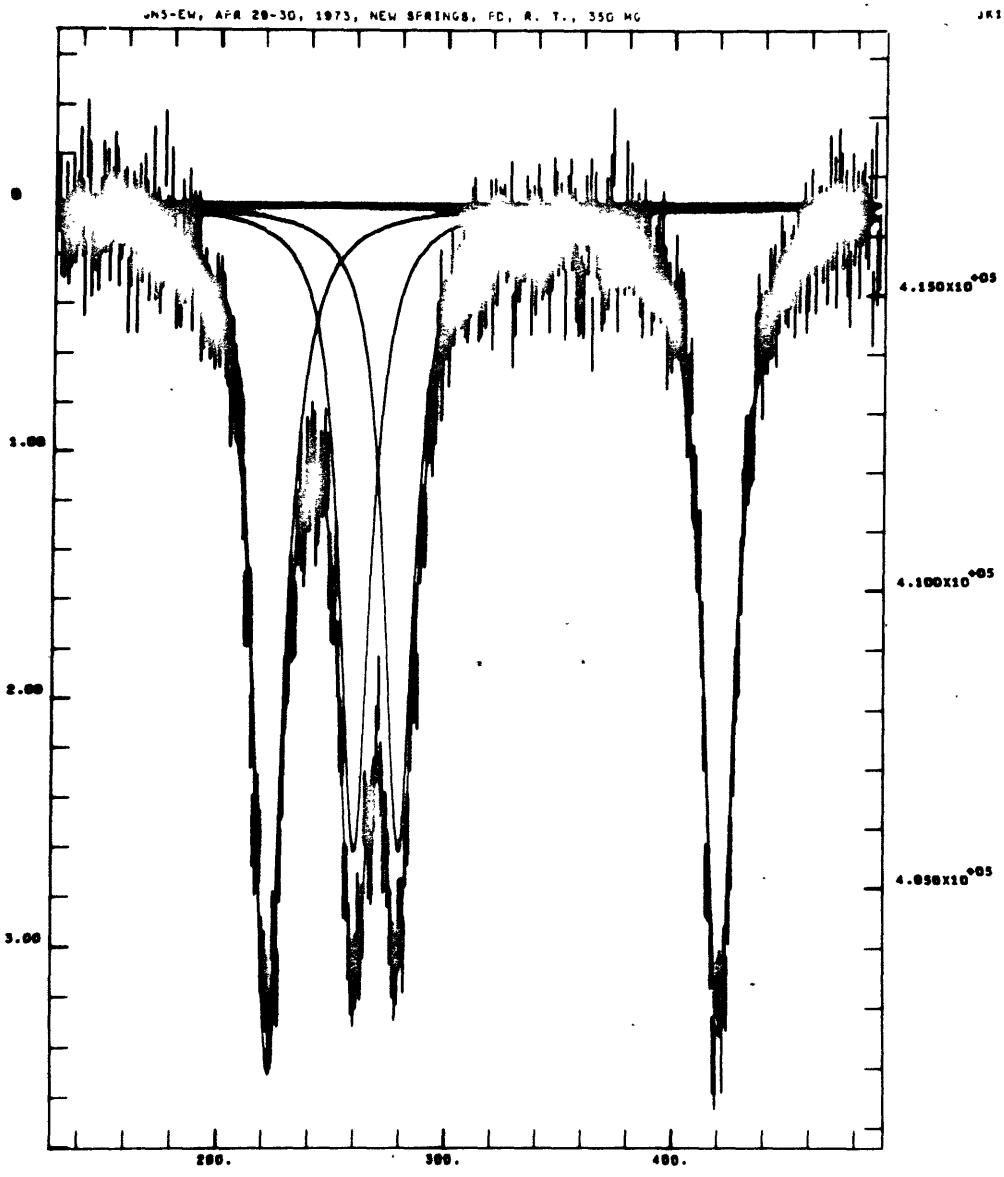

FIG. 10.

Spessartite Garnet GN5. Ferrous peaks have largest amplitude.

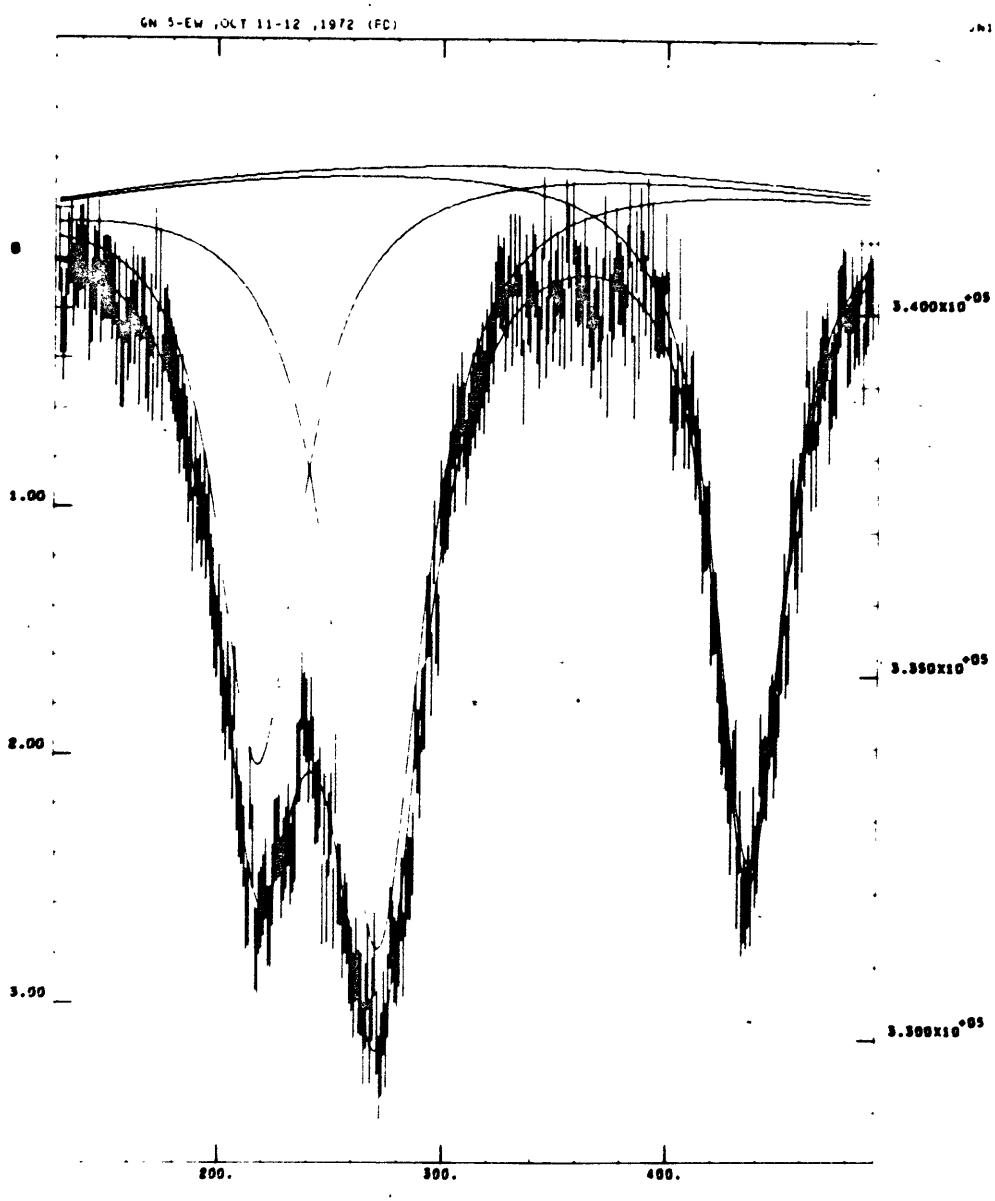

FIG. 11.

Spessartite Garnet GN5. Poor resolution.

Effects of Stone's computer interpretation upon the ferrous-ferric ratio and site occupancy of the minerals must be considered. If exactly the same numerical data are processed, the final answer will usually be the same in a spectrum interpreted more than once. An exception was a 6 peak fit on CPX3, in which the two low velocity ferrous peaks could be reversed in position. Occasional bizarre interpretations also arise. The negatively bowed baseline of GN2B was set to be positive in the initial estimates, in a test of the computer program's reproducibility; the result was the same as before with a negatively bowed baseline.

The bowing (sine function) of the baseline is a function of the number of lines fitted. As the number of lines increases, the bowing (positive sine value in these cases) decreases. Thus, the baseline bowing is not reproducible with varying interpretations of a spectrum (see the discussion in the appendix) and is not solely a function of the inverse square law of the source radiation. Examples are given in Table 8a, none of which have been corrected by Program Mosscorr. CR1 (8 lines), HB1 and CPX3 employ full constraints, all ferrous widths equal and all ferric widths equal. CR1 (6 lines) employs only two width constraints, one for the outer ferrous doublet and one for the ferric doublet. The same relations were shown by the left side of Bancroft's mirror run on HB1, as well as the HB1 run above. The channel drift values and the values of chi-squared also improve with the increase in the number of lines(see chi-squared for CPX4, 8, and 10 peaks, Table 10).

The bowing of the baseline may be also a function of statistics, as mentioned in the appendix. This was observed in the use of Program Mosscorr,

which always increases the value of chi-squared. The sine wave value (considering positive values) always increased after the use of Program Mosscorr (Table 10).

There were also indications, difficult to show conclusively, that runs with high values of chi-squared gave large sine wave values. A number of these runs are shown in Tables 8a and 8b, which also list three mirror runs which are discussed in the next section under HB1 and HB2. Mirror runs have a different sine wave and statistics relation.

In complex spectra, such as amphiboles and pyroxenes, the reproducibility of the type of spectrum (meaning the sequence of lines, not their exact position) is surprising. All three calcium amphiboles of this study showed the same type of spectrum, despite large differences of composition. Similarly, in the pyroxenes a ten-line fit was obtained on the titanaugite CPX4. This fit used 3 ferrous doublets and (like CPX3) two ferric doublets (all widths of each type equal; full constraints) and a sine wave and channel drift value constrained to the same value as the eight-line fit (sine = 0.068%, drift = 0.81 ppm). The ten-line fit possibly eliminates the M1 site multiplicity of CPX4 (see end of section; Table 9 and 10 for parameters). The line positions of the ferric lines (10 lines) are very similar to those of CPX3 (8 lines; probably no M1 site multiplicity in CPX3). In CPX3 and CPX4, it is doubtful whether the outer ferric doublet represents tetrahedral ferric iron, because of the center shift. Ferrous line widths were 0.35 mm/sec; those of ferric iron were 0.44, which contrast with the 8-line fit.

G. M. Bancroft contends that lines that overlap more closely than one-half a line width cannot be accurately determined by computer interpretation. This may hold true for amplitudes and areas, but relative line positions (i.e.,

Table 8a. Interpretation vs. sine wave values.*

	CR1		CPX3		HB1 (left side, mirror**)		HB1 (mirror**)
	6†† peaks	8 peaks	6††† peaks	8 peaks	6 peaks	8 peaks	8 peaks
sine wave (%)	0.175	0.127	0.139	0.062	0,284	0.204	0.005
channel drift (ppm/chan.)	2.77	1.85	0.77	0.44†	5.16	3.23	0.46
chi-squared	726	613	773	560	2286	1230	3533
R(area) (= Fe^{+2}/Fe^{+3})	1.28	1.47	0.269	0.310	3.10	2.73	2.80

*full constraints, all ferrous widths equal, all ferric widths equal

**not Bancroft's run, see also Table 8b

†constrained

††only two constraints, widths

†††one ferric doublet.

Table 8b (see Table 8a)

Statistics vs. sine wave values.*

	HB1 (r. side, mirror**)	HB1	HB1	HB2 (l. side, mirror)	HB2 (r. side, mirror)	HB2 (mirror)	GN7 (free fit)†	GN7 (free fit)††
sine wave (%)	0.325	0.145	0.177	0.215	0.220	-0.003	0.092	0.120
channel drift (ppm/chan.)	-1.63	7.02	2.20	2.35	-1.93	0.43	1.82	0.96
chi-squared	1032	968	605	591	630	1958	646	662
R(area)	2.79	2.92	3.10	2.39	2.41	2.49	0.151† (hi vel. peaks)	0.183†† (hi vel. peaks)

*full constraints, all ferrous widths equal, all ferric widths equal; 8 peaks except GN7

**not Bancroft's run, see Table 8a

†low vel. peaks' sum 100.4% of high vel. sum

††low vel. peaks' sum 93% of high vel. sum.

Table 8b (Cont.)

	CPX4 (8 peaks) *	CPX4 (8 peaks) *	M3 (6 peaks) **	M3 (6 peaks) **	GN2B* (l. side, mirror)	GN2B* (r. side, mirror)	GN2B* (mirror)	GN2B*
sine wave (%)	0.068	0.118	-0.083	-0.098	-0.144	-0.124	0.002	-0.101
channel drift (ppm/chan.)	0.81	2.13	0.57	0.07	0.53	0.59	0.34	-0.77
chi-squared	533	548	526	514	558	520	1636	559
R(area)	2.89	3.08	2.23	1.58	0.507	0.487	0.495	0.492

*full constraints, all ferrous widths equal, all ferric widths equal

**no area constraints, all ferrous widths equal, ferric widths equal. Low velocity ferric peak too small.

sequence of lines) are remarkably reproducible. Full constraints undoubtedly aid reproducibility of amplitudes and areas, because of restrictions of one peak of a doublet on the parameters of the other peak.

Ferrous-ferric ratios are not so sensitive to computer interpretation as site occupancy, because the ferric areas are determined by difference (see section on Fitting of Mossbauer Spectra and Site Occupancy). The ratio, however, does depend on an adequate fit. A case in point is the ferrous-ferric ratio of CPX4 in the 8 line and 10 line fits, where R was 2.86 and 2.50 respectively (using Program Mosscorr). Compared with chemistry, the 10 line fit of CPX4 agrees more closely with CPX3 and BAB1 than the 8 line fit.

In the garnets, used to test the doublet equality and reproducibility of spectra, the site multiplicity and consequent line shape problems (esp. of ferric iron in GN2A) may affect the ferrous-ferric ratio. This, however, does not explain the variability of the ferrous-ferric ratio in various runs, and the variable doublet inequality in the free fits, except possibly for problems of the sine wave value variation (area stealing taken into account). The sine wave's effects are probably small, for a fully constrained fit of GN2A in one run gave R = 0.580 (good doublet equality in free fit; sine wave = -0.071, drift = -0.12 ppm/channel) while R = 0.570 for a straight baseline (sine wave and drift zero). For GN2B, R = 0.492 (good doublet equality in free fit; sine wave = -0.101, drift = -0.77 ppm/channel) and R = 0.494 for a straight baseline (Table 8b).

Hornblendes had positively bowed baselines, sometimes extremely bowed (Tables 8a, 8b), yet straightening of the baselines in certain mirror

spectra did not greatly change the ferrous-ferric ratio. In these mirror interpretations, the ratio is a combination of the two halves of the spectrum. The results are discussed in "Fitting of the Mössbauer spectra and the Site Occupancy of Iron," for the minerals HB1 and HB2, and presented in Tables 8a and 8b.

Channel-count statistics may affect computer interpretations, but the overall areas of the high velocity and low velocity envelopes cannot be greatly affected, unless the counter malfunctions. For instance, in a spectrum with a baseline count of only 360,000 (GN2A), one standard deviation is 600, and if the average peak height count is about 8,000 (isolated peak; 10,800 counts or 3% absorption) then one standard deviation is 7.5% of the average peak height. Since most of the area is covered by about 20-30 channels, the area variation of the peak due to statistics alone is very small. The statistical variation of envelopes will be much smaller.

Resolution of spectra may also affect the computer interpretation. An example of good and bad resolution is given in Figures 10 and 11. The amplitudes of ferrous peaks in these figures are different relative to the amplitudes of the ferric peak(s) and different in percentage absorbtion. This is due to counts being transferred laterally (i.e., from channel to channel) with consequent decrease in peak amplitude and loss of resolution. This is mentioned above, and its effects on the correction of the amplitudes of peaks by Program Mosscorr is mentioned in the appendix on the last page of the discussion of the absorption amplitude. Figure 11 of GN5 was not the only spectrum which showed signs of resolution problems. For example, better resolved spectra of CR1 were obtained (but without as much ferric iron). The bad fit of the high velocity ferric peak of CR1, Figure 4, (worse in the 6 peak

fit) may be due to resolution, and consequently amplitude problems. The 6 peak fit had a high value of chi-squared (916 vs. 619 for 8 peaks), and the 6 peak fit may be better than appears by its value of chi-squared, if the resolution and the consequent amplitude distortion did not exist in the spectrum.

Electronic relaxation may cause differences of peak amplitudes in a doublet, especially in ferric iron. This is discussed in an article by Goldanskii and Makarov (ref. 103; p. 96-98), which provides a good explanation of the phenomenon. There is also an advanced article on relaxation in ref. 103. Relaxation effects are almost certainly absent in ferric iron in the minerals used in this study, because there was no evidence of amplitude differences in the garnets studied, even at 77° K (GN2B and GN7). The amplitude of the resultant absorption at the low velocity ferric peak position of GN2B (which is most heavily overlapped) is always slightly greater than that of the high velocity ferric peak. In GN7, where the ferrous peaks are small, the ferric amplitudes are more nearly equal. The free fits of GN2B and GN7 show good amplitude equality even at 77° K, which confirms the lack of relaxation effects.

A. D. Law (ref. 64) has conclusively shown that minimization of chi-squared in fittings of Mossbauer spectra does not always lead to a more accurate interpretation of the site occupancy of a mineral, when chi-squared decreases as doublets are added to the interpretation of a spectrum. A specimen of the orthorhombic amphibole holmquistite was shown conclusively to contain no iron in the M2 site, by means of X-ray scattering. Despite this, the Mossbauer spectrum, using three ferrous doublets (for M1, M2 and M3), showed a value of X^2 less than that for the spectrum interpreted by two ferrous doublets (for M1 and M3 only, corresponding to the X-ray result). Thus, the

interpretation with three ferrous doublets, though it possesses a lower value of X^2, must be incorrect. From Law's result, it is evident that Mossbauer spectroscopy is not the ultimate tool for the determination of iron site occupancy, but must be used in conjunction with other methods, such as X-ray scattering and chemical analysis (as in pyroxenes). The pyroxenes, especially, pose severe problems in site occupancy by Mossbauer spectroscopy, due to site multiplicity of ferrous iron, and as yet unresolved problems in ferric iron site occupancy (see this work) possibly due to inhomogeneous pyroxenes (hourglass zoning).

In this work, the crossite CR1 may possess problems in interpretation similar in principle to those found by A. D. Law (see previous paragraph). Alkali amphiboles, such as crossite, have been shown to possess an M2 site considerably smaller than the M1 and M3 sites, probably two small to accomodate much ferrous iron (ref. 104-106). The eight peak fit of CR1 in Table 9 shows a suspiciously high value for the center shift of the M2 doublet, when compared with the center shifts of the M2 doublet (relative to M1 and M3) in the calcium amphiboles HB1, HB2, and HB3. (Possibly, this center shift may be characteristic of the alkali amphibole system.) Calcium amphiboles appear to have an M2 site comparable in size to that of the M1 and M3 sites (ref. 105) and the eight peak fits of HB1, 2 and 3 are more likely to be correct. Moreover, if aluminum in the mineral formulae (Table 8) of HB1, 2 and 3 is used to fill the silicon deficiency, and the remainder of the aluminum, together with all the ferric iron, is placed in the M2 site, all the M2 content of ferrous iron determined by the spectra can easily be accomodated in the M2 site. A large ferrous iron content in the M2 site of a calcium amphibole has been quoted, by X-ray methods from

another work, by Burns and Greaves (ref. 62; see also 105). Only 0.06 ferrous iron (per formula unit) at most can be so fitted into the M2 site of CR1, if all the ferric iron is on M2. For the M2 site occupancy of CR1 to be true, roughly 38 per cent of the iron on the M2 site must be ferrous, and the remainder of the ferric iron must be on other sites. (Some support for this is the width of the ferric iron lines, which may indicate occupancy of ferric iron on more than one site, rather than site multiplicity.) Because of the suspicious center shift of the M2 site (8 peaks) of CR1, and the known small size of the M2 site in crossite, it is possible that no ferrous iron exists on the M2 site of CR1, and a situation exists similar to Law's example of holmquistite. Therefore, a six peak fit of the crossite (fully constrained, all ferrous widths equal) has been included in this work for comparison (Tables 9 and 10).

In deciding the correctness of the 6 peak or 8 peak fit, one must remember that the X-ray site population cannot distinguish between ferrous and ferric iron, and that the M2 site occupancy of ferrous iron is judged upon the criterion of ionic size, a subjective judgment (except for Law's case, where there is no M2 iron). Note also that the crystal field stabilization of ferrous iron is increased by small site size. The M2 content of ferrous iron is therefore a balance between site size and crystal field effects, not site size alone.

Besides the greater width of the ferric iron lines (above), other evidence exists that the eight peak fit of CR1 may be correct. Papike and Clark (ref. 104) found by X-ray methods that in a glaucophane the iron content of M3 was roughly twice that of M1 (per site), and therefore the total iron content of both sites was about equal. This agrees with the results of the eight

peak fit of CR1 (for ferrous iron distribution only), but not for the six peak fit where the ferrous contents (per site) are roughly equal in M1 and M3 (there being two M1 sites per each M3 site). If in CR1 some ferric iron is not on the M2 site, and is evenly distributed between M1 and M3 (per site), then the X-ray results on glaucophane and the present Mossbauer results on the crossite CR1 can agree, using the eight peak fit. This would imply that ferric iron is not solely on the M2 site in glaucophane.

The value of chi-squared for the six peak fit of CR1 is 916, and for the eight peak fit it is 619. This is a far greater difference than the difference in the values of chi-squared for holmquistite by A. D. Law, which were 575 and 537 for six and eight peak fits, and this greater difference is more likely to be significant. A less constrained six peak fit of CR1 (width of outer ferrous doublet, width of ferric doublet; sine wave not constrained) in Table 8a gives chi-squared equal to 726. Additional constraints (such as other ferrous doublet width, sine wave constrained to 0.1 or less) would increase the value of chi-squared. The ferric peaks are unequal, the low velocity being about 25% greater in amplitude, which suggests a poor fit. The low value of chi-squared (619, eight peaks, full constraints, all ferrous widths equal, sine wave constrained to less than 0.1) equalizes the ferric peaks. Releasing the area constraints on the eight peak fit (except the small M2 doublet; all ferrous widths equal) results in reasonable peak equality in the doublets, which indicates a good fit.

The M1 and M3 contents of ferrous iron in the six peak fit of CR1 agree with the results of six peak fits of sodic amphiboles of Ernst and Wai (ref. 106, P. 1245). In light of the X-ray result of Papike and Clark (above), these six peak fits may not be correct, because the X-ray result (one sample) appears to show a different distribution between M1 and M3 (see previous paragraph).

Special problems in fitting also occur in cases of site multiplicity. The site multiplicity problems of pyroxenes have been partly solved (ref. 79, 107) and used in this work on the titanaugite CPX4 in its ten peak fit (Tables 9 and 10; see also section on Fitting of Mossbauer Spectra and Site Occupancy of Iron). Titanaugite CPX3 has so much calcium that the M1 site multiplicity probably does not exist (Table 8).

In pyroxenes, each M1 site shares edges with three M2 sites. If the multiplicity is assumed to be due to presence or absence of calcium on M2, with no appreciable contributions from other M1 sites, a simplistic mathematical solution may be obtained. If Me represents absence of Ca from M2 (i.e., presence of Fe, Mg, Na), then the various combinations of three M2 sites surrounding one M1 site are

$$3\,Ca,\quad 2\,Ca + Me\quad ,\qquad Ca + 2\,Me\quad ,\qquad 3\,Me.$$

The statistical distribution of these combinations is given by the terms of the binomial expansion. In this case (Ca + Me = 1.000),

$$\underset{}{(Ca+Me)^3} = \underset{(3\,Ca)}{Ca^3} + 3\,\underset{(2\,Ca+Me)}{Ca^2\,Me} + 3\,\underset{(Ca+2\,Me)}{Ca\,Me^2} + \underset{(3\,Me)}{Me^3}\quad .$$

For CPX4, Ca ≅ 0.88 and Me ≅ 0.12, therefore

$$(Ca + Me)^3 = \underset{(3\,Ca)}{0.68} + \underset{(2\,Ca+Me)}{0.28} + \underset{(Ca+2\,Me)}{0.038} + \underset{(3\,Me)}{0.0017}\quad .$$

If the (3 Ca) term (peaks) may be contained only in the inner M1 doublet (ref. 107) (Table 9, ten peak fit), then the ratio of the three Me terms (peaks) to the (3 Ca) term (peaks) is 0.39 - 0.47, by the reasoning above. The answer

in Table 9 is 0.44, from the Mossbauer spectrum of ten peaks. The good agreement between prediction and experiment may be fortuitous. If it is not fortuitous, then the site multiplicity problem of ferrous iron in CPX4 may be solved for practical purposes. The values of the C.S. and Q.S. for the two M1 doublets are similar, but not identical, to the values of Dowty and Lindsley (ref. 107) for $Fs_{.60}$.

FITTING OF THE MOSSBAUER SPECTRA AND SITE OCCUPANCY OF IRON

The purpose of this section is to describe the adjudged correct fits of the spectra and the reasons for them, and to discuss some of the problems, principles and techniques encountered.

The term , "full constraints" will mean areas and widths constrained in pairs.

A fundamental difference in necessary conditions exists between determining the site occupancy of a mineral by Mossbauer spectra, and determining the ferrous-ferric ratio. When the site occupany is determined, the resulting spectrum should be as "realistic" as possible, with each line in its proper position, with proper width and intensity. Technically, this is not a necessary condition for the determination of the ferrous-ferric ratio in most minerals (micas an exception). This is because all the ferric iron contributes to the low velocity region (envelope of lines) of the spectrum, and the ferrous iron is equally in the low velocity envelope and the high velocity envelope. Thus, when area constraints of ferrous iron are made, the ferric iron (in the low velocity envelope) is determined by difference in the low velocity envelope. Therefore, any large number of lines which give a good fit can be used for the ferrous-ferric ratio, whether they correspond to real lines or not.

The above approach was tried in this work, but was finally rejected because a spectrum of correct site occupany will also give the correct ratio.

The basic principle stated above, however, clarifies why thickness corrections to the spectra may at times be critical. The low velocity envelope

is almost inevitably the biggest, with the greatest amplitude, and will have an even greater amplitude with respect to the high velocity envelope when corrected for "thickness." The ferric iron area must be affected, even in micas where ferrous area constraints cannot be used.

The computer fits were done by a program written by Stone (ref. 35), with the option of a computer plot of the spectrum, examples of which are included in the thesis. Convergence could be greatly speeded by constraining the sine wave and channel drift in the first stage (10 iterations) or two and/or by peak separation (POSN 1. -1. constraint) in the low velocity envelope, also dropped after the first or second stage. No spectrum used the POSN constraint in the final fit.

The sine wave value was seldom allowed to be greater than 0.1%, for reasons outlined in the appendix. When it was much greater than 0.1%, the spectrum was redone, constraining the sine wave at 0.065% to 0.1%. Mirror spectra had a small sine wave value, less than 0.005%, except for Bancroft's run on HB1, which was (minus) 0.039.

Spectra with negative sine wave values were redone (GN2A, GN2B and M3) constraining the sine wave and channel drift to zero (not mirror spectra, which are both + and -).

Center shifts and quadrupole splittings were determined by 1 mil iron foil.

When area and/or width constraints were used, they were constrained to be equal. Unequal area constraints were tried (M3, ferric) but none used in the final fits.

A special technique was used for finding the area of extremely small peaks, which is outlined in this section under the titanium garnets.

I. GARNETS

GN1A (almandine)

This consists of a single, narrow, ferrous doublet of large Q.S. No ferric iron is seen, agreeing with the chemical analysis.

Three runs showed one peak or the other slightly greater in area, indicating no visible anisotropy. This also varied in some runs on the type of computer fit.

GN2A and 2B (grossular; two fractions of the same collection of garnet pieces)

These spectra are nearly the simplest ferrous-ferric spectra possible, a ferric doublet at low positive velocity, bracketed by a ferrous doublet of large quadrupole splitting. The three low velocity peaks overlap a bit, but are very distinct.

Since all the peaks at low velocity are distinct, this spectrum, along with the iron foil calibration, is a crucial test of the (low velocity) characteristics of the spectrometer. This is discussed in "Investigation of the Mossbauer Spectrometer."

The garnets show no indication of anisotropy in the doublets. They are granular and without cleavage, which preclude crystal orientation or the crystal shape effect. The only possible anisotropic effect is the Goldanski-Karayagin effect, which is not seen. All garnets were 200 + mesh when spectra were taken.

The amplitudes of the ferric peaks are only a little greater than the ferrous. In GN2A the ferric peak is consistently wide and indicates site

multiplicity. It is interesting that GN2A shows considerable optical anisotropy (common in grossular) and one wonders if the wide lines and optical anisotropy are related.

In any given run, the best answer for the ferrous-ferric ratio is the fully-constrained value. The best test of the low velocity characteristics of the spectrometer is the free or unconstrained fit. One should note that these are two different concepts, and that the value of the fully-constrained fit is often poor if the low velocity characteristics of the spectrometer are poor, which is reflected in the free fit.

Even if the low velocity characteristics are not good, the correct answer can often be obtained from the free fit by using only the two high velocity peaks. This recourse is not as reliable as an obvious good-quality spectrum.

Because the garnet spectra are so simple, whose quality can be checked, they are ideal for low versus high temperature measurements.

Site occupancy rules in these garnets appear to conform to well-established ideas,

1. All ferrous iron is in eight-fold sites.

2. All ferric iron is in octahedral sites (except for titanian garnets, which contain tetrahedral ferric iron).

This seems to be true also for GN5 and GN7, which are manganiferous garnets.

In the titanian garnets, GN3, GN4 and GN6, some evidence exists for ferrous iron on octahedral sites. See below, and especially the section on charge transfer problems in the titanian garnets.

In contrast to most minerals, the spectra of GN2A and 2B consistently showed negatively bowed baselines. In the final fits, the baseline was

constrained straight (sine wave and channel drift both zero) and full constraints used.

GN5 (Spessartite; Franklin, N. J.; ref. 52)

In this manganese garnet, the octahedra are so regular (see ref.60 , p. 811-12) that the ferric peak electric field gradient is small (Burns, unpublished, in other Mn garnets). The quadrupole splitting of the ferric peaks is consequently small. Manganese strongly effects garnet site-shape regularity.

One spectrum of this garnet shows extremely wide peaks, 0.65-0.75 mm/sec for the ferrous iron, while the ferric peaks are coalesced into one peak 0.83 mm/sec wide! The resolution is very poor. This widening and poor resolution is due to difficulties with the spectrometer, and is discussed in the section, "Investigation of the Mossbauer Spectrometer." A well-resolved spectrum of this garnet shows narrow lines and two ferric peaks.

In the final fit, the baseline was constrained straight, and full constraints used.

GN7 (Mn andradite, Franklin, N. J.)

The spectrum of this garnet is the same as GN2A and 2B, except that the ferrous peaks are much smaller.

In the best spectrometer run, the free fit shows the low velocity ferrous peak to be only 75% as great as the high velocity. Consideration of the small size of the ferrous peak, however, shows this to be a good run. The ferrous-ferric ratio was obtained from the size of the high velocity ferrous peak alone, using the free fit, which is justified because the run is of excellent quality.

The ferric peaks corroborate this, being nearly equal in area, the low velocity ferric peak being a little greater, due to "area-stealing" in the computer fit. The ferrous iron area in the fully constrained fit is too low, because of the influence of the low velocity peak (plot shows the poor fit at the high velocity peak).

Titanian Garnets (schorlomites and melanite)

These garnets show charge-transfer effects, and melanites are semi-conductors (ref. 59 , p. 835). Their spectra are often more complex than the low-titanium garnets, because the schorlomites show distinct tetrahedral ferric iron.

Due to charge transfer effects, the ferrous iron content of the spectra is much less than the chemical analysis would indicate. These ferrous peaks are so small that a special technique must be used to find their areas, because even the isolated high velocity peak is affected or overwhelmed by the large ferric peaks. A very high count is preferable to determine the small, high velocity peak.

The procedure is,

1. Spectrum of high baseline count, and large absorption.

2. Lose all channels in the spectrum, except 20-30 channels (0.38-0.57 mm/sec) on either side of the high velocity ferrous peak in a 512 channel spectrum.

3. Fix (absolutely) the width of the single peak to a reasonable value ($\cong$ 0.32 mm/sec).

4. Fix (absolutely) the sine wave function to zero.

5. Allow the channel drift to vary, to allow for the slope in the count near the peak.

6. Compare with one ferric peak, found in the usual way (include tetrahedral ferric).

The results, of course, cannot be of high accuracy, but are far superior to the usual fitting procedure.

GN3 (schorlomite, Magnet Cove, Ark.) and GN4 (schorlomite; Atlas Mtns., Africa; ref. 54)

These two schorlomites were investigated previously by R. G. Burns (ref. 50). His observation of loss of ferrous peak area due to charge transfer effects is reaffirmed. There is an alternative, however, to his claim of trivalent titanium in these garnets.

Tetrahedral ferric iron, about 7% of the total iron in both, was determined under full constraints, with all ferric widths equal, on 50 mg of these garnets in a hole of 3.8 cm^2 (i.e., at low absorption, to minimize thickness effects). When 100 mg was used, the tetrahedral ferric content was double, although this may have been coincidental. Quite likely, it is not coincidental, because (the large oct. ferric) absorption peaks at high absorption are more "squat" than at low absorption compared with a Lorenztian, and have more room under their wings to accommodate extra peak area (tetr. ferric).

In GN3, a high velocity eight-fold ferrous peak was not seen. That of GN4 was distinct on one high-count spectrum (3 million-plus counts per channel).

For possible occupancy of the octahedral sites in schorlomites and melanites by ferrous iron, see the section on the charge transfer problems. Note that no ferrous iron in typical octahedral site peak position was seen in the spectra (also true for GN6).

GN6 (melanite; Oka, Quebec)

By definition, melanites contain less than 8% by weight TiO_2 (schorlomites more).

This melanite shows charge transfer effects, and is opaque like the schorlomite. There was, however, no visual indication of tetrahedral ferric iron on the plot. The bulge due to the small low velocity (eight coord.) ferrous iron peak could be seen.

The amplitude of the high velocity ferric peak was the same as that of the low velocity ferric peak. If tetrahedral ferric iron were present, the heavy overlap on the high velocity side would cause the high velocity peak to be greater in amplitude, as it was in the schorlomites.

II. Amphiboles

Amphiboles possess complex spectra and the correct interpretations of these are still controversial.

Six-peak fits were discussed by Bancroft and Burns (ref. 61) for alkali amphiboles (see Special Problems in Computer Fitting of M. Spectra).

Crystal chemical arguments indicate that eight-peak fits are closer to the truth, assuming only one doublet for ferric iron in all types of sites, because of three distinct sites for ferrous iron (M_1, M_2 and M_3). The occupancy by iron of the M_4 site, preferred by Na, Ca and Mn is excluded in this discussion, where it is assumed that M_4 is populated only by Na, Ca and Mn. In antho-phyllites and cummingtonites, the M_4 site is populated by ferrous iron, and the ferrous peaks of the other three sites are overlapped such that one doublet of low quadrupole splitting appears for M_4, and another for the remaining three sites. These spectra are different than those of the amphiboles discussed here.

One eight-peak fit was obtained by Bancroft and Burns on a magnesioriebeckite (#7), but the position of the M2, low velocity ferrous peak lies to the low velocity side of both ferric peaks, whereas in Burns and Greaves (ref. 62), this peak lies between the ferric peaks in all their cases. The results of the present work support Burns and Greaves.

Two amphiboles used here were identical (or nearly) to two used previously. The crossite (CR1) is the identical batch used by Bancroft and Burns (#4) (J. H. Scoon, personal communication). A disagreement exists between J. H. Scoon and the author on the ferrous iron content of the crossite. A good eight-peak spectrum was obtained on the crossite in this work. The hastingsite (HB1)

of this work is nearly identical to that of Burns and Greaves (#4). The original hastingsite concentrate contained 4% anthophyllite, and the purification methods of Burns and Greaves, versus Whipple, probably differ. Whipple used a magnetic separation, which probably affected the average composition. The chemical analyses differ a little. The ferrous iron (also by J. H. Scoon) is nearly the same as the author's and the author obtains a little more total iron (as with the crossite).

The assignment of the ferrous peaks in this work is that of Burns and Greaves,

1. Outer doublet, ferrous iron in M1 position.
2. Middle doublet, ferrous iron in M3 position.
3. Inner doublet (small), ferrous iron in M2 position.

The inner doublet is small because M2 is a small site, which concentrates ferric iron and probably aluminum (ref. 61) and consequently rejects ferrous iron (see Special Problems in Computer Fitting of M. Spectra).

The site occupany of ferrous iron in the four amphiboles of this work is listed in Table 9 , (full constraints, all ferrous widths equal). The ferrous site occupancies are all for uncorrected spectra, as for all the groups of minerals. Correction by Program Mosscorr results in little change.

There is enough Na, Ca and Mn to fill all the M_4 positions in each of these amphiboles.

Of these four amphiboles, the crossite CR1 and the hastingsite HB1 are of metamorphic origin, and the two kaersutites HB2 and HB3 are volcanic. No correlation between geological origin and site occupany is evident.

The concentration of ferrous iron in the various sites (taking into account the existence of only one M3 site in the structure) shows that in three of the

four amphiboles, ferrous iron is approximately twice as concentrated in M3 as in M1. In HB1 (hastingsite), the concentrations are approximately equal. M2 has the least concentration, due to occupancy by ferric iron and aluminum (see Table 9).

The reason for the difference between HB1 and the other three is not understood. The site occupancy of HB1 agrees with the results of HB1 (#4) of Burns and Greaves. The latter also found variability in the site occupancy of various calcium amphiboles (actinolites), but found no such large M3 occupancies as in CR1, HB2, and HB3 (8 peak fits).

It may be necessary to reassign the various ferrous doublets to other sites, but whatever the correct assignment the variation of site occupancy in different amphibole samples is large.

For an interesting critique on the fitting of Mossbauer spectra, and the site occupancy of holmquistite, see Law (ref. 64).

CR1 (Crossite; Laytonville, Calif.; Bancroft and Burns #4; ref. 61)

The most reliable fit (eight peaks) was considered to be the fully constrained one, with all ferrous widths equal. The sample was finely ground, to avoid the crystal shape effect. The width of the ferric iron lines is greater than that of the ferrous, which is common and thought to be due to the overlap of the various sites occupied by ferric iron (largely M2 in this case).

Mossbauer runs on CR1 are also mentioned in the section on "Investigation of the Mossbauer Spectrometer." One half of a mirror run gave more ferric iron than the value accepted, but agreement between the two halves of the mirror was very poor, and the statistics bad, and the value was rejected.

Because of the small size of the M2 site in alkali amphiboles, it is possible that the M2 site of CR1 may contain no ferrous iron. In this case, the eight line fit of CR1 is incorrect, and an interpretation problem exists in CR1 similar to that encountered by A, D. Law in holmquistite. A thorough discussion of this problem in Law's paper and in CR1 is given near the end of the section on Special Problems in Computer Fitting of Mossbauer Spectra. A six line fit of CR1 has been included for comparison with the eight line fit in Tables 9 and 10. The value of R was little changed. The values of the sine wave and channel drift were constrained to 0.065 and 0.0 (0.085 and 1.69 for 8 lines, the channel drift free). Full constraints were used, all ferrous widths equal.

HB1 (Hastingsite; Hastings County, Ontario; ref. 102)

Fit, etc., same as CR1, except for the early ones, including one run done by Bancroft, which were not finely ground. There was never evidence of anisotropy. This is virtually identical to the analysis #13, p. 288 of Deer, Howie and Zussman (ref. 3), and Burns and Greaves #4 (ref. 62).

This Mossbauer sample contained much more iron per cm^2 than the other amphiboles, and required correction by Program Mosscorr. HB3 was also corrected.

The value of the ferrous-ferric ratio was taken from a mirror run of 512 channels done by G. M. Bancroft, When analyzed separately, the two halves of the mirror run gave ratios of 2.54 and 2.66. When analyzed as a mirror spectrum, the ratio was 2.64 (all values uncorrected). The two halves of the mirror run gave excessive values of the sine wave, 0.184 and 0.288, whereas the mirror run value was -0.039. The values of chi-squared were 259 and 274, versus the mirror value 632. The high sine wave values of the halves, when reduced to a lower value in the mirror spectrum, lead to a high value of chi-squared in the mirror spectrum. This is true also for three mirror runs by the author on HB1, HB2 and GN2B, using 1024 channels. With GN2B, the sine values of the halves were negative, and the ratio given by the mirror lay between the values of the ratio for the halves (see HB2). In these cases, the ratios given by the two halves agreed well, and the ferrous-ferric ratios for HB1 and GN2B were 2.80 and 0.495 for the mirror runs, uncorrected.

Other Mossbauer runs on HB1 are mentioned in the section on "Investigation of the Mossbauer Spectrometer."

HB2 (kaersutite; San Carlos, Ariz.; ref. 65)

Fit, etc., same as CR1, but not finely ground, > 100 mesh; no evidence of anisotropy.

This kaersutite is not as pure as HB3, and contains opaque inclusions, which are probably ilmenite.

The value of the ferrous-ferric ratio was taken from a mirror run of 1024 channels. When analyzed separately, the two halves of the mirror run gave ratios of 2.39 and 2.41. When analyzed as a mirror spectrum, the ratio was 2.49. When analyzed separately, the values for the sine wave for both halves were excessive, 0.215% and 0.220%; the mirror run was much more reasonable, -0.003%. The values of chi-squared for the separate halves were 591 and 630; for the mirror, chi-squared was 1958. As with HB1, when the high values of the sine wave for the halves were reduced to a lower value in the mirror, the value of chi-squared in the mirror was increased.

The agreement of the ratios of the halves was good (above), and the ratio of the mirror interpretation was accepted (2.49).

HB3 (kaersutite; Kakanui, N. Z.; ref. 95)

Fit, etc., same as CR1. This sample is UNusually pure, and contains no visible opaque minerals!

It was originally > 100 mesh, and then more finely ground for the Mossbauer sample. Correction by Program Mosscorr produced very little change. The values for the sine wave and channel drift were a little different for the corrected spectrum. For an exact comparison between an uncorrected and corrected spectrum, the values for the baseline, sine wave and channel drift must be constrained identical. This was not done for any of the samples.

III. Orthopyroxene

OPX1 (enstatite; Webster, N.C.; ref. 99)

This was the only orthopyroxene used, and was useful only in the development of the ferrous iron analytical technique since its analysis is difficult.

Spectra, done by James Besancon of MIT, showed no ferric iron, in agreement with the chemical analysis (98.5% ferrous iron, 1.5% ferric iron) and other results on orthopyroxenes by Mossbauer spectroscopy (Virgo and Hafner, ref. 78). On p. 206, Virgo and Hafner state that they never saw more than 1% ferric iron of the total iron in any of the orthopyroxenes investigated by them (a sampling of 37 localities).

A Mossbauer spectrum doneat 77°K showed 88% of the ferrous iron in the M2 site. The composition of OPX1 is Fs 0.11.

IV. Clinopyroxenes

The clinopyroxenes are a very complex group of minerals from the point of view of Mossbauer spectroscopy. Not only do they commonly contain significant amounts of tetrahedral ferric iron, whose line positions have been given by Hafner and Huckenholz (ref. 73), but also show an extra peak of the M1 site when there is a marked deficiency of calcium content (i.e., large M2 content of ferrous iron), as shown by Williams, Bancroft et al. (ref. 79). The M1 site shows two doublets under these conditions, when M2 is deficient in calcium (see esp. ref. 107).

Thus, under many conditions an accurate computer fit of a clinopyroxene will be a minimum of ten lines! Moreover, the ferric iron content is usually low, which makes the determination of the ferrous-ferric ratio even more difficult. Beyond this, they show a complication not even possessed by the

amphiboles, which themselves are complex, namely that all lines except two (or three in a ten-line fit) lie under the low velocity envelope and the only lines outside the low velocity envelope which can impose constraints in the low velocity region are the two resolvable (or three in a ten-line fit) ferrous lines in the high velocity envelope. The amphiboles (8 lines) have three lines in the high velocity envelope for constraints in the low velocity region, which is better control (if tetrahedral ferric iron is resolved in amphiboles, the problems will be equal, with ten lines). Thus the four ferric lines in the low velocity envelope have no external control in the high velocity region (as with most minerals) for an exceedingly complex and overlapped spectrum. This last difficulty affects the site occupancy values, but not the ferrous-ferric ratio.

Because titanaugites are relatively oxidized compared to other clinopyroxenes, they are more tractable cases for chemical and Mossbauer work. A possible disadvantage is that they are also more impure generally.

CPX1 (diopside; Farm Point, Quebec)

This diopside contains so little iron (0.36%) that a Mossbauer spectrum could barely be done. The small ferric content (0.10%) is probably partly due to a small hematite content, visible in some parts of the hand specimen.

The most salient point of the spectrum is that the M1 and M2 sites are about equally populated, showing that the calcium deficiency is very low. The spectrum was fitted to two ferrous doublets, full constraints, all widths equal. Because the ferric iron was not taken into account, the spectrum is not accurate, and could not be because of the extremely low fractional absorption (1%).

CPX2 (diopside; Orange Co., N.Y.)

This pyroxene has a high iron content, but so little ferric iron that the ferrous-ferric ratio is too high ($R \cong 12$). The accuracy of the chemical determination of the ratio begins also to break down when the ratio is high.

This specimen was therefore not used for spectra.

CPX3 (titanaugite; Oka, Quebec, ref. 96, 98)

A thorough x-ray and chemical study of titanaugite from this site has been done by Peacor (ref. 75). Its high ferric iron content is noteworthy (77% of total).

A possible serious contaminant of this mineral, as inclusions, is pyrrhotite. Area per area, in a thin section, pyrrhotite (if as thick as the section) has 570 times the reducing power of the pyroxene! This is due to the eight-electron change of the sulfide as a reducing agent, the high iron and sulfur content of the sulfide compared with the pyroxene, and the higher density of the sulfide. In the chemical preparation of this pyroxene, diluted hydrofluoric acid was used to strip away all the matrix to rid it of sulfide. In thin section, a very small amount was seen as inclusions.

The Mossbauer spectrum shows nearly equal amounts of ferrous iron in M1 and M2. Since the ferrous iron content is so low (1.38% by weight), the calcium deficiency must be very small (see microprobe analysis, Tables 5, 6 and 8; also true for Peacor's sample) and the M1 site multiplicity (see section on Special Problems in Computer Fitting of Mossbauer Spectra, and discussion of CPX4 below) should be nil. A three-doublet fit for ferrous iron (one ferric doublet) with full constraints, all ferrous widths equal, produced a dip in the high velocity peak which did not exist in the absorption counts, which is evidence against M1 site multiplicity.

Peacor states by X-ray results that the tetrahedral ferric content is nil. Whether this is true relative to the ferric iron content is another matter. (The specimen analyzed here is not the specimen of Peacor.) A computer fit with two ferric doublets, eight peaks, all ferric widths equal

and all ferrous widths equal, and full constraints, shows that the two ferric doublets have nearly the same center shift. Thus, the center shift of the outer ferric peaks does not have the same value as the center shift of tetrahedral ferric iron in ferridiopside. All ferric iron parameters are very similar for both CPX3 and CPX4. The ferric lines are very wide and the width and the center shift may represent a "smearing" of peak positions due to the heterogeneity in composition of CPX3 (hourglass zoning). Then again, the similar center shifts for the ferric doublets may be due solely to octahedral ferric site multiplicity, the ferric iron being probably on the M1 (smaller) site and subject to the same influences as ferrous iron on M1 (see ref. 107), except for the unpaired electron of ferrous iron. The latter explanation is not so likely, because CPX3 may be nearly free of M1 site multiplicity problems (see previous paragraph). The quantity of tetrahedral ferric iron represented in the spectrum is unknown. The outer ferric doublet is more intense in both CPX3 and CPX4, and CPX3 at 77° K (Table 9). The different ferrous iron site occupancies at 77°K and 295°K for CPX3 are probably due to spectrometer variability, because another run at 77° K showed approximately the same ferrous site occupancy as at 295° K.

The value of chi-squared decreased from 773 with two ferric lines, to 560 with four ferric lines. The ferric peaks narrowed from 0.63 mm/sec to 0.51 mm/sec and the sine wave decreased from 0.139% to 0.062%. With two ferric peaks, their quadrupole splitting was 0.80 mm/sec; with 4 ferric peaks, the octahedral ferric peaks had a quadrupole splitting of 0.54 mm/sec, which is far closer to the usual values.

Substantial amounts of tetrahedral ferric iron have been found by Burns, Abu-Eid and Leung in a titanaugite by electronic absorption and Mossbauer means (ref. 68).

Spectra of CPX3 were taken at 77° K, and showed a lower ferrous-ferric ratio than at 295° K (using 4 ferric peaks). This indicates that the recoil-free fraction of ferrous iron is greater than that of ferric iron in CPX3.

CPX4 (titanaugite, Crawfordjohn essexite, Gt. Britain; ref. 101)

In contrast to CPX-3, this titanaugite is a little more reduced than some titanaugites (Deer, Howie and Zussman, tables, ref. 3). Also in contrast to CPX3, there was little sulfide in the matrix, and none was seen as inclusions. Both contain magnetite as inclusions. There is no indication of magnetite in the low velocity baseline of CPX4, where one moderate-intensity magnetite line would occur.

Eight line fits with full constraints, all four ferrous widths equal and all four ferric widths equal, showed ferrous widths greater than that of the ferric. This was probably due to the site multiplicity of the M1 site (see above) which is not taken into account in an eight peak fit. The microprobe analysis (average of nine grains, nine trials) shows a significant deficiency of calcium, which could cause the multiplicity.

One spectrum of CPX4 was taken at 77°K, but the ferrous-ferric ratio was so high (ferric iron so low) that the value reflected difficulties with spectrometer. This value is included in the table of Mossbauer results at 77° and 295°K.

One should note that in neither CPX3 nor CPX4 (8 lines) do the parameters of the ferric iron lines correspond with those of ferridiopside. The only parameter of ferric iron in these two minerals which accords reasonably well with ferridiopside is the center shift of the octahedral lines in CPX3.

To eliminate (completely?) the M1 site multiplicity of CPX4, a ten line fit was obtained, constraining the sine wave and channel drift, full constraints, all ferrous widths equal and all ferric widths equal (Tables 9 and 10). Surprisingly, the ferric iron parameters (4 lines) accord with those of CPX3, which should have no M1 site multiplicity problem, but not

ferridiopside! This may be due to "smearing" of the line positions due to the great inhomogeneity of CPX3 and CPX4, which conceivably can give an effect similar to that of site multiplicity. The inhomogeneity of CPX3 and CPX4 is due to hourglass zoning, and is striking (Tables 6 and 7). It is also possible that the four ferric lines imply no tetrahedral character at all, but merely octahedral site multiplicity. Then again, the ferrous iron M1 site multiplicity of CPX4 may be imperfectly removed by the ten line fit, with a consequent distortion in the ferric line positions. However, CPX3 with no M1 site multiplicity problem (?) and much less ferrous iron gives the same ferric line positions as the ten line fit of CPX4. The problem of interpretation of the ferric lines (and perhaps the ferrous lines) in these pyroxenes is unresolved. See also the section on Special Problems in Computer Fitting of Mossbauer Spectra (esp., end of section, which deals with the ferrous site multiplicity).

The value of R_{Chem}/R_{Moss} for the ten line fit of CPX4 accords better with those of CPX3 and BAB1 than the eight line fit (Table 10). In the ten line fit of CPX4, the width of ferric lines is greater than that of ferrous lines, which is the usual relation, in contrast with the eight line fit.

V. Babingtonite

Although a heavy overlap of the low velocity peaks in this spectrum exists, the high velocity peaks are so isolated that this mineral is almost as ideal as garnets for measuring the ferrous-ferric ratio. The Mossbauer spectrum of babingtonite was first done by Burns (unpublished). It is free of titanium, but has manganese.

The structure is partly known, with one octahedral site for Fe^{+2} and one octahedral site for Fe^{+3}, and is a pyroxenoid type (ref. 80). From the narrowness of the Mossbauer lines, strictly one site for each iron ion may exist. Babingtonite is a mineral of low temperature paragenesis and may be very well ordered (ref. 81).

BAB1 (Babingtonite; Holyoke, Mass.; ref. 82)

The specimen appeared to be very pure. Originally > 100 mesh, it was ground more finely for the Mossbauer specimen.

If no anisotropy exists in this spectrum, the area of the resultant low velocity peak, due to the heavy overlap of the low velocity ferrous and ferric peaks, should equal the sum of the high velocity ferrous and ferric peaks which are isolated. In the uncorrected spectrum, the low velocity peak (two lines) is less than this sum. In the corrected spectrum, the sums are much closer to being equal, which forms a consistent picture of roughly equal doublet lines, and the efficacy of Program Mosscorr (see appendix, An Experimental Test of Program Mosscorr and Sign of the Quadrupole Splitting).

Babingtonite has a pyroxenoid structure, and the spectrum at 77°K shows shifts of line position reminiscent of pyroxenes (ref. 77). Free fits were used at both 77° and 295°K, using four lines. At 77°K, the low velocity lines

are a little more separated than at 295°K, and the resultant low velocity peak has less amplitude than at 295°K.

The ferrous-ferric ratio was obtained from the two high velocity peaks only, because of possible error from the heavy overlap of the low velocity peaks.

VI. Micas

Because of their platy habit, natural micas are nearly impossible to produce in random orientation even when mounted in sucrose. When the iron content is high, these are probably subject to the crystal shape-effect also, such as M2. The nature of the crystal shape-effect is such that it always increases the effect of the crystal preferred orientation, but does not decrease it.

The anisotropy can be reduced to a low degree quite easily by fine grinding (under acetone) and/or passing through a 200 mesh sieve, and by mounting in sucrose.

Because the area of the high velocity peaks (all ferrous) cannot equal the area of the ferrous peaks in the low velocity envelope, attempts to constrain the areas of the ferrous peaks seriously affect the ferric iron area, which is entirely in the low velocity envelope. Therefore, the ferrous peak areas were left free. However, the ferric peaks, which are all in the low velocity envelope, can often be constrained equal in area to a good approximation, especially if the ferric content is low, which is usually the case (see M2).

One mica (M1; phlogopite, Burgess, Ont.; Jakob's #1) had too low an iron content to be practical for spectra.

Eight peak fits were unsuccessful in these micas. Ferric doublets in the micas are non-centrosymmetric, the tetrahedral ferric peaks being both to the low velocity of their octahedral counterparts (ref. 83).

Synthetic micas, because of their small grain size, can be obtained in random orientation (ref. 83) and eight-peak spectra can be obtained (Burns, unpublished).

Two different octahedral sites are present in micas, which are determined by the configuration of two hydroxyl groups. There are twice as many sites in which the hydroxyl groups are trans (opposite; A sites) than those which are cis (proximal; B sites). The cis sites are larger (Robert Hazen, MIT term paper).

M2 (titanian biotite; South Sweden, Jakob's #3; ref. 88)

This mica could be fitted with only six peaks. When the ferric doublet was left unconstrained in area, the low velocity ferric peak was 50% greater than the high velocity ferric peak. This was probably unreasonable, since the ferrous peaks showed anisotropies of only 10-14% (the low velocity being more intense).

The final fit was four ferrous peaks all equal in width, and the ferric doublet fully constrained. The ferric doublet was in the octahedral position. A pronounced shoulder of octahedral ferric iron on the low velocity envelope helps control its area, which is small.

When the ferric doublet was fully constrained, both low velocity ferrous peaks were 12-13% greater than their high velocity counterparts.

This mica had the highest ferrous-ferric ratio (7.98) deemed useful of any of the mineral specimens.

M3 (Mn phlogopite; Oka, Quebec)

This mica is unusually oxidized, containing nearly equal amounts of ferrous and ferric iron, but a low iron content. Its color is also unusual, red or pink. It is very heterogeneous and sometimes hexagonally zoned with green phlogopite, and full of magnetite inclusions. Small pieces were hand-selected, free of inclusions, but some zoned material was accepted. Only about 3% of the crude mica was acceptable.

M3 was ground to 200 + mesh size under acetone for the Mossbauer spectrum.

The spectrum could be fitted with only 6 peaks; the ferric peaks were fully constrained and all ferrous widths equal. The baseline was negatively bowed when allowed to vary, so the final fit used a straight baseline (sine wave and channel drift constrained to zero).

The center shift of the ferric peaks indicates that the ferric iron is in tetrahedral sites. The microprobe and chemical analyses (Tables 8 and 10) indicate that the sum of the ions Mg, Mn, Fe^{+2} and Ti^{+4} is approximately 3.06 in the phlogopite formula. This is more than enough to force all the ferric iron onto the tetrahedral sites. The deficiency in Si and Al is approximately sufficient to accept the ferric iron in tetrahedral sites. Therefore, the ferric iron is tetrahedral in this mica for compositional reasons.

The ferric lines are very wide compared to the ferrous lines. Because this mica is very heterogeneous in composition, some compositions may allow octahedral ferric iron to exist, which could widen the ferric iron

lines, because octahedral ferric lines are in a different position.

As with M2, the low velocity ferrous peaks are more intense, the outer peak by 2% and the inner by 53%. The area constraint of the intense ferric doublet appears to entail more error in M3 than in M2, in which the ferric doublet is small. Constraining the low velocity ferric peak to be 10% greater than the high velocity peak reduced the outer low velocity ferrous peak to less area than the high velocity ferrous peak, which does not accord with the known anisotropy of ferrous iron in micas. Failure to fit octahedral ferric iron may also account for the assumed irregularities in the ferrous iron anisotropy.

Table 9

Mossbauer Parameters of Minerals

Values in mm/sec, with respect to Fe foil, in a holder of 3.8 cm^2

Mineral	$\frac{mgFe}{cm^2}$	°K	Doublet	% area	C.S.	Q.S.	Width
GN1A almandine	3.9	295	8-fold Fe^{+2}	100.0	1.29	3.54	0.28
GN2A grossular	4.8	295	8-fold Fe^{+2} oct. Ferric	36.3 63.7	1.27 0.38	3.56 0.60	0.31 0.53
GN2B grossular	4.8	77	8-fold Fe^{+2} oct. Ferric	35.8 64.2	1.33 0.44	3.55 0.58	0.32 0.38
GN2B grossular	4.8	295	8-fold Fe^{+2} oct. Ferric	33.0 67.0	1.27 0.38	3.57 0.59	0.32 0.40
GN5 spessartite	4.0	295	8-fold Fe^{+2} oct. Ferric	56.4 43.6	1.26 0.34	3.50 0.34	0.29 0.29
GN7 andradite	2.6	77	8-fold Fe^{+2} oct. Ferric	13.9 86.1	1.39 0.45	3.63 0.53	0.27 0.29
GN7 andradite	2.6	295	8-fold Fe^{+2} oct. Ferric	13.2 86.8	1.28 0.43	3.58 0.55	0.35 0.39
GN3 schorlomite	2.3	295	oct. Ferric tetr. Ferric	93.4 6.6	0.40 0.17	0.58 1.16	0.28 0.28
GN4 schorlomite	2.3 (4.6)	295	8-fold Fe^{+2} oct. Ferric tetr. Ferric	0.7 92.4 6.9	high, at 3.02 0.39 0.20	 0.57 1.28	0.28* 0.32 0.32
GN6 melanite	4.4	295	8-fold Fe^{+2} oct. Ferric	1.5 98.5	high, at 3.06 0.42	 0.60	0.41* 0.49
CR1 crossite (8 peaks)	3.4	295	M1, Fe^{+2} M2, Fe^{+2} M^3, Fe^{+2} Ferric	22.8 13.2 23.6 40.4	1.16 1.26 1.17 0.37	2.99 2.00 2.65 0.54	0.32 0.32 0.32 0.42

*Assumed.

Table 9 (cont.)

Mineral	$\frac{mg\ Fe}{cm^2}$	°K	Doublet	% area	C.S.	Q.S.	Width
HB1 hastingsite	5.0	295	M1, Fe^{+2}	33.8	1.07	2.59	0.33
			M2, Fe^{+2}	21.4	1.03	1.66	0.33
			M3, Fe^{+2}	17.4	1.04	2.22	0.33
			Ferric	27.4	0.34	0.60	0.48
HB2 kaersutite	3.2	295	M1, Fe^{+2}	24.0	1.06	2.71	0.35
			M2, Fe^{+2}	16.4	1.03	1.83	0.35
			M3, Fe^{+2}	30.9	1.04	2.30	0.35
			Ferric	28.7	0.34	0.64	0.63
HB3 kaersutite	3.3	295	M1, Fe^{+2}	31.0	1.12	2.60	0.34
			M2, Fe^{+2}	11.8	1.07	1.85	0.34
			M3, Fe^{+2}	27.2	1.10	2.23	0.34
			Ferric	30.0	0.46	0.65	0.56
HB3 kaersutite	3.3	77	M1, Fe^{+2}	31.5	1.20	2.77	0.33
			M2, Fe^{+2}	10.5	1.15	1.88	0.33
			M3, Fe^{+2}	30.7	1.18	2.39	0.33
			Ferric	27.3	0.51	0.68	0.52
CPX3 titanaugite	3.2	77	M1, Fe^{+2}	14.2	1.12	2.79	0.43
			M2, Fe^{+2}	8.6	1.13	2.19	0.43
			oct. Ferric	31.9	0.48	0.57	0.53
			"tetr." Ferric *	45.3	0.48	1.07	0.53
CPX3 titanaugite	3.2	295	M1, Fe^{+2}	10.1	0.91	2.69	0.43
			M2, Fe^{+2}	13.6	0.96	2.07	0.43
			oct. Ferric	32.4	0.38	0.53	0.51
			"tetr." Ferric *	43.9	0.34	1.05	0.51
CPX4 titanaugite (8 peaks)	3.2	295	M1, Fe^{+2}	23.7	1.15	2.37	0.44
			M2, Fe^{+2}	50.4	1.12	1.95	0.44
			oct. Ferric	13.5	0.53	0.39	0.37
			tetr. Ferric	12.4	0.39	1.12	0.37

* Parameters are unusual, and in doubt. The ferrous-ferric ratio is probably correct. For the reason, see the section on The Fitting of the Mossbauer Spectra and Site Occupancy of Iron.

Table 9 (cont.)

Mineral	$\frac{mg\ Fe}{cm^2}$	°K	Doublet	% area	C.S.	Q.S.	Width
BAB1 babingtonite	4.5	77	oct. Fe^{+2}	48.9†	1.25	2.76	0.33
			oct. Ferric	51.1†	0.45	0.84	0.31
BAB1 babingtonite	4.5	295	oct. Fe^{+2}	47.9†	1.16	2.47	0.35
			oct. Ferric	52.1†	0.43	0.80	0.32
M2 biotite	2.7	295	M1, Fe^{+2}(A)	60.3	1.13	2.51	0.38
			M2, Fe^{+2}(B)	25.6	1.11	2.06	0.38
			oct. Ferric	14.1	0.57	0.60	0.55
M3 phlogopite	2.9	295	M1, Fe^{+2}(A)	33.2	1.12	2.69	0.32
			M2, Fe^{+2}(B)	22.4	1.12	2.36	0.32
			tetr. Ferric	44.4	0.19	0.55	0.65

†From high velocity peaks only.

CR1 crossite (6 peaks)	3.4	295	M1, Fe^{+2}	41.06	1.17	2.86	0.38
			M3, Fe^{+2}	19.38	1.16	2.34	0.38
			Ferric	39.56	0.41	0.45	0.42
CPX4 titanaugite (10 peaks) Mosscorr	3.2	295	M1, Fe^{+2}	14.9	1.17	2.48	0.35
			M1, Fe^{+2}	33.9	1.15	2.07	0.35
			M2, Fe^{+2}	22.6	1.16	1.72	0.35
			oct. Ferric	11.2	0.43	0.51	0.44
			"tetr." Ferric*	17.4	0.37*	1.04*	0.44

*Like CPX3, the parameters are unusual, and the tetrahedral character of the doublet is in doubt. For the reason, see the sections on The Fitting of the Mossbauer Spectra and Site Occupancy of Iron and Special Problems in Computer Fitting of Mossbauer Spectra.

RESULTS AND DISCUSSION

Comparisons between the chemical and Mossbauer spectrum determinations of the ferrous-ferric ratio in minerals have been published by several authors (see refs., Mossbauer Spectra, vs. chemistry) mostly for micas and amphiboles.

The Mossbauer spectra sometimes give more ferric iron than the chemical methods, and sometimes less. Individual comparisons may be correct, or reflect errors in the chemistry, the Mossbauer spectra, or both. Because of the considerable difficulties with both methods, and the difficulty in judging the accuracy of either the chemistry or the Mossbauer spectrometers used by the above authors, comparisons of the results of the present work with previous works will be avoided.

A collection of computer plots of several spectra is given in a separate section. Other plots appear in isolated sections. The Mossbauer values, those corrected by Program Mosscorr, and the chemical values for the ferrous-ferric ratio appear in Table 10. Parameters of Mossbauer spectra appear in Table 9. Values at 77°K and 295°K are in Table 11. Compositions of the minerals are given in Tables 2 thru 8 and 10.

The easiest way to compare the Mossbauer and chemical ferrous-ferric ratios is to divide the chemical ratio by the Mossbauer ratio. If no charge transfer effects are active in the mineral, this ratio is equal to a simple ratio of recoil-free fractions.

$$R_{Moss} = \frac{Fe^{+2}}{Fe^{+3}} \left(\frac{f'_2}{f'_3}\right) = R_{chem} \left(\frac{f'_2}{f'_3}\right)$$

$$\left[\frac{R_{chem}}{R_{Moss}} = \frac{f'_3}{f'_2}\right] .$$

It is easiest to assume no charge transfer at first, and then discuss how it would affect the chemical ferrous-ferric ratio, that is, to estimate the true ferrous-ferric ratio in the mineral.

The simplest Mossbauer spectra known for silicate minerals containing both ferrous and ferric iron are those of the garnets, babingtonite and howieite (ref. 18). The garnets give especially good results with the spectra because the quality of a given run on the spectrometer may be criticized by equality or inequality in area of the peaks of a doublet (using the free fit, i.e., no constraints). The value of the ferrous-ferric ratio is best obtained from a fully constrained fit of a garnet spectrum with a good free fit.

The comparison between the Mossbauer and chemical results on the grossulars GN2A and GN2B, the spessartite GN5 and the manganiferous andradite GN7 shows a large and consistent difference between the two methods. If no charge transfer effects are present, the recoil-free fraction of ferric iron is 1.29 times as great as that of the eight-fold coordinated ferrous iron. The value of R_{chem} over R_{Moss} is

$$\frac{R_{chem}}{R_{Moss}} = \frac{f'_3}{f'_2} = 1.29\ (\pm 2\%) \quad .$$

This is the most precise series of comparisons in this study. The errors include all those of the chemistry, the spectra and Program Mosscorr. The value for GN7 was appreciably changed by correction by the program, from 1.22 to 1.29.

If titanium is directly involved in charge transfer in these garnets, it is by the electron exchange reaction (charge transfer of one type),

$$Ti^{+4} + Fe^{+2} \rightarrow Ti^{+3} + Fe^{+3}.$$

which increases the value of R_{chem}/R_{Moss} above the value it would have if no charge transfer occurred. This is because the reaction increases the content of ferric iron in the mineral (spectrum) versus the content for no charge transfer (i.e., the chemistry gives too much ferrous iron). Manganese can have the opposite effect by the reaction,

$$Mn^{+2} + Fe^{+3} \rightarrow Mn^{+3} + Fe^{+2} \quad .$$

The titanium content of the spessartite GN5 is undetectable by the electron microprobe and is far too low to have any effect. In GN2A, GN2B and GN7, if all the titanium were trivalent (unlikely in the extreme) the values for R_{chem} would be changed and R_{chem}/R_{Moss} would be respectively 1.10, 1.18, and 1.18, and therefore the ratio of the recoil-free fractions must be at least 1.10-1.18. Because the values of all four agree so well, the charge transfer reaction occurs little or not at all, and the ratio of the recoil-free fractions is 1.29.

The large manganese contents of GN5 and GN7, 31.46% and 10.72% MnO respectively, and the agreement of the four values of the garnets show that manganese has no charge transfer effect in garnets and all manganese (in the eight-fold site) is divalent.

Charge transfer effects involving Ti and Mn appear to be absent in these garnets, but other types of charge transfer are possible, such as

$$Fe^{+2} \rightarrow Fe^{+3} + e \qquad \text{(to a hole or band)} \quad .$$

However, none of these four garnets has the dark visual colors often associated with charge transfer, excepting perhaps the andradite GN7, and therefore charge transfer is probably insignificant.

Spectra of two of the four garnets were taken at 77°K, and correction factors derived from the simple Debye theory (see appendix, "Variation of $\frac{f'_2}{f'_3}$ with Temperature") were applied to the value of ψ_R, determined from the measurements at 295°K and 77°K. The value of ψ_R times the correction factor should be equal to R_{chem}/R_{Moss}. From the appendix,

$$\frac{Fe^{+2}}{Fe^{+3}} = R_{77}\left(\frac{1}{\psi_{77}}\right) \quad ; \qquad \frac{1}{\psi_{77}} = \frac{f'_3}{f'_2}\,(77\ K)$$

where $\frac{1}{\psi_{77}}$ is correction factor in Table 13.

$$\psi_R = \frac{\psi_{77}}{\psi_{295}} = \frac{R_{77}}{R_{295}} \quad ; \qquad \frac{Fe^{+2}}{Fe^{+3}} = R_{chem}$$

$$\frac{Fe^{+2}}{Fe^{+3}} = \psi_R\, R_{295}\left(\frac{1}{\psi_{77}}\right)$$

$$\therefore \left[\frac{\frac{Fe^{+2}}{Fe^{+3}}}{R_{295}} = \frac{R_{chem}}{R_{Moss}} = \psi_R\left(\frac{1}{\psi_{77}}\right) = \frac{f'_3}{f'_2}\,(295\,K)\right]$$

When the value of ψ_R for the two garnets GN2B and GN7 (and the kaersutite HB3) were corrected, the value was much less than the value of R_{chem}/R_{Moss} (Table 11). There are three possible explanations for the difference.

1. Low temperature did not reach 77°K.

2. Extent of charge transfer differs at 77°K and 295°K.

3. The simple Debye Theory is inadequate for silicates.

If the Debye Theory is inadequate, it must be replaced by a theory which has less temperature dependence of the recoil-free fraction.

The titanian garnets, the schorlomites GN3 and GN4, and the melanite GN6 show charge transfer effects and are discussed in the next section. The charge transfer gives rise to the high values of R_{chem}/R_{Moss} because the chemical value for ferrous iron is higher than the true content (the spectra).

Spectra of GN4 and GN6 were done at 77°K, and no qualitative changes in the spectra were observed. The ferrous-ferric ratio of GN6 varied, but this may be due to error of measurement of the small ferrous peak.

The amphiboles CR1 (crossite, a sodium amphibole), HB1 (hastingsite) and HB2 and HB3 (kaersutites) show the same relations as the garnets, but the precision is not nearly as good. This may be due to variation of recoil-free fraction or possibly charge transfer with composition, and certainly is partly due to difficulties with the spectrometer. Amphiboles give complex spectra, and it is more difficult to know when the spectrometer is functioning well. The "maximum ferric iron" rule was used for these spectra (see section on "Investigation of the Mossbauer Spectrometer") in criticizing individual runs. One spectrum of poor quality indicated that CR1 should have more ferric iron than the value accepted.

The values of R_{chem}/R_{Moss} vary from 1.13 (CR1) to 1.36 (HB1), indicating that the recoil-free fraction of ferric iron is greater. The titanium content of CR1 is so low that it can affect this value by only 1.2%. The manganese content of CR1 is high enough to change the value of R_{chem} to 1.81 if all the manganese were trivalent. If so, R_{chem}/R_{Moss} would be 1.23.

The values for the ratio Ti^{+4}/Fe^{+2} (atomic) are, for CR1 and HB1-HB3 respectively, 0.005, 0.06, 0.35 and 0.58. There is enough titanium in HB2 and HB3 to cause a large value for R_{chem}/R_{Moss}, yet these values are less than that of HB1, which has much less titanium. Allowing for some error in the Mossbauer ratios of HB2 and HB3, it is evident that the Mossbauer ratios are nevertheless independent of the titanium content. Therefore, titanium is not converted to Ti^{+3} in charge transfer reactions in these amphiboles. These amphiboles show dark colors indicative of charge transfer reactions, and it is not certain therefore if all the difference between the chemical and Mossbauer measurements can be ascribed to recoil-free fraction differences. If all the difference is due to recoil-free fraction, HB1, 2, and 3 give $f'_3/f'_2 = 1.28$.

The manganese contents of HB1 versus HB2 and HB3 are in the wrong direction, relatively, to make their values of R_{chem}/R_{Moss} agree more closely.

Two measurements at 77°K were made on HB3, and the lower ferrous-ferric ratio of the two chosen using the "maximum ferric iron" rule. As with the garnets, the two Mossbauer measurements at 77° and 295° did not account for all the difference between the Mossbauer and the chemical results. One run at 77°K was made on CR1, but it gave less ferric iron than the chemical value, and was therefore discarded.

With the pyroxenes, the titanaugites CPX3 and CPX4, and babingtonite BAB1 which has a pyroxenoid structure, the comparison of the chemical and Mossbauer ferrous-ferric ratios shows approximate equality of the two methods, in contrast to the garnets and amphiboles. The values of R_{chem}/R_{Moss} for these are respectively 0.98, 0.89, and 1.01. Due to difficulties with the spectrometer, the value for CPX4, 0.89, can be somewhat greater, but it is unlikely that the value can be greater than approximately 1.05(8 peak fit).

Enough manganese is present in these three minerals to change R_{chem} to 0.315, 2.68 and 1.06 respectively, if all the manganese were trivalent. The values of R_{chem}/R_{Moss} then become 1.04, 0.94 and 1.17. The ferrous and ferric recoil-free fractions in CPX3 and CPX4 must therefore be approximately equal, or the ferrous recoil-free fraction a little greater.

The titanaugites CPX3 and CPX4 contain enough titanium to greatly change the value of R_{chem}/R_{Moss}. However, if titanium is present as Ti^{+3}, the quantity of ferric iron is increased in the mineral. In CPX3 and CPX4, the Mossbauer spectra show more ferrous iron than in the garnets and amphiboles,

and this is in the opposite direction of the effect of titanium. Titanium therefore has little or no effect in titanaugites and is quadrivalent.

A very small amount of pyrrhotite is present as inclusions in CPX3. Area per area in a thin section, pyrrhotite is 570 times as effective as a reducing agent as the pyroxene, if it all reacts with pentavalent vanadium in the ferrous iron determination! (See the section on "Fitting of the Mossbauer Spectra and Site Occupany of Iron.") The ferrous iron content of CPX3 should therefore be lower than the chemical analysis indicates, and the value of R_{chem}/R_{Moss} lower than 0.98.

Mossbauer spectra of CPX3, CPX4 and the babingtonite were done at 77°K. The ferrous-ferric ratios of CPX3 and the babingtonite at 77°K and 295°K are nearly the same. This, and especially the chemical data, indicate that the recoil-free fractions of ferrous and ferric iron are nearly the same in the pyroxenoid structures (if manganese is not involved in charge transfer in babingtonite) and the ferrous iron recoil-free fraction perhaps even a little greater than that of ferric iron (see CPX3 at 77° and 295°K). The ratio at 77°K for CPX4 is almost certainly too high, due to difficulties with the spectrometer. Using the "maximum ferric iron" rule, one run at 295°K for CPX4 was obtained with more ferric iron than the first attempt (i.e., the accepted run). With little doubt, the same could be done for the run at 77°K also.

The values of R_{chem}/R_{Moss} are conflicting for the biotite M2 and the phlogopite M3. The value for the biotite M2 is 1.18 and for the phlogopite M3 is 0.78.

Enough titanium and manganese are present in M2 to change its value greatly. Because titanium appears to have no effect on the spectra of the

hornblendes and pyroxenes, an effect in this biotite is probably absent also. If manganese is trivalent, then R_{chem} is increased, and R_{chem}/R_{Moss} and f'_3/f'_2 are both greater than 1.18.

Like the amphiboles, M2 has dark color indicative of charge transfer, and it is not certain whether all of the value 1.18 can be attributed to greater recoil-free fraction of ferric iron.

The low value of M3 is difficult to explain. It may be due either to a high (relative) recoil-free fraction of ferrous iron, or the effect of the small amount of manganese in this mica. The amount of manganese is comparable to the amount of ferric iron.

The red color of this mica may be due either to Mn^{+3} or the ferric iron, which is in tetrahedral coordination in M3. The color is similar to that of piedmontite, which contains Mn^{+3}. It is also similar to the color of synthetic ferric orthoclase, in which the ferric iron is tetrahedral (Frank Huggins, personal communication).

In the three groups of minerals, the garnets, the amphiboles (except CR1) and the pyroxenoids (excepting perhaps the two micas, in which the ferric iron is comparable to the amount of manganese, and manganese charge transfer can affect the ferrous-ferric ratio to a large or unknown extent) the results are most precise if manganese is assumed not to be involved in charge transfer. This is beyond doubt in the garnet group, where all manganese must be divalent.

Because titanium is not involved in charge transfer in the low-titanium garnets, the amphiboles and the titanaugites, whether manganese is involved or not, the recoil-free fraction of ferrous iron in the titanaugites is equal to or a little greater than that of ferric iron. This poses a problem in the

titanaugites CPX3 and CPX4, because much of the ferric iron in these is in tetrahedral coordination and intuitively should have a greater recoil-free fraction than octahedral ferric iron, because of the small size of the tetrahedral site. The comparison of these titanaugite spectra with the chemical ferrous-ferric ratios should show the same relation as with the garnets and amphiboles, only more pronounced, but the opposite is true. This implies that the recoil-free fraction of tetrahedral ferric iron is less than that of octahedral ferric iron, or that the recoil-free fraction of ferrous iron is unusually high in titanaugites.

In the mica M3, the ferric iron is in tetrahedral coordination. If the recoil-free fraction of tetrahedral ferric iron is less than that of ferrous iron, then its low value for R_{chem}/R_{Moss} is easily explained.

An electronic absorption spectrum of M3 was done by Rateb Abu-Eid of MIT, with the plane of polarization perpendicular to the flake, having absorption in the following bands

6,800 Å	–	charge transfer (?)
5,500	–	Mn^{+3}
4,950	–	
4,500	–	both Mn^{+2} and Fe^{+3} (?)
4,250	–	Mn^{+2}
4,120	–	

with some contribution from a spin-forbidden transition in Fe^{+3} at 4,950 Å. Abu-Eid estimates that roughly one-third of the manganese is trivalent. This is roughly the correct amount to cause the observed value of R_{chem}/R_{Moss} in M3. The difficulty with M3 may thus be better explained by trivalent

manganese than by low recoil-free fraction of tetrahedral ferric iron. The trivalent manganese, a Jahn-Teller ion, is probably in the site which is most asymmetrical, probably the B site in which the two hydroxyl groups are cis to each other, which should result in a charge assymetry due to the hydrogen ions. Other electronic spectroscopic evidence exists for trivalent manganese in phlogopite (Burns, p. 58-59, ref. 1).

Table 10

Chemical and Mossbauer Results

Mineral	Total Fe (chem)%	Fe^{+2} (chem)%	$\frac{Fe^{+2}}{Fe^{+3}} = R_{chem}$	Uncorr $\frac{Fe^{+2}}{Fe^{+3}} = R_{295°}$ chi^2	Mosscorr $R_{295°}$ chi^2	R chem R_{Moss} 295° (corr)	TiO_2 (wt. %)	MnO (wt. %)
GN2A grossular	3 .062 (±0.2%)	1.278 (±0.5%)	0.716 (±1.2%)	0.570 462	0.568 490	1.26	~0.15	~0.22
GN2B grossular	4.558 (±0.2%)	1.752 (±0.3%)	0.624 (±0.8%)	0.494 582	0.484 652	1.29	~0.15	~0.22
GN5 spessartite	4.382 (±0.5%)	2.766 (±0.4%)	1.71 (±2.5%)	1.29 523	1.31 553	1.31	0.00	31.46
GN7 andradite	12.334 (±0.1%)	1.915 (±0.5%)	0.184 (±0.8%)	0.151 646	0.142 685	1.29	0.18	10.72
GN3 schorlomite	17.20 (±0.2%)	0.692 (±2.6%)	0.042 (±2.9%)	0.000† 675		v. high	~14.5*	~0.70*
GN4 schorlomite	17.64 (±0.1%)	1.632 (±1.1%)	0.102 (±1.3%)	0.0068† 707		15.0 (not corr)	~8.6*	~0.65*
GN6 melanite	16.590 (±0.3%)	0.887 (±1.0%)	0.0565 (±1.4%)	0.0150† 1556**		3.8 (not corr)	2.73	0.84

† Low value due to charge transfer.

* Values from Howie (ref. 54).

** As two peaks.

Table 10 (cont.)

Mineral	Total Fe (chem)%	Fe^{+2} (chem)%	$\frac{Fe^{+2}}{Fe^{+3}} = R_{chem}$	Uncorr $\frac{Fe^{+2}}{Fe^{+3}} = R_{295°}$ chi^2	Mosscorr $R_{295°}$ chi^2	R chem R_{Moss} 295° (corr)	TiO_2 (wt. %)	MnO (wt. %)
CR1 crossite (8 peaks)	21.682 (±0.2%)*	13.531 (±0.5%)*	1.66 (±2.0%)*	1.47 619		1.13	0.04 †	0.51 †
HB1 hastingsite	11.158 (±0.2%)	8.630 (±0.3%)	3.41 (±2.2%)	2.64 632**	2.51 910**	1.36	0.68 †	0.27 †
HB2 kaersutite	13.441 (±0.3%)	10.165 (±0.3%)	3.10 (±2.5%)	2.49 1958**		1.25	5.04	0.22
HB3 kaersutite	7.852 (±0.2%)	5.820 (±0.2%)	2.86 (±1.6%)	2.33 498	2.30 593	1.24	4.79	0.11
CPX3 titanaugite	6.048 (±0.2%)	1.384 (±0.2%)	0.297 (±0.5%)	0.310 560	0.302 587	0.98	3.96	0.13
CPX4 titanaugite (8 peaks)	6.093 (±0.3%)	4.375 (±0.5%)	2.55 (±2.9%)	2.89 533	2.86 618	0.89	2.97	0.10
BAB1 Babingtonite	17.082 (±0.1%)	8.158 (±0.3%)	0.914 (±0.8%)	0.920 554	0.909 611	1.01	0.00	0.77

† By J. H. Scoon.

* Different value than J. H. Scoon.

** Mirror spectrum, see text.

Table 10 (cont.)

Mineral	Total Fe (chem) %	Fe^{+2} (chem) %	$\frac{Fe^{+2}}{Fe^{+3}} = R_{chem}$	Uncorr $\frac{Fe^{+2}}{Fe^{+3}} = R_{295°}$ chi^2	Mosscorr $R_{295°}$ chi^2	R chem / R_{Moss} 295° (corr)	TiO_2 (wt. %)	MnO (wt. %)
M2 biotite	20.890 (±0.1%)	18.564 (±0.4%)	7.98 (±4.7%)	6.10 657	6.74 780	1.18	3.16	1.31
M3 phlogopite	3.697 (±0.1%)	1.917 (±0.8%)	1.077 (±1.9%)	1.25 546	1.38 572	0.78	0.14	1.02
CR1 crossite (6 peaks)	21.68 (±0.2%)	13.53 (±0.5%)	1.66 (±2.0%)	1.53 916		1.09	0.04†	0.51†
CPX4 Titanaugite (10 peaks)	6.093 (±0.3%)	4.375 (±0.5%)	2.55 (±2.9%)		2.50 531	1.02	2.97	0.10

Table 10 (cont.)

Minerals Unimportant for Spectra

Mineral	Total Fe (chem) %	Fe^{+2} (chem) %	$\frac{Fe^{+2}}{Fe^{+3}}$ (= R_{chem})
GN1A almandine	26.34 (±0.4%)	26.11 (±0.3%)	~110
OPX1 enstatite	6.043 (±0.3%)	5.952 (±0.4%)	~ 65
CPX1* diopside	0.362 (±0.4%)	0.262 (0.6%)	2.61 (±3.8%)
CPX2† diopside	10.5 (± ?)	9.67 (± ?)	11.6 (± ?)
M1 phlogopite	0.883 (±1.2%)	0.707 (±0.1%)	4.02 (±6.6%)

*Hematite in sample.

†Approximate values.

Table 11

Mossbauer Spectra at 77°K and 295°K

Mineral (mg Fe/cm^2)	No. peaks	$R_{77°}$ chi^2	$R_{295°}$ chi^2	ψ_R*	Corr.* $\left(\frac{1}{\psi_{77}}\right)$	ψ_R^* (corrected)	$\frac{R_{chem}}{R_{295°}}$
GN2B (4.8)	4	0.557 561	0.494 582	1.128	1.05	1.18	1.26
GN2B Mosscorr	4	0.547 618	0.484 652	1.130	1.05	1.19	1.29
GN7 (2.6)	4	0.161 507	0.151 646	1.066	1.03	1.10	1.22
GN7 Mosscorr	4	0.149 544	0.142 685	1.049	1.02	1.07	1.29
GN6 (4.4)	3	0.025 826**	0.015 1556**				3.8
HB3 (3.3)	8	2.66 559	2.33 498	1.142	1.05	1.20	1.23
HB3 Mosscorr	8	2.62 642	2.30 593	1.139	1.05	1.20	1.24
CPX3 (3.2)	8	0.295 502	0.310 560	0.952	0.98	0.93	0.96
CPX4 (3.2)	8	3.41† 569	2.89 533	1.180†	1.07	1.26†	0.88
BAB1 (4.5)	4	0.956 520	0.920 554	1.039	1.02	1.06	0.99
BAB1 Mosscorr	4	0.953 619	0.909 611	1.048	1.02	1.07	1.01

†Spectrometer trouble, value falsely high.

*See appendix for theory.

**As two peaks.

JAKOB'S TITANIAN MICAS

In 1937, J. Jakob (ref. 88) published analyses of three titan ian micas which he claimed contained trivalent titanium. His basis for his claim was that these micas contained more reducing power than the total iron could account for. The excess he attributed to trivalent titanium.

With the help of the Natural History Museums of Bern and Vienna, two of Jakob's micas were procured for this work. The phlogopite from Burgess, Ontario (M1; Jakob's #1) is the same specimen number (Vienna, H .3752) as that used by Jakob. The biotite (M2; Jakob's #3) from Sweden (Bern) is possibly not the same specimen number. Jakob's phlogopite #2 contains so little iron that accuracy would be minimal, and was not procured.

The results of this work show that Jakob's analytical chemistry was in error. Both micas are rather reduced, but in neither case does the reducing power (Fe^{+2}) exceed the total iron. A large error occurs in Jakob's #1 (Burgess phlogopite; M1). In this mica, Jakob recovered only 26% of the total iron content (0.23% versus 0.88%)! This was probably due to failure to dissolve the large amount of MgF_2 formed by the HF attack on the phlogopite, much iron being occluded in it. The analysis of Jakob's #1 appears in Deer, Howie and Zussman (ref. 3), p. 46, Anal. #2 and is incorrect.

CHARGE-TRANSFER IN TITANIAN GARNETS

Compared to the ferrous iron determined by chemical means, the spectra of the three titanian garnets studied show much less ferrous iron. Two of these, of high enough titanium content to be classified as schorlomite, have been studied previously by Burns (ref. 50) using samples of nearly the same composition as those schorlomites in Howie and Wooley (ref. 54). The results of the present study agree with Burn's data. The third garnet, a melanite (less titanium) from Oka, Quebec, also shows a deficiency of ferrous iron in its spectrum.

The ferrous iron cannot be due to mineral impurities, since these contain octahedral ferrous iron only, and no octahedral ferrous iron lines appear in the spectra. The only ferrous lines which sometimes appear are those of ferrous iron in the garnet eight-fold site.

Charge transfer has been invoked to explain the loss of ferrous iron in the spectra, according to the reaction

$$Fe^{+2} + Ti^{4} \rightarrow Fe^{+3} + Ti^{+3} \quad .$$

The information from both the spectra and the chemical analyses indicates considerable Ti^{+3} content (0.6%−1.5%, by weight).

This seems reasonable until one considers the energy of Ti^{+3} as a reducing agent. In oxides, Ti^{+4} can be reduced to Ti^{+3} only with purified hydrogen, or stronger reducing agents at high temperature. Under these conditions, all ferric iron is reduced to ferrous and ferrous iron may be reduced to the metal unless it is in a dilute solid solution, which can stabilize it. The coexistence of Fe^{+3} and Ti^{+3} is therefore thermodynamically unsound.

The crystal field stabilization of the above reaction is far too small to effect the direction of the reaction.

An equivalent way of expressing the same result is to calculate the Gibbs Free Energy of the reaction

$$FeO_{1.5} + TiO_{1.5} \rightarrow FeO + TiO_2 \quad .$$

According to the Janaf tables (1966-7), the Gibbs free energies of the oxides by formation from the elements are

$Fe_2O_3(298°) = -177.7$ kcal, (-88.9×2)

$Ti_2O_3(298°) = -342.8$ $\quad (-171.4 \times 2)$

$FeO\ (298°) = -60.1$

$TiO_2\ (298°) = -212.6$ (rutile) .

$\Delta\mathring{G}$ (295 K) for the above reaction is -12,400 cal. At equilibrium (295°K),

$$\Delta G = 0 = \Delta\mathring{G} + RT\ \ell n\ K$$

and

$$\log_{10} K = 9.2 \quad \text{or,} \quad K = \frac{a_{FeO}\ a_{TiO_2}}{a_{FeO_{1.5}}\ a_{TiO_{1.5}}} = 10^{9.2} \quad .$$

Therefore, if all four oxides (ions) are to be present in comparable amounts in a silicate, the activity coefficients for $FeO_{1.5}$ and $TiO_{1.5}$ must be reduced 3×10^4 times relative to the activity coefficients of FeO and TiO_2. The relative change of activity coefficient is exceedingly large and very unlikely. Because the reaction involves only a simple electron transfer between iron and titanium, the reaction is not "frozen in" at 295°K, but can procede unhindered to equilibrium.

The incompatability of much FeO in a silicate with comparable Ti_2O_3 and TiO_2 contents is shown by the composition of the Ti^{+3} fassaite from the Allende Meteorite (Dowty and Clark, ref. 71). This pyroxene contains no detectable iron, and the chondrule containing it posseses very little (ref. 70). The strongly reducing conditions that produced the Ti^{+3} content eliminated a possible large iron content of the pyroxene by reduction of ferrous iron to metal. The chondrule shows signs of a "magmatic" sequence of crystallization of its minerals which accounts for the separation of the minerals from the iron, which has a very high cosmic abundance and must have been present originally.

High Ti^{+3} contents in minerals therefore appear to be compatible with low (ferrous) iron content. Terrestrial minerals containing ferric iron must contain a very small concentration of Ti^{+3}.

The mineral ilmenite is known to be composed of Fe^{+2} and Ti^{+4}, not Fe^{+3} and Ti^{+3}, by the nature of its magnetic properties (see references on ilmenite).

The mineral neptunite

$$Li\,Na_2\,K\,(Fe^{+2}, Mg, Mn)_2\,(TiO)_2\,[Si_8O_{22}]$$

possesses a structure in which all octahedra are joined by edges, with all the iron and the large titanium content in these sites. The edge-sharing facilitates charge transfer of d_{xy} electrons, and neptunite has a favorable chance of containing both trivalent titanium and trivalent iron. The Mossbauer spectrum, however, contains no ferric lines. If the manganese is not involved in charge transfer (all Mn is divalent), then all the titanium in neptunite is quadrivalent (see references on neptunite).

From consideration of electronic spectroscopic evidence in the literature, Dowty (1971, ref. 51) concluded that there was no such evidence for the presence of trivalent titanium in garnets. In a titanaugite, a line thought to be due to Ti^{+3} has been shown to be due to Fe^{+3} (Manning and Nickel, 1969, ref. 74) at 22,000 cm^{-1} (4,500 Å). The latter claim a Ti^{+3} transition in titanaugite in a band at 19,000 cm^{-1}, but Dowty contests the assignment of this band in garnets to Ti^{+3}.

In the kaersutites and titanaugites, the titanium is not converted to Ti^{+3} by charge transfer (except perhaps to a small degree) as described in the Results and Discussion in the present work, and is quadrivalent.

The small ferrous iron content of the Mossbauer spectra of melanites and schorlomites, compared to the chemical value for the ferrous iron (reducing power) is therefore very difficult to explain. If reducing agents other than ferrous iron (such as V^{+3} or Mo^{+3}) were present, then the result is easily explained, but none have been detected in these garnets. Trivalent titanium is ruled out because of the arguments above.

The chemical composition tables of Howie and Wooley (ref. 54) for melanites and schorlomites show that much of the ferrous iron (determined by chemical means) cannot fit in the 8-fold calcium sites because the calcium deficiency is not great enough. Therefore, considerable ferrous iron (in the chemical, "formal", sense) must be present on the octahedral or tetrahedral sites.

A possible clue to a solution to this problem has been offered by Moore and White (1971, p. 835; ref. 59) who found that whereas andradite is an insulator, melanite garnet is a semiconductor. The disappearance of much

of the ferrous iron from the spectra may thus be due to the different electrical properties of the structure, possibly due to a charge transfer reaction such as

$$Fe^{+2} \rightarrow Fe^{+3} + e(\text{to a hole or band}) \quad .$$

The physics of this effect may well be worthy of the efforts of a solid-state physicist.

APPENDIX

INTRODUCTION

When Mossbauer spectra are to be used for quantitative purposes, many details need to be clarified and/or put on a quantitative basis. This is the purpose of this appendix.

Much of this appendix is the result of well-established theory. The crystal shape effect has not yet been demonstrated experimentally.

TWO MÖSSBAUER ABSORPTION MODELS

When Mossbauer spectroscopy is performed as absorption spectroscopy, which is usually the case, the physical model of the absorber must be described so that the amounts of the various radiations passing through the absorber can be quantified.

One absorber model can be accurately described as the layer model. This consists of a solid piece of one absorber material. The iron foil used to calibrate the spectrometer conforms to this model. In this model, the 14.4 kev radiation (both resonant and non-resonant) and the 122 kev radiation from the source have different absorption coefficients, but the relative amounts of each are simply related after absorption.

The second absorber model can be described as the cylinder model for simple mathematical purposes. It consists of two or more materials present as discrete solid areas of each in the absorber field. The usual finely-ground mineral sample mounted in sugar conforms partly to this model. The ideal cylinder model is as diagrammed,

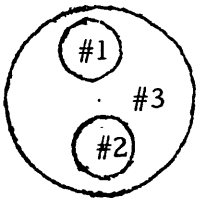

where #1 and #2 are cylinders of two different minerals and #3 is solid sugar. Each cylinder has its own particular absorption coefficients for each radiation, and can be simply treated by the layer model.

In practice, as with sugar-mounted minerals, the working model is a mixture of overlapping layers, and spaces of sugar free of mineral which are of

the cylinder model. The above models are over-simplifications which show phenomena to be expected in practice. (see Bowman, et. al., ref.28)

Where radiation passes around mineral grains and through sugar only, the sugar areas can be thought of as holes in the sample.

SYMBOLS

I_R = intensity of resonant 14.4 kev gamma rays in absorber from source (counts/cm^2)

I_N = intensity of non-resonant gamma rays ($\cong$ 14.4 kev) in absorber from source (counts/cm^2)

I_S = intensity of other radiation from source, which is countable, in absorber, not 14.4 kev (counts/cm^2). This is largely 122 kev.

I_0 = total intensity of radiation incident on absorber (counts/cm^2)

I_{0R} = as I_0, but only for resonant radiation

I_E = radiation at any value of σ (counts/cm^2), passed to counter (or in absorber) $I_E = I_R + I_N + I_S$

I_{10}, I_{20} and I_{30} = total intensity of radiation incident on absorbers mineral #1, mineral #2 and sugar #3 (counts/cm^2)

$I_0 = I_{10} = I_{20} = I_{30}$

I_1 (etc.) = total radiation from #1, #2 and #3 passed to counter (counts) at any value of σ_1 and σ_2

B = I when no resonance occurs ($\sigma_1 = \sigma_2 = 0$), baseline (counts)

B_E = I_E when no resonance occurs ($\sigma = 0$), baseline (counts/cm^2)

R = absorbance peak height (depth) (counts)

R_E = absorbance peak height (counts/cm^2)

Q = area in cm^2

F = fractional absorption = $\frac{R}{B}$ or $\frac{R_E}{B_E}$, the apparent depth of the absorption curve

{#1} etc. = sum of exponentials for any value of σ_1, (terms with σ, k_{RN}, k_N and k_S) in cylinder model

$\{\#1b\}$ etc = sum of exponentials when $\sigma_1 = 0$ (baseline) in cylinder model

n_R, n_N, n_S = fractions of I_0 of resonant, non-resonant (14.4 kev) and other radiation (S) such as 122 kev.

k_{RN}, k_N, k_S = absorption constants as above (cm^{-1}). k_{RN} is for absorption for resonant radiation by non-resonant means

f = recoil-free fraction of source (= 0.66 for Pd source)

f' = recoil-free fraction of absorber

W' = number of Fe^{57} atoms/cm^3

W = number of Fe^{57} atoms/cm^2

t = absorber linear thickness (cm)

T = absorber thickness (dimensionless)

$$T = \sigma f' W$$

σ = Fe^{57} resonant nuclear cross-section (cm^2) = $\sigma_0 \frac{\Gamma^2}{(2S)^2 + \Gamma^2}$

σ_0 = σ at full resonance (max)

$\overline{\Gamma}$ = natural line width of source or absorber (in energy, cm/sec or channels)

Γ = line width of absorbance curve (ideally $2\overline{\Gamma}$)

S = distance from center of Lorentzian curve.

ABSORPTION EQUATION, LAYER MODEL

In the following treatments, the resonant absorption is expressed in an over-simplified way. The coefficient of absorption used is $\sigma f' W = T$ and the fraction of resonant radiation absorbed is expressed as $(1 - e^{-T})$. In reality, the absorption is an integral of $(1 - e^{-T})$ combined (as a convolution) with a function which represents the source line shape. This function (the integral) expressed as an approximation, is used to correct amplitudes in Program Mosscorr.

In each material, each radiation has its own absorption coefficient and its intensity must be integrated separately from the others as it passes through the absorber.

The differential expressions for absorption of each radiation type (R, resonant 14.4 kev; N, non-resonant 14.4 kev; and S, other countable radiation) are

$$dI_R = -I_R(\sigma f' W' + k_{RN})\, dt$$

$$dI_N = -I_N\, k_N\, dt$$

$$dI_S = -I_S\, k_S\, dt$$

where dI_R contains both resonant and non-resonant terms. t is the linear thickness. Therefore

$$\frac{dI_R}{I_R} = -(\sigma f' W' + k_{RN})\, dt$$

and

$$\frac{I_R}{I_{0R}} = e^{-(\sigma f' W' t + k_{RN} t)} ,$$

where $I_{0R} = n_R I_0$. n_R is the fraction of the total countable radiation which is resonant. Note that

$$n_R + n_N + n_S = 1 .$$

From above,

$$I_R = n_R I_0 \, e^{-(\sigma f' W' t + k_{RN} t)} ,$$

Similarly,

$$I_N = n_N I_0 \, e^{-k_N t}$$

$$I_S = n_S I_0 \, e^{-k_S t}$$

and

$$I_E = I_R + I_N + I_S$$

by definition. I_E is the total radiation passed to the counter. B_E is the baseline count.

$$I_E = I_0 \left\{ n_R \, e^{-(\sigma f' W' t + k_{RN} t)} + n_N \, e^{-k_N t} + n_S \, e^{-k_S t} \right\}$$

$$B_E = I_0 \left\{ n_R \, e^{-k_{RN} t} + n_N \, e^{-k_N t} + n_S \, e^{-k_S t} \right\} \quad \text{when } \sigma = 0$$

These two are the basic equations for all derivations (in counts/cm^2).

All the above equations are standard for absorption physics.

Note that I_E, I_R, I_N and I_S have become intensities <u>after</u> passage through the absorber. B_E is the baseline count (the maximum) which has no resonant absorption (all in counts/cm^2).

The depth of the absorption curve is the difference between the count I_E and the baseline count B_E

$$R_E = B_E - I_E \qquad \text{(depth of curve, counts/cm}^2\text{)}$$

$$= I_0 \left\{ n_R e^{-k_{RN}t} - n_R e^{-\sigma f' W' t} e^{-k_{RN}t} \right\}$$

$$= I_0 n_R e^{-k_{RN}t} \left(1 - e^{-\sigma f' W' t} \right) .$$

By definition,

$$W't = W \qquad (Fe^{57} \text{ atoms/cm}^2)$$

and

$$T = \sigma f' W .$$

Therefore, the fractional absorption F is

$$F = \frac{R_E}{B_E} = \frac{(1 - e^{-T})}{\left(1 + \frac{n_N}{n_R} e^{-(k_N - k_{RN})t} + \frac{n_S}{n_R} e^{-(k_S - k_{RN})t} \right)} .$$

Because the resonant and non-resonant 14.4 kev radiations are almost exactly equal in energy

$$k_N = k_{RN} ,$$

$$\left[F = \frac{(1 - e^{-T})}{\left(1 + \frac{n_N}{n_R} + \frac{n_S}{n_R} e^{-(k_S - k_{RN})t}\right)} \right]$$

If $n_S = 0$ (counter is gated extremely well, counting no 122 kev or other radiation), then

$$n_R + n_N = 1 \quad .$$

and

$$F = \frac{R_E}{B_E} = n_R (1 - e^{-T}) \quad .$$

In this case, $n_R = f$ (recoil-free fraction of the source) and

$$\left[F = f(1 - e^{-T}) \cong f T \left(1 - \frac{T}{2}\right) \right] \quad .$$

This is a form quoted in the literature. For a palladium source, $f = 0.66$.

One should note that the exponentials are always positive, and that the terms in the denominator are always positive in the unsimplified form.

If the 122 kev radiation from the source did not exist (or the counter is perfectly gated), then $n_S = 0$ and the simple relation is valid. In practice $n_S \neq 0$ and value of the fractional absorption F must be less than the ideal value given by the simple equation.

In the cylinder model, there is an additional reason why F should be less than its ideal value.

The actual fractional absorption observed in an Fe^{57} spectrum is smaller by a factor of 7 to 40 in the spectra than the value of the thickness T. For an

explanation of this great difference, and the factors involved, see the section on the Absorption Amplitude, except for the effects of the cylinder model which follow.

ABSORPTION EQUATION; CYLINDER MODEL

It is useful to include two minerals and the sugar matrix in the cylinder model. The number 3 refers to the sugar.

For each mineral and the sugar, the radiation passed to the counter is (counts/cm^2)

$$I_1 = I_{10}\{\#1\}$$

$$= I_{10}\left\{n_R e^{-\sigma_1 f_1' W_1' t_1} e^{-k_{RN_1} t_1} + n_N e^{-k_{N_1} t_1} + n_S e^{-k_{S_1} t_1}\right\}$$

$I_2 = I_{20}\{\#2\}$, similar to #1, but with subscripts 2 .

$$I_3 = I_{30}\{\#3\}$$

$$= I_{30}\left\{n_R e^{-k_{RN_3} t_3} + n_N e^{-k_{N_3} t_3} + n_S e^{-k_{S_3} t_3}\right\}$$

and

$$I_{10} = I_{20} = I_{30} = I_0$$

also,

$$I = Q_1 I_1 + Q_2 I_2 + Q_3 I_3$$

where Q is area in cm^2; I is in counts. Therefore,

$$I = I_0 [Q_1\{\#1\} + Q_2\{\#2\} + Q_3\{\#3\}]$$

$$B = I_0 [Q_1\{\#1b\} + Q_2\{\#2b\} + Q_3\{\#3\}]$$

where b refers to the baseline value. B and I are in counts, not counts/cm^2, because I_1 (counts/cm^2) has been multiplied by area (cm^2).

The peak height R is

$$R = B - I = I_0 \left[Q_1 n_R e^{-k_{RN_1} t_1} \left(1 - e^{-T_1}\right) + Q_2 n_R e^{-k_{RN_2} t_2} \left(1 - e^{-T_2}\right) \right]$$

$$\left[F = \frac{R}{B} = \frac{R}{Q_1\left(n_R e^{-k_{RN_1} t_1} + n_N e^{-k_{N_1} t_1} + n_S e^{-k_{S_1} t_1}\right) + Q_2(\quad) + Q_3(\quad)} \right].$$

The terms next to Q_2 and Q_3 are similar to that of Q_1.

The fractional absorption for either mineral in the cylinder model must be less than the layer model because of the terms for the other mineral and the sugar in the denominator. The sugar constitutes a "hole" in the sample which lets radiation through which cannot undergo resonant absorption. This radiation contributes to the background and lowers the fractional absorption.

More important, the relative value of amounts of iron represented by absorptions, by two different minerals mixed physically, is very difficult to obtain. This is because Q_1 and Q_2 (the areas) are difficult to determine, and

$$k_{RN_1} t_1 \neq k_{RN_2} t_2$$

in the expression for R. This fact is not generally appreciated.

Intuitively this fact can be understood by imagining that mineral #2 is nearly opaque to the 14.4 kev resonant radiation, due to non-resonant absorption. If so, then almost no radiation will reach the counter from #2 and almost no resonant absorption detected. Almost all the resonant absorption at any

velocity will be due to mineral #1. A quantitative comparison between the two minerals cannot therefore be made.

TOTAL AREA OF A DOUBLET AND RELATIVE RECOIL-FREE FRACTIONS

The chance of an Fe^{57} nucleus interacting with a resonant gamma ray depends upon the state of polarization of the gamma ray and the angle the incoming gamma ray makes with the electric field gradient (efg) at the nucleus. The state of polarization of the gamma ray determines whether the nucleus will make the transition

$$m = \frac{1}{2} \rightarrow m = \frac{3}{2} \text{ (excited) or } m = \frac{1}{2} \rightarrow m = \frac{1}{2} \text{ (excited)} \quad .$$

The first gamma ray is fully circularly polarized while the second is $\frac{2}{3}$ linearly polarized and $\frac{1}{2}$ circularly polarized. Each of these has its own probability of interaction with the nucleus, which depends on the angle θ of the incoming gamma ray with the efg at the nucleus. (ref. 2 , p. 98)

The probability functions are, including the recoil-free fraction at the angle θ (ref. 2 , p. 71) ~~(i.e., σ_θ varies with θ)~~ ERW

$$\begin{cases} \frac{3}{2}(1 + \cos^2\theta)\, f' \\ \frac{1}{2} \rightarrow \frac{3}{2} \text{ (ex.)} \end{cases} \quad \text{and} \quad \begin{cases} \left(1 + \frac{3}{2}\sin^2\theta\right) f' \\ \frac{1}{2} \rightarrow \frac{1}{2} \text{ (ex.)} \end{cases} \quad .$$

The $\frac{1}{2} \rightarrow \frac{3}{2}$ (ex.) transition gives rise to one peak of the doublet and the $\frac{1}{2} \rightarrow \frac{1}{2}$ (ex.) to the other peak.

The total line strength at angle θ that the iron nucleus (understood to be of <u>one</u> valence at <u>one</u> type of site) exhibits is the sum of the <u>two</u> transition probabilities (<u>both</u> lines) times the recoil-free fraction

$$\frac{3}{2}(1+\cos^2\theta)\,f' + \left(1+\frac{3}{2}\sin^2\theta\right) f' = 4f'$$

(i.e., for the doublet) which is a constant, except for f'.

The total line strength for all directions is the spherical integral of the above. Using spherical coordinate angles, one of which is the conic angle θ above, we find that f' is a function of both these angles (α and θ) because the iron nucleus' vibration, and therefore f', is anisotropic. (Note that the spherical integral is applicable only where there is true random orientation of crystals in the Mössbauer absorber.) The gamma ray transition probability is a function only of θ, which has conic symmetry, the axis of which is the efg.

The total (intrinsic) line strength therefore is a spherical double integral,

$$\int_{\theta=0}^{\theta=\pi}\int_{\alpha=0}^{\alpha=2\pi} 2\pi \sin\theta \left[\frac{3}{2}(1+\cos^2\theta) + 1+\frac{3}{2}\sin^2\theta\right] f'\, d\alpha\, d\theta$$

$$= 8\pi \int_{\theta=0}^{\theta=\pi}\int_{\alpha=0}^{\alpha=2\pi} \sin\theta\, f'\, d\alpha\, d\theta = 8\pi\, f' \text{ (effective)}$$

$$= f' \text{ (effective, normalized)} \quad .$$

This integral cannot yet be evaluated because of lack of knowledge of the angular dependence of f'.

For two valences of iron, each in one particular site, the relative intrinsic line strength, ψ, is (for ferrous and ferric iron)

$$\psi = \frac{f_2' \text{ (effective)}}{f_3' \text{ (effective)}} \quad .$$

Since the ratio of these integrals in different minerals cannot be exactly the same except by chance, ψ must be expected to vary somewhat from mineral to mineral. Whether this variation is large enough to affect the practical results is a moot question.

For a non-random (preferentially oriented) Mössbauer absorber, similar arguments hold depending upon the type and degree of orientation, because f' depends upon the angles α and θ, and ψ can vary with orientation.

VARIATION OF $\psi \left(= \frac{f'_2}{f'_3}\right)$ WITH TEMPERATURE

The theory of variation of recoil-free fraction with temperature uses the concept of the Debye, or characteristic, temperature. For the Mössbauer effect this is not the same value as the Debye temperature, because the characteristic frequency for the Mössbauer effect is not the same as for the specific heat.

The most complex case that can be treated mathematically is that for a cubic, monatomic solid. In the present work, this is equivalent to an iron-57 atom with iron ligands. Because silicate minerals seldom have cubic sites, and the ligands are oxygen, one must be ready to criticize the use of this simplified theory in silicates.

The result of the theory is the relation

$$f'(T) = \exp - \frac{6E_R}{k\theta_D}\left[\frac{1}{4} + \left(\frac{T}{\theta_D}\right)^2 \int_0^{\frac{\theta}{T}} \frac{t\,dt}{e^t - 1}\right]$$

There are simplified expressions of this for high and low temperatures (Gruverman, vol. 2, p. 8-9, ref. 4 ; there is a misprint in equation 7a).

Another way of expressing the above integral is by the table of A. H. Muir (ref. 40). Muir's computations may be used when θ (the Debye temperature) is unknown by recasting his data into a different form. Muir presents the data in the form

$$f' = \exp\left[\frac{-E_R}{\theta} R_Z\right] \quad , \qquad E_R = 1.94 \times 10^{-3} \text{ ev} = \text{recoil energy}$$

where R_Z is tabulated relative to $\frac{\theta}{T}$ (Table 12). The more convenient form is to relate R_Z to $\frac{T}{\theta}$ times a correction factor. The form is

$$R_Z = 7.15 \times 10^4 \left(\frac{T}{\theta}\right) (\text{corr})$$

so that

$$f' = \exp\left[-\frac{E_R T}{\theta^2} (7.15 \times 10^4) (\text{corr})\right] = \exp\left[-139 \frac{T}{\theta^2} (\text{corr})\right]$$

Table 12 lists Muir's form and the new form.

Within limited ranges, the correction factor (corr) can be related to $\frac{\theta}{T}$ with good accuracy. For instance, if T = 77 °K and 450° > θ > 250° (allowing for the ranges of both θ_2 and θ_3 for ferrous and ferric iron) then the range of $\frac{T}{\theta}$ is 0.17-0.31. In this range,

$$\text{corr} = \left[\frac{\theta}{T} - 4.2\right] (0.18) + 1.41 = 0.18 \frac{\theta}{T} + 0.65$$

An expression for ψ can be derived from this, where

$$f' = \exp\left[(-139)\left(\frac{k_1}{\theta} + \frac{k_2 T}{\theta^2}\right)\right] .$$

The higher the value of the Debye temperature, the higher the value of the recoil-free fraction becomes.

In order to use this form, one must have an estimate of the value of θ. Estimates for ferrous and ferric iron in garnets have been made by Russian workers (ref. 56-58). For ferric iron in the octahedral site, estimates

Table 12

$\frac{\theta}{T}$	$\frac{T}{\theta}$	$\frac{T}{\theta} \times 7.15$	R_Z	Corr.
1.0	1.0	7.15	7.15 ($\times 10^4$)	1.00
1.5	0.67	4.80	4.93	1.03
2.0	0.50	3.58	3.85	1.07
2.5	0.40	2.86	3.24	1.13
3.0	0.333	2.38	2.86	1.20
3.5	0.286	2.04	2.60	1.27
4.0	0.25	1.79	2.42	1.35
4.5	0.222	1.59	2.29	1.44
5.0	0.200	1.43	2.19	1.53
5.5	0.182	1.30	2.11	1.62
6.0	0.1666	1.19	2.06	1.73
6.5	0.154	1.10	2.01	1.83
7.0	0.143	1.023	1.97	1.92
7.5	0.133	0.953	1.94	2.04
8.0	0.125	0.894	1.92	2.15
8.5	0.1178	0.842	1.90	2.26
9.0	0.111	0.795	1.88	2.36
9.5	0.1052	0.753	1.87	2.48
10.0	0.10	0.715	1.86	2.60

are $f_3' \cong 0.82$ at R. T. (θ_3 = 460 K) and θ_3 = 400-460 K. For ferrous iron in the eight-fold site, $f_2' \cong 0.78$ at R. T. (θ_2 = 410 K) and θ_2 = 340-410. For tetrahedral ferric iron, $f_3'(\text{tetr}) \cong 0.88$ at R. T. (θ_3 tetr = 585 K) and $\theta_3(\text{tetr})$ = 550-585 K. (Room temperature has been assumed to be 295 K.) The Russian values are uncertain because their values for θ and the corresponding values for f' do not satisfy the mathematical relation between them. The Russian values for θ are the lower of the two values stated. The higher value of θ accords with their value for f', by Muir's form of the equation.

As the temperature is lowered to 77 °K, the ferrous-ferric ratio determined by Mössbauer spectra increases if $\theta_3 > \theta_2$ ($f_3' > f_2'$), where the subscript 3 refers to ferric iron and 2 to ferrous iron. In addition, both f_3' and f_2' approach unity, and the Mössbauer ratio is closest in value to that it would have if $f_3' = f_2'$.

If one is to correct the Mössbauer ratio to the value it would have if $f_3' = f_2'$, one should correct the low temperature ratio because it is closest to this value and the correction factor is least. In doing this, there are two unknown variables, θ_3 and θ_2. One variable can be eliminated by using the measurement of ψ_R (see below). This leaves one unknown variable in the equations, which is chosen to be θ_2.

In order to calculate the correction factor at 77 °K, one uses the ratio of $\psi(= f_2'/f_3')$ taken at 77 °K and 295 °K, which is ψ_R.

$$\psi_R = \frac{\psi_{77\,K}}{\psi_{295\,K}} = \frac{f_2'/f_3'\,(77\text{ K})}{f_2'/f_3'\,(295\text{ K})} \quad .$$

The experimental determination of ψ is very difficult, but that of ψ_R is easy. Because

$$R_{\text{Moss, 77 K}} = \frac{Fe^{+2}}{Fe^{+3}} \cdot \frac{f_2'}{f_3'}(77\text{ K}) = \frac{Fe^{+2}}{Fe^{+3}} \psi_{77\text{ K}}$$

$$R_{\text{Moss, 295 K}} = \frac{Fe^{+2}}{Fe^{+3}} \cdot \frac{f_2'}{f_3'}(295\text{ K}) = \frac{Fe^{+2}}{Fe^{+3}} \psi_{295\text{ K}}$$

therefore

$$\psi_R = \frac{R_{\text{Moss, 77 K}}}{R_{\text{Moss, 295 K}}}$$

where the R_{Moss} terms are the ferrous-ferric ratios taken at the two temperatures. This relation is very useful.

To calculate the correction factor for the Mössbauer spectra, to correct to the value the spectra would have if $f_2' = f_3'$, one must derive an equation for ψ_R, valid in a limited range.

$$f_2'(295°\text{K}) = \exp -139\left[\frac{k_7}{\theta_2} + \frac{T_2 k_8}{\theta_2^2}\right] \quad \begin{array}{l} T_2 = 295°\text{K} \\ \frac{T}{\theta_2} = 1\text{-}0.84 \\ \theta_2 = 300\text{-}350 \end{array}$$

$$f_2'(77°\text{K}) = \exp -139\left[\frac{k_1}{\theta_2} + \frac{T_1 k_2}{\theta_2^2}\right] \quad \begin{array}{l} T_1 = 77°\text{K} \\ \frac{T}{\theta_2} = 0.33\text{-}0.18 \\ \theta_2 = 230\text{-}430 \end{array}$$

$$f_3'(295°\text{K}) = \exp -139\left[\frac{k_3}{\theta_3} + \frac{T_2 k_4}{\theta_3^2}\right] \quad \begin{array}{l} \frac{T}{\theta_3} = 1.2\text{-}0.5 \\ \theta_3 = 250\text{-}600 \end{array}$$

$$f_3'(77°K) = \exp - 139 \left[\frac{k_5}{\theta_3} + \frac{T_1 k_6}{\theta_3^2}\right] \quad \begin{matrix} \frac{T}{\theta_3} = 0.25\text{-}0.125 \\ \theta_3 = 310\text{-}620 \end{matrix}$$

The above range is for $\theta_2 = 300\text{-}350$ K and $\theta_3 = 310\text{-}600$ K. The values for the constants in this range are

$$k_1 = 0.17 \qquad k_3 = 0.06 \qquad k_5 = 0.20 \qquad k_7 = 0$$

$$k_2 = 0.68 \qquad k_4 = 0.94 \qquad k_6 = 0.53 \qquad k_8 = 1 \quad .$$

The general expression for ψ_R is

$$\psi_R = \frac{\exp - 139\left[\frac{k_1}{\theta_2} + \frac{T_1 k_2}{\theta_2^2}\right]}{\exp - 139\left[\frac{k_5}{\theta_3} + \frac{T_1 k_6}{\theta_3^2}\right]} \Bigg/ \frac{\exp - 139\left[\frac{k_7}{\theta_2} + \frac{T_2 k_8}{\theta_2^2}\right]}{\exp - 139\left[\frac{k_3}{\theta_3} + \frac{T_2 k_4}{\theta_3^2}\right]} = \frac{\frac{f_2'}{f_3'}(77\ K)}{\frac{f_2'}{f_3'}(295\ K)} \quad .$$

If $\rho = \frac{\theta_3}{\theta_2}$, one can derive the relations

$$\frac{1}{\rho} = \frac{\theta_2(k_5 - k_3) + \theta_2 \sqrt{(k_5 - k_3)^2 + 4(T_2 k_4 - T_1 k_6)\left(\frac{T_2 k_8 - T_1 k_2}{\theta_2^2} + \frac{(k_7 - k_1)}{\theta_2} - \frac{\ell n \psi_R}{139}\right)}}{2(T_2 k_4 - T_1 k_6)}$$

and

$$\psi_{77} = \exp\left\{\frac{139}{\theta_2}\left[\left(\frac{k_5}{\rho} - k_1\right) + \frac{T_1}{\theta_2}\left(\frac{k_6}{\rho^2} - k_2\right)\right]\right\} \quad .$$

The true ferrous-ferric ratio is

$$\frac{Fe^{+2}}{Fe^{+3}} = R_{\substack{Moss \\ 77\ K}} \frac{1}{\psi_{77}} = R_{\substack{Moss \\ 77\ K}} \frac{f_3'}{f_2'} (77\ K) \quad .$$

The correction factor is $\frac{1}{\psi_{77}}$

$$\frac{1}{\psi_{77}} = \exp\left\{\frac{139}{\theta_2}\left[\left(k_1 - \frac{k_5}{\rho}\right) + \frac{T_1}{\theta_2}\left(k_2 - \frac{k_6}{\rho^2}\right)\right]\right\} \quad .$$

To obtain the value for the correction factor, $\frac{1}{\rho}$ must be calculated from the values of T_1 (= 77 K), T_2 (=295 K), the values of the constants for the range of the calculation, the value of ψ_R from experiment, and the estimated value of θ_2. $\frac{1}{\rho}$ is then substituted to obtain the value of $\frac{1}{\psi_{77}}$.

Table 13 shows the value for this correction factor at various values of θ_2 and ψ_R, and that the correction factor, $\frac{1}{\psi_{77}}$, varies <u>very little</u> with the unknown Debye temperature θ_2, but varies mostly with ψ_R, which is known.

When ψ_R and θ_2 become large, the value of θ_3 becomes unreasonably large (assumed > 600 K) and these values are not included. The value of $\frac{1}{\rho} = \frac{\theta_2}{\theta_3}$ is included in the table.

The columns of values for θ_2 = 250 K and 400 K are made using different values for the constants $k_1 - k_8$, because the approximations for the recoil-free fractions are in a different range.

Table 13

Values of $\frac{1}{\rho}\left(=\frac{\theta_2}{\theta_3}\right)$ and correction factor $\frac{1}{\psi_{77}}$

↓ ψ_R θ_2 →	$\left(f_2' = 0.52 \text{ at } 295°K\right)$ 250 °K	$\left(f_2' = 0.635 \text{ at } 295°K\right)$ 300 °K	$\left(f_2' = 0.71 \text{ at } 295°K\right)$ 350 °K	$\left(f_2' = 0.77 \text{ at } 295°K\right)$ 400 °K
	$\frac{1}{\rho} = \frac{\theta_2}{\theta_3}$; $\frac{1}{\psi_{77}}$			
1.06	0.941 1.019	0.901 1.025	0.858 1.025	0.821 1.024
1.08	0.919 1.026	0.869 1.032	0.807 1.033	0.753 1.033
1.10	0.898 1.033	0.831 1.040	0.755 1.041	0.678 1.042
1.12	0.875 1.040	0.799 1.046	0.703 1.049	$\theta_3 > 600$ K
1.14	0.853 1.047	0.767 1.053	0.644 1.058	$\theta_3 > 600$ K
1.16	0.830 1.055	$\frac{1}{\rho} = 0.729$ 1.060	0.585 1.067	$\theta_3 > 600$ K
1.18	0.808 1.062	$\frac{1}{\rho} = 0.692$ 1.068	$\theta_3 > 600$ K	$\theta_3 > 600$ K

THE CRYSTAL SHAPE EFFECT

Topics concerning granular Mossbauer absorbers are developed in a mathematical way by Bowman et al. (ref. 28). The purpose of this section is to discuss an anisotropy effect which can occur in granular, crystalline absorbers in a simple way, in order to understand it intuitively. Some evidence is presented to show that the effect may be significant under some conditions.

If a powdered mineral sample is truly randomly oriented, then the mass is randomly oriented and is usually thought to produce equal peaks in a doublet (neglecting the Goldanski-Karayagin effect).

To produce a Mossbauer absorption spectrum in which the doublet peaks are equal, equal amounts of resonant radiation must be transmitted and absorbed by each increment of mass. It is the purpose of this section to show that crystal shape and non-resonant absorption can combine together to produe unequal peaks in a doublet even when the powder sample is truly randomly oriented. This is produced by resonant absorption which is non-random in intensity.

Assume that a crystal is a square prism of length ℓ and side s. The angle θ is the angle of the length ℓ from the incident gamma ray beam.

By treating each crystal as an absorber,

$$\text{Volume, } V = \ell s^2$$

and R, the height of the peak, is for that crystal

$R_{\theta=90°}$ = area normal to beam × baseline × fractional absorption

$$= \ell s \, B_E \, F$$

where B_E is in counts/cm^2, R is in counts and

$$B_E = I_0 \, e^{-k_{RN} s} ,$$

assuming that $k_{RN} = k_N$, $n_S = 0$, and letting $I_0 = 1$. (See beginning of Appendix.) Then

$$R_{\theta=90°} = \ell s \, e^{-k_{RN} s} \, f(1 - e^{-\sigma f' W' s}) .$$

Similarly,

$$R_{\theta=0°} = s^2 \, e^{-k_{RN} \ell} \, f(1 - e^{-\sigma f' W' \ell}) .$$

Because

$$\ell s = \frac{V}{s} , \qquad s^2 = \frac{V}{\ell}$$

and

$$(1 - e^{-\sigma f' W' s}) \cong \sigma f' W' s$$

$$R_{\theta=90°} \cong \frac{V}{s} \frac{f \sigma f' W' s}{e^{k_{RN} s}}$$

$$\left[\begin{array}{l} R_{\theta=90^\circ} \cong \dfrac{V f \sigma f' W'}{k_e R N^s} = \dfrac{\text{const}}{k_e R N^s} \\ \\ R_{\theta=0^\circ} \cong \dfrac{\text{const}}{k_e R N^{\ell}} \end{array}\right]$$

The important feature of the values of R at $\theta = 90^\circ$ and $\theta = 0^\circ$ is that they are different because the denominators are different. In the expressions for R, the probability functions for the absorptions of the resonant radiation with respect to the direction of the electric field gradient in the crystal have been neglected.

Each orientation has its own particular anisotropy, or inequality of the low and high velocity peaks of the doublet. The anisotropy at $\theta = 0^\circ$ is less represented quantitatively in the spectrum than the anisotropy at $\theta = 90^\circ$ because $\ell > s$.

Intuitively, this effect can be understood on the same basis as the two-phase Mössbauer absorber can be understood (see the cylinder model). The crystal oriented at $\theta = 0^\circ$ is more opaque to the resonant radiation per unit mass because the radiation passes through a greater thickness. It is consequently less represented in the spectrum, just as the more opaque of the two phases of the Mössbauer absorber is less represented.

A priori, it is not known whether the high velocity line or the low velocity line will be the greater with a given orientation of the crystal. This depends upon the direction of the electric field gradient in the crystal, which is unknown. All that is known is that the anisotropy of the parallel ($\theta = 0^\circ$)

orientation is less represented, and the spectrum will contain an undue proportion of the anisotropy of the orientation where $\theta = 90°$.

Two factors enhance the crystal shape effect. One is elongation of shape. If $\ell < m$, then the crystal is a plate, and similar arguments hold to those for the prism. The second factor is anything which increases the non-resonant absorption coefficient (k_{RN}) for the resonant radiation. Heavy metals tend to increase absorption, due to their many electrons, so one should expect that high contents of metals such as Ca, Mn, Fe and especially Ba should increase the crystal shape effect. High non-resonant absorption produces greater opacity in the parallel ($\theta = 0°$) orientation.

One sure way to defeat this effect is to grind the mineral so finely that both s and ℓ are very small, and the exponentials in the denominators are both nearly unity.

Table 14 gives experimental data on transmittance (absorbance) and k_{RN} for various of the mineral specimens. The data in this table are very crude, because the transmittances represent both 14.4 kev and 122 kev radiation. The 14.4 kev radiation will be more strongly absorbed than the 122 kev, and the values for k_{RN} will be greater than the table indicates. Extra transmittance due to the cylinder model decreases the value of k_{RN}.

In Table 14 the mineral is assumed to be a solid layer of thickness t, calculated from the weight of the sample, its density, and the area of the holder.

The values of k_{RN} vary from 17 to 58, which are highest for minerals containing much Fe and Mn. For the value 58,

Table 14

(Area of holder = 3.9 cm^2)

Mineral wt(mg)	Transmittance	Assumed density	t (cm)	Exp. of transmittance ($-k_{RN}t$)	$k_{RN}(cm^{-1})$	Fe content (%)	Mn content (%)	Ca content (%)
Sucrose	1.00 (assumed)	—	—	$\cong 0$	—			
CR1 (60)	0.78	3.3	0.0047	-0.248	53	21.6	0.4	0.9
HB1 (169)	0.66	3.2	0.014	-0.416	30	11.2	0.2	7.3
M3 (300)	0.63	2.8	0.027	-0.462	17	3.7	0.8	0.0
GN2A (600)	0.32	3.65	0.042	-1.14	27	3.06	0.2	24.6
GN5 (350)	0.28	4.1	0.022	-1.27	58	4.4	24.4	1.8
GN7 (80)	0.73	3.8	0.0054	-0.315	58	12.4	8.3	15.0

$$\begin{cases} e^{k_{RN}s} = e^{0.58} = 1.79 , & s = 0.1 \text{ mm} = 0.01 \text{ cm} \\ e^{k_{RN}\ell} = e^{1.74} = 5.7 , & \ell = 0.3 \text{ mm} = 0.03 \text{ cm} \end{cases}$$

This is for a prism three times as long as it is wide, and of a common size (100 mesh = 0.150 mm). The terms in the denominator are scarcely negligible relative to each other, and the prisms must be reduced to much less than 0.1 mm in cross section, or much less than 100 mesh. Easily cleaved minerals (irregular shape) must be fine; garnets are an exception because they are granular.

If $s = 0.01$ mm and $\ell = 0.03$ mm

$$\begin{cases} e^{k_{RN}s} = 1.06 \\ e^{k_{RN}\ell} = 1.19 \end{cases}$$

and the denominators are nearly the same. Any crystal shape effect will be nil.

When minerals are put into Mössbauer holders to do the spectrum, a little anisotropy is sometimes produced even when sucrose is used as the mounting medium. The nature of the crystal shape effect is such that it augments the anisotropy (for a flat holder mounted at right angle to the beam).

THE SINE FUNCTION, STONE'S PROGRAM

The sine function in Stone's computer program was originally meant to correct for the physical motion of the source, by the inverse square law of radiation. The reasoning for this is outlined below.

The sine function is variable on the same absorber sample from run to run, and is often far too large in practice to be due to source distance only, since the motion of the source is exceedingly small.

By the inverse square law, it is easy to find the maximum increase of the baseline (maximum of the sine function) relative to the baseline itself. In Stone's program, the maximum is multiplied by a sine wave whose value is determined by its position (channel) in the spectrum.

The change in the inverse square value with distance r is

$$\frac{d\left(\frac{1}{r^2}\right)}{dr} = -2\,r^{-3} \quad \text{or} \quad d\left(\frac{1}{r^2}\right) = \frac{-2\,dr}{r^3} \quad .$$

Compared to the original value of $\frac{1}{r^2}$

$$\frac{d\left(\frac{1}{r^2}\right)}{\frac{1}{r^2}} = \frac{-2\,dr}{r} \quad \text{or} \quad \frac{\Delta\left(\frac{1}{r^2}\right)}{\frac{1}{r^2}} = -\frac{2\,\Delta r}{r} \quad .$$

The relative increase of the baseline, $\frac{2\,\Delta r}{r}$, is determined from a least-squares fit of the spectrum.

The maximum value the sine function may have in practice can be estimated from some characteristics of the spectrometer, assuming that it is dependent only on the inverse square law.

The real motion of the source has a stepped, "sawtooth" shape. If the motion is treated as a constant acceleration, then the amplitude of the motion can be easily deduced.

$$v = \int_{t=0}^{t} a\,dt = at$$

$$d = \int_{0}^{t} v\,dt = \frac{1}{2}at^2 = \frac{1}{2}vt \quad .$$

If the dwell time per channel is about 40 microseconds plus 20 microseconds waiting, and there are 256 channels in one sweep, either positive or negative (512 channels in a full spectrum; not a mirror), there are

$$(2.56 \times 10^{2})(60 \times 10^{-6}) = 1.54 \times 10^{-2} \text{ sec/sweep}$$

then

$$d_{max} = \frac{1}{2} v_{max} t_{max} \quad ; \qquad v_{max} \cong 4.5 \text{ mm/sec}$$

and

$$[d_{max} = \Delta r = 3.46 \times 10^{-2} \text{ mm}] \quad .$$

If the distance of the sample from the source is 6 inches (152 mm), 6 to 8 inches being the usual distance,

$$\frac{2\,\Delta r}{r} = \frac{6.92 \times 10^{-2}}{152} = 0.45 \times 10^{-3}$$

which is only 0.045% variation due to the inverse square law.

In practice, the sine function is often much greater than 0.045%, sometimes greater than 0.2%. Moreover, minerals like GN2A, GN2B and M3 in this study consistently give negatively bowed baselines under exactly the same experimental conditions in which the other minerals give positively bowed baselines. The bowing of the baseline, the sine function, is therefore a function of the type of spectrum, as well as other variables.

When spectra were corrected by Program Mosscorr, the sine function, when left unconstrained, always increased in value (considering only positive bowing). Since the value of chi-squared usually increased 10% or 20% on correction, the bowing of the baseline may also be a function of the statistics of the spectrum.

The function $\frac{2\,\Delta r}{r}$ is a sawtooth-shaped function, whereas the sine wave is a smooth curve of a different shape. The sine wave in Stone's program might best be replaced with this function, which more closely represents the variation due to the inverse square law.

THE ABSORPTION AMPLITUDE

In absorption spectroscopy, amplitudes and areas of peaks are not linear with the amount of material which is absorbing. In many cases, the absorption amplitude is an exponential function. If T is the thickness of the absorber, then the absorption amplitude is proportional to

$$(1 - e^{-T}) \quad .$$

Mössbauer amplitudes do <u>not</u> follow this simple function, but undergo an effect known as "saturation." At T = 30, the absorption amplitude is approximately 80 per cent and the curve has become nearly flat ("saturates"), whereas the exponential function gives virtually 100 per cent absorption.

The absorption amplitude is given in the literature in the form of a graph (ref. 31, 33) but no table of values appears to have been published. If one is to correct the amplitudes and areas of Mössbauer spectra for saturation effects, one must deduce an approximation for the amplitude. Amplitude is also given by a complicated integral with no analytic solution which is useless in that form (ref. 32).

The function which gives the area of a single Mössbauer peak, the function L(T), has been tabulated by numerical integration (ref. 31). Table 15 lists L(T) and T (and the amplitude estimates from the graph plus the algebraic approximations). L(T) is non-linear with T. A good approximation for L(T) to T = 2 is

$$(1 - e^{-T})(1 + 0.26\,T - 0.008\,T^2 + 0.01\,T^3)$$

<u>or</u>

$$(1 - e^{-T})(1 + 0.26\,T) \quad .$$

As a single Mössbauer line becomes increasingly thick with increasing T, the width of the peak increases. This is because of a geometric effect. The amplitude at the peak maximum is decreased proportionally far more than at the limbs. The width (at half-height) is therefore measured to a point where the curve is wider than at the half-height of the undistorted curve. A width relation has been published by Frauenfelder (ref. 30) which is

$$\frac{\Gamma}{\Gamma_0} = 1 + 0.135\ T \quad .$$

Mössbauer curves, even when thick, are good approximations to the Lorentzian shape (ref. 32). Therefore, if the relative area that a peak should have is

$$(1 - e^{-T})(1 + 0.26\ T) = L(T)$$

and the width is increased by

$$1 + 0.135\ T$$

then the relative amplitude must be approximately

$$\frac{(1 - e^{-T})(1 + 0.26\ T)}{1 + 0.135\ T} \quad .$$

The function which best fits the published amplitude curve in the graph is

$$\frac{(1 - e^{-T})(1 + 0.26\ T)}{1 + 0.11\ T} \quad . \qquad \text{(to } T = 2.5\text{)}$$

In Table 15 at the values of T = 0.21, and 0.45, the values of the amplitude taken from the graph, 2(1-I), are greater or nearly equal to L(T). This cannot be, because it is known that the amplitude saturates more rapidly than the area, i.e.

Table 15

Area and Amplitude Functions

T	L(T) (= area)	$(1 - e^{-T}) \times (1 + 0.26\ T)$ ($\cong$ L(T))	2(1 - I) ($\cong$ TOB) graph	$\frac{(1 + 0.26\ T)(1 - e^{-T})}{(1 + 0.11\ T)}$ ($\cong$ TOB)
0.0	0.0	0.0	0.0	0.0
0.02		0.0199		0.01986
0.20	0.1905	0.1907		0.1866
0.21		0.1997	0.2	0.1957
0.40	0.3637	0.3640		0.3486
0.45		0.4048	0.4	0.3857
0.50		0.4446	0.43	0.4214
0.60	0.5220	0.5216		0.4893
0.75		0.6305	0.6	0.5824
0.80	0.6673	0.6652		0.6114
1.00	0.8015	0.7964	0.72	0.7175
1.50	1.0966	1.0799	0.92	0.9269
2.00	1.3473	1.3143	1.06	1.0773
2.50	1.5656	1.5145	1.18	1.1879
5.00	2.3831	2.2845	1.47	1.4739
7.00	2.8714	2.8174	1.53	1.5918
10.00	3.4751	3.5998	1.63	1.7142

L(T) > amplitude function.

Therefore, the values taken from the graph (or the graph itself in this region) are not precise. The amplitude function, which has a denominator greater than unity, is always less than L(T).

The amplitude function is only a proportionality factor; the value of the amplitude is one-half that of the factor. This is because, for very thin spectra,

$$\text{amplitude} \cong \frac{1}{2} T \frac{\Gamma^2}{(2S)^2 + \Gamma^2} \quad \text{(ref. 32 , p. 137)}$$

Here, T is understood to be the maximum value. Previously, it has been assumed that T is a variable equivalent to

$$T \frac{\Gamma^2}{(2S)^2 + \Gamma^2} \quad \text{(for a single line)}$$

and that the T's for overlapping lines are additive. In this work, T will continue to be used as a variable.

T is the true thickness at any point on the curve, for single or overlapping lines

$$T = \sigma_0 f' W \frac{\Gamma^2}{(2S)^2 + \Gamma^2} \quad \text{(single line)} \quad .$$

The uncorrected thickness is proportional to the actual peak height observed in the spectrum, and is termed TOB ("thickness observed") in the computer program. In very thin spectra,

$$\text{amplitude} = \frac{1}{2}\,\text{TOB} \cong \frac{1}{2}\,T \quad .$$

The correction of the amplitudes in the program is done in the subroutine by the equation

$$\text{TOB} = \frac{(1 - e^{-T})(1 + 0.26\,T)}{1 + 0.11\,T} \quad , \text{ (used in another form).}$$

The amplitude must be greater by the factor

$$\frac{T}{\text{TOB}} \ (>1)$$

and the correction factor is

$$\frac{T}{\text{TOB}} - 1 \quad .$$

The counts proportional to the correction factor are sub tracted from the count in the spectrum. T is the root of the amplitude equation and the subroutine extracts this root.

In the program, FOB ("F observed") is the amplitude observed in the spectrum. For a spectrum containing only <u>one</u> type of resonant radiation

$$\text{"T observed"} = 2\ \text{FOB} \quad .$$

FOB is understood to be the value <u>after</u> correction for the background radiation (FR 122) and the recoil-free fraction of the source (F).

In iron-57 spectra, there are <u>two</u> types of resonant radiation ($3/2 \rightarrow 1/2$ and $1/2 \rightarrow 1/2$). When a peak is undergoing absorption due to <u>one</u> type of radiation, the other type constitutes a background radiation and the amplitude observed is <u>one-half</u> the true amplitude of the transition. Therefore, the program contains the statement

2.000, mistake, ERW

TOB = 4.0000*FOB

which applies to spectra with only two types of resonant radiation.

The thicknesses observed in the spectra are considerably smaller than the iron they represent indicates. This is because they are 1.5—4 times wider than the theoretical value. The theoretical value of T is

$$T(max) = \sigma_0 f' W$$

where

$$\sigma_0 = 2.36 \times 10^{-18} \text{ cm}^2 \text{ (for random orientation)}$$

$$W = \text{number of iron-57 nuclei/cm}^2 \quad .$$

For natural iron (2.19% iron-57),

$$\sigma_0 W = (0.558) \text{ (mg Fe/cm}^2) \quad .$$

If $f' \cong 0.75$, which is "reasonable" in silicates,

$$[T \cong (0.42) \text{ (mgFe/cm}^2)] \quad .$$

This relation is understood to be valid only for the maximum amplitude of a single isolated peak, because σ_0 is used.

The amplitude of peaks observed as "fractional absorption" in the final spectrum is, as mentioned above, 7 to 40 times less than the value of T indicates. The factors producing the low amplitude are,

1. Background radiation, largely 122 kev radiation from the source.

2. The non-resonant fraction of the 14.4 kev radiation. This also constitutes a background radiation.

3. The factor of one-half in the equation relating the amplitude (one resonant type) to the uncorrected thickness (TOB).

4. The non-linear relation between T and TOB in the amplitude function (T > TOB).

~~5. The presence of two resonant radiation types, one of which is background with respect to the other during resonant absorption.~~ Incorrect, ERW

6. Increased line width, greater than the theoretical width. This can be due to site multiplicity or the spectrometer. If the increased width is due to the spectrometer, it is at the cost of amplitude and the peak area cannot be fully restored by an amplitude-correction program.

7. Holes in the absorber (cylinder model) which permit excess background radiation.

8. See Bowman, et. al., ref. 28 , for effects of granular absorbers.

THE USE OF PROGRAM MOSSCORR

Many of the theoretical details of the absorption are given in the section on the absorption amplitude. This section is more concerned with the practical use of the program.

Program Mosscorr is designed to correct Mossbauer spectra of isotopes which undergo two types of resonant transition, not more. Because each type of resonant radiation has its own correction factor for amplitude, independent of the other, overlapping of peaks of the two types requires an estimate of the peak heights of one of the types. It is therefore necessary to analyze the spectrum before it is corrected, via Stone's program. This is equivalent to stating that the correction factors applied to a spectrum are not independent of the peak positions in the spectrum.

In this section, the high velocity peak of any doublet will be assumed to be of one transition type ($\frac{1}{2} \rightarrow \frac{1}{2}$). This is not necessarily so, but simplifies the discussion. Some direct evidence for this, in iron Mossbauer spectra of silicates, is presented in "The Sign of the Quadrupole Splitting," which follows this section.

In iron-57 spectra of silicates, the high velocity peaks ($\frac{1}{2} \rightarrow \frac{1}{2}$) are usually less overlapped, and their resultant amplitude is less than that of the low velocity peaks. The correction is less for the high velocity peaks and therefore is less subject to errors in input data than the heavily overlapped low velocity peaks. Data for the high velocity peaks, the position, width and area, in that order, from Stone's program are entered in Program Mosscorr for the high velocity peaks whose parameters are (1 set to a card)

POSNFE	GFE	AREAFE
POSFE2	GFE2	AREFE2
	etc.	
POSFE5	GFE5	AREFE5 .

Not necessary, ERW set to zero.

(Five of these lines (cards) provided) If a line is not to be used, set the area to 0.0 (do not set the width to zero). All values must contain a decimal point. The program adds the amplitudes for these peaks, assumed to be Lorenztian, makes the correction, and determines the height for the low velocity ($\frac{1}{2} \rightarrow \frac{3}{2}$) peaks by difference from the net count (CABS). If the amplitude (area) is too large, the program is set to make a correction on no amplitude greater than that of the net count. The error in the areas may not be large, because this will affect the size of the "tails" in the low velocity region. One channel must be added to the position from Stone's program, because the latter numbers from 0 to 511 instead of 1 to 512.

The term SUM in the program is the sum of the amplitudes of the five peaks at any channel. SUMNEW is the same except when the sum is greater than the count, in which case it is less than the sum and 99 per cent of the count. The term H is the amplitude of the low velocity peaks. I is the channel number from 1 to any number (512). The term CORR is the correction in counts for the low velocity peaks; CORRFE is that for the five peaks entered (high velocity). T is the thickness of the low velocity peaks, calculated by the subroutine (see section on the absorption amplitude) and TFE is the thickness of the five peaks entered (high velocity). These are also in print output.

Enough lines in the program printout are allowed for three 512-channel spectra. If more are to be corrected, the "WRITE (6, 6010)" card must be removed from the program.

The program requires input of five other numbers,

1. The number of data points (usually 512) as an integer without a decimal point. (N)

2. The recoil-free fraction of the source, with a decimal point. For a Pd source, F = 0.66. See ref. 34 for a list of these.

3. The "base" (BASE) which is the baseline count without the number of millions, and with a decimal point.

It may be determined by

(a) Averaging the first 10-20 channels on the low-velocity side, and then adding the tails of the peaks at the first channel.

(b) By Stone's program, keeping the baseline straight (setting sine wave and channel drift to zero absolutely).

4. The background radiation, mostly 122 kev. FR122 is the fraction of the 122 kev radiation, with a decimal point.

This is measured by inserting 0.005 inch nickel foil between the sample and the counter, and counting for 10 minutes. The 122 kev radiation is transmitted. Also measure the sample without the foil. (ref. 36).

There remains some question of the accuracy of the nickel foil measurement.

5. The number of millions of the baseline, as an integer without a decimal point (M).

The input data, plus the (52) cards containing the channel counts, are in the following order:

1. Title card

2. Number of data points (N) and then the recoil-free fraction of the source (F) on the second card.

3.—7. Five cards for the five lines, each number in the order position, width, area, each with a decimal point.

8. Value for the base (BASE), then the fraction of background radiation (FR122) and finally the number of millions (M) on one card.

Last. Cards with the channel counts (usually 512 channels, 52 cards) in F6.0, 9F7.0 format.

In order to correct another spectrum, add another set of cards. The very last card must be /* (only one of these in all).

The card output is in 10 F 8.0 (10I8) format with the number of millions. To use Stone's program, eliminate the "add million" card and change the format to (10F8.0).

An example of a typical input is, card by card, for a garnet with a baseline less than one million,

```
Garnet 21,        June 3—4, 1973,    295 deg K, Mosscorr
512                    0.66
291.560               19.159            1,161,567.0
425.678               16.058              340,217.0
250.                  20.                       0.0
250.                  20.                       0.0
250.                  20.                       0.0
966,523.0              0.127                    0
{52 cards with channel counts, in correct order
/*
```

Program Mosscorr makes no provision for deviant channel counts. All deviant counts must be replaced by reasonable values. This is very important.

Along the baseline, statistical variation may cause negative amplitudes. To avoid increasing the count, absolute values of the amplitudes are used. The count is never increased, but either remains the same, or is decreased.

Program Mosscorr is best used to correct spectra which are not thick, probably where $T < 1$. When spectra become thick, amplitudes are large and errors in input data for F and FR122 play a larger role than in thinner spectra. Effects like those described in Bowman, et. al.(ref. 28) in granular absorbers add to the error. Problems with the source thickness may also add error; the source thickness has been assumed to be zero for Program Mosscorr.

AN EXPERIMENTAL TEST OF PROGRAM MOSSCORR

Experimental tests of a Mossbauer correction program must be chosen carefully. A good test should meet several criteria, which are listed below.

1. The test may be done in one run, within a single spectrum, or in two or more runs.

2. If done in two runs, a single line, varying in T in the runs, should show T proportional to the iron in the absorber hole. Better, a material after correction should show the same ferrous-ferric ratio independent of the thickness. One set of the lines should be big, and the other small (example, GN7).

3. If done in a single spectrum, a pair of lines A and B should overlap strongly and be equal to the sum of two other lines C and D which are not overlapped. Babingtonite has this type of spectrum (assuming no anisotropy). Before correction, there should be marked inequality and the spectrum should not be thin.

4. The material should not have too high an iron content. If the iron concentration is too high, there will be "holes" in the absorber (like the cylinder model) and the fractional absorption cannot be typical for the thickness of the absorber. The spectrum will be undercorrected. Magnetite, otherwise a good material, probably suffers from this disadvantage.

Two spectra of babingtonite, at 77° and 295°K, were available for the test. At 295°, the intense low velocity peak, composed of overlapping low velocity ferrous and ferric lines, was 88.7% of the sum of the high velocity

lines. At 77°, it was 85.1%, but should have been more than 88.7%, 186
because the amplitude was less, relative to the high velocity peaks. This low temperature run was of lesser quality.

After correction, the low velocity peak (sum of two lines, as above) of the 295° run was 97.3% of the sum of the high velocity peaks. That of the 77° run was 93.6 percent. More than half of the inequality was eliminated in both cases. At maximum amplitude of the 295° run, T = 1.03 and the increase in amplitude due to the correction was 40%, from 11% fractional absorption to 15%. This was the greatest value of T encountered in this work.

```
IV G1  RELEASE 2.0            MAIN            DATE = 73159        20/25/29

      C
      C     PROGRAM MOSSCORR, TO CORRECT THE NON-LINEAR AMPLITUDES OF MOSSBAUER
      C     SPECTRA.
      C
            DIMENSION TITLE(20)
            EXTERNAL FCT
            COMMON/LAURA/TX
            REAL*4 C(1200)
            INTEGER K(1)
            EQUIVALENCE(C,K)
     1      READ(5,1000,END=900)TITLE
     1000 FORMAT(20A4)
            WRITE(6,2000)TITLE
     2000 FORMAT('1',20A4)
            READ(5,*)N,F,POSNFE,GFE,AREAFE,POSFE2,GFE2,AREFE2,
           1  POSFE3,GFE3,AREFE3,POSFE4,GFE4,AREFE4,POSFE5,GFE5,AREFE5,
           2  BASE,FR122,M
            WRITE(6,3000)N,F,POSNFE,GFE,AREAFE,POSFE2,GFE2,AREFE2,
           1  POSFE3,GFE3,AREFE3,POSFE4,GFE4,AREFE4,POSFE5,GFE5,AREFE5,
           2  BASE,FR122,M
     3000 FORMAT(' ','N =',I5/' F = ',F6.4//' POSNFE = ',F8.3/' GFE = ',F8.3
           1  /' AREAFE = ',F12.0//' POSFE2 = ',F8.3/' GFE2 = ',F8.3/
           2  ' AREFE2 = ',F12.0//
           3  ' POSFE3 = ',F8.3/' GFE3 = ',F8.3/' AREFE3 = ',F12.0//
           4  ' POSFE4 = ',F8.3/' GFE4 = ',F8.3/' AREFE4 = ',F12.0//
           5  ' POSFE5 = ',F8.3/' GFE5 = ',F8.3/' AREFE5 = ',F12.0//
           6  ' BASE = ',F8.0/' FR122 = ',F8.6/' M = ',I2/
           7   //8X,'OLD',7X,'NEW',5X,'  CORR',5X,'CURFE  ',
           8   5X,'I',9X,'H',7X,'SUM',5X,'SUMNEW',11X,'T  ',18X,'TFE  '/)
            READ(5,5000)(C(I),I=1,N)
     5000 FORMAT(10(F6.0,1X))
            MM=M*1000000.
            RESCN=(BASE+MM)*(1.-FR122)*F
      C
      C     BASE IS THE ESTIMATED BASELINE, (NO MILLIONS ), ASSUMED TO BE STRAIGHT.
      C     FR122 IS THE BACKGROUND RADIATION (MOSTLY 122 KEV),F,RECOIL-FREE  FRACTION
      C     OF THE SOURCE.
      C
      C     RESCN IS THE TOTAL NUMBER OF COUNTS OF RESONANT RADIATION OF BOTH
      C     TRANSITION TYPES. ALL AMPLITUDE CORRECTIONS ARE BASED UPON THIS NUMBER.
      C     THE 122 KEV RADIATION IS ONLY BACKGROUND, AND HAS  NO PHYSICAL EFFECT
      C     ON THE AMPLITUDES OF THE  PEAKS. AMPLITUDES (COUNTS) BEGIN WITH LETTER H.
      C     AREAFE, AREFE2, ETC.,ARE AREAS OF IRON PEAKS OF THE SAME TRANSITION TYPE.
      C     THE AMPLITUDES OF THESE   PEAKS MUST BE ADDED TOGETHER BEFORE CORRECTION
      C     BECAUSE THEIR NON-LINEAR EFFECTS ARE NOT SEPARATE.
      C     THESE   IRON PEAKS ARE USED IN THE PROGRAM ONLY WHEN PEAKS OF THE
      C     3/2-1/2 TRANSITION TYPE ARE HEAVILY OVERLAPPED BY PEAKS OF THE 1/2-1/2
      C     TRANSITION TYPE.  SETTING AREAFE AND AREFE2, ETC., TO ZERO ELIMINATES THIS
      C     PART OF THE PROGRAM. WHEN OVERLAP OCCURS, THE POSITIONS (POSNFE, POSFE2,
      C     ETC.),WIDTHS (GFE, GFE2, ETC.) AND AREAS OF THESE   PEAKS ARE ENTERED
      C     IN UNITS OF COUNTS AND CHANNELS FROM THE UNCORRECTED SPECTRUM.
      C     1 CHANNEL SHOULD BE ADDED TO THE POSITION FROM STONE'S PROGRAM
      C     BECAUSE STONE NUMBERS FROM 0 TO 511 INSTEAD OF 1 TO 512.
```

```
C
C     DO NOT SET WIDTHS TO ZERO.
C
      DO 10 I=1,N
      XI=I
      DENOM=(GFE**2)+4.0*((POSNFE-XI)**2)
      DENOM2=(GFE2**2)+4.0*((POSFE2-XI)**2)
      DENOM3=(GFE3**2)+4.0*((POSFE3-XI)**2)
      DENOM4=(GFE4**2)+4.0*((POSFE4-XI)**2)
      DENOM5=(GFE5**2)+4.0*((POSFE5-XI)**2)
      HFE=(0.6366*AREAFE)*(GFE/DENOM)
      HFE2=(0.6366*AREFE2)*(GFE2/DENOM2)
      HFE3=(0.6366*AREFE3)*(GFE3/DENOM3)
      HFE4=(0.6366*AREFE4)*(GFE4/DENOM4)
      HFE5=(0.6366*AREFE5)*(GFE5/DENOM5)
C
C     EQUATIONS HFE=, HFE2=, ETC., ARE THE MAXIMUM AMPLITUDES (COUNTS) TIMES
C     THE LORENTZIANS FOR THE   IRON PEAKS OF THE SAME TRANSITION TYPE.
C     GFE, ETC.,   (WIDTHS IN CHANNELS) HAVE BEEN FACTORED FROM THESE EQUATIONS.
C
C     ALONG THE BASELINE, WHERE CORRECTIONS ARE SMALL, THE CORRECTION FACTOR
C     (FACTOR AND FACTFE) IS GIVEN ACCURATELY BY 0.350 TIMES THE UNCORRECTED
C     THICKNESS (TOB AND TOBFE; OB MEANS OBSERVED). THIS AVOIDS THE ROOT
C     CALCULATION BY RTNI (TO GET THE TRUE THICKNESS T AND TFE), SAVING COMPUTER
C     TIME. FOB AND FOBFE ARE THE OBSERVED FRACTIONAL ABSORPTIONS (WITH
C     RESPECT TO THE RESONANT RADIATION).
C           TOB AND TOBFE ARE REALLY NOT 'OBSERVED', BUT ARE  DERIVED FROM THE
C     'OBSERVED ' FRACTIONAL ABSORPTIONS FOB AND FOBFE, WHICH ARE WITH
C     RESPECT TO THE RESONANT 14.4 KEV RADIATION ONLY. FOB AND FOBFE REQUIRE
C     KNOWLEDGE OF THE RECOIL-FREE FRACTION OF THE SOURCE AND THE BACKGROUND
C     RADIATION (MOSTLY 122 KEV).
C
C     IF AREAS ARE ACCIDENTLY SET TOO HIGH, AMPLITUDES OF THE IRON PEAKS
C     MAY EXCEED THE REAL HEIGHTS OF THE PEAKS AS DETERMINED BY THE COUNTS.
C     THE FIRST 'IF' STATEMENTS AVOID THIS POSSIBLE TROUBLE.
C
      SUM=(HFE+HFE2+HFE3+HFE4+HFE5)
      CABS=ABS(BASE-C(I))
      IF (SUM .LT. CABS)GO TO 45
      IF (SUM .GE. CABS)GO TO 44
   44 SUMNEW=0.99*CABS
      GO TO 46
   45 SUMNEW=SUM
   46 FOBFE=SUMNEW/RESON
      TOBFE=(4.0000)*FOBFE
      IF (TOBFE .GT. 0.02)GO TO 56
      IF (TOBFE .LE. 0.02)GO TO 57
   56 TX=TOBFE
      CALL RTNI(TFE,FF,DFF,FCT,TOBFE,.0001,100,IER)
      FACTFE=(TFE/TOBFE)-1.
      B=TFE
      GO TO 59
   57 FACTFE=0.350*TOBFE
```

2,000
ERW

```
      B=TCBFE
   59 CORRFE=FACTFE*SUM
C
C     BASE IS THE ESTIMATED BASELINE , WHICH IS ASSUMED TO BE STRAIGHT.
C     CABS IS THE ABSOLUTE VALUE OF THE BASE (NO MILLIONS ) MINUS THE COUNT,
C     WHICH IS THE AMPLITUDE (IN COUNTS).
C
      H=(CABS-SUMNEW)
      FCB=(ABS(H))/RESON
      TCB=(4.0C00)*FCB
      IF (TCB .GT. 0.02)GC TO 96
      IF (TCB .LE. 0.02)GC TO 97
   96 TX=TCB
      CALL RTNI(T,FF,DFF,FCT,TCB,.0001,100,IER)
      FACTCR=(T/TCB)-1.
      A=T
      GO TO 99
   97 FACTCR=0.350*TCB
      A=TCB
   99 CORR=FACTOR*(ABS(H))
C
C     CORRECTIONS CORR ANC CORRFE (FCR THE MAIN ENVELOPE OF PEAKS AND THE PEAKS
C     OF DIFFERENT TRANSITION TYPE) ARE SUBTRACTED FROM  THE EXPERIMENTAL
C     COUNT C(I). XNEW, PLUS THE NUMBER OF MILLIONS, MM, IS THE FINAL RESULT.
C
      XNEW=C(I)-CCRRFE-CCRR
      I1=C(I)+.5+MM
      I2=XNEW+.5+MM
      I3=-CCRR
      I4=-CCRRFE
      I5=H+C.5
      I6=SUM+0.5
      I7=SUMNEW+0.5
C
C     REMCVING WRITE STATEMENT DELETES PRINT.
C
      WRITE(6,601C)I1,I2,I3,I4,I,I5,I6,I7,A,B
 6010 FORMAT(' ',8I10,6X,E14.7,6X,E14.7)
      K(I)=I2
   10 CONTINUE
      WRITE(7,7C00)(K(I),I=1,N)
 7C00 FORMAT(1CI8)
      GO TC 1
   9CC STOP
      END
```

2,000
ERW

```
IV G1  RELEASE 2.0              MAIN              DATE = 73159          20/25/29

C
C      THE EQUATION F= (ZERO UNDERSTOOD) IN SUBROUTINE FCT (RTNI) IS THE MOST
C      IMPORTANT RELATION IN THE PROGRAM. IT RELATES THE TRUE THICKNESS T WITH
C      THE OBSERVED THICKNESS TOB. T IS THE ROOT TO BE EXTRACTED BY THE SUB-
C      ROUTINE. DF IS THE DERIVATIVE OF EQUATION F= .
C
       SUBROUTINE FCT(T,F,DF)
       COMMON/LAURA/TX
       F=((1.0+0.26*T)*(1.0-EXP(-T))/(1.0+0.110*T))-TX
       DF=(0.26)*(1.0-EXP(-T))/(1.0+0.110*T)+(1.0+0.26*T)*((EXP(-T))/
      1  (1.0+0.110*T)+(0.110)*(EXP(-T)-1.0)/((1.0+0.110*T)**2))
       RETURN
       END
```

Incorrect, ERW

THE SIGN OF THE QUADRUPOLE SPLITTING

In the correction of the spectra by Program Mosscorr, the question arises whether any one peak is of the $\frac{1}{2} \rightarrow \frac{1}{2}$ or $\frac{1}{2} \rightarrow \frac{3}{2}$ transition type. In the present work, it has been assumed that the high velocity peak of any of the doublets is of one transition type ($\frac{1}{2} \rightarrow \frac{1}{2}$). This assumption, if correct, enables the spectra to be corrected more accurately than without this assumption.

In the case of babingtonite, the spectrum provides direct evidence of this. The anisotropy of the uncorrected spectrum of babingtonite has been described in the previous section on "An Experimental Test of Program Mosscorr." If the low velocity ferrous peak were type $\frac{1}{2} \rightarrow \frac{3}{2}$ and the low velocity ferric peak were type $\frac{1}{2} \rightarrow \frac{1}{2}$, the amplitudes would add separately, the correction factors would be separate, and the low velocity peak (overlapped Fe^{+2} and Fe^{+3}) would be equal to the sum of the high velocity peak (assuming no anisotropy and no spectrometer error) in the uncorrected spectrum. This is not the case.

The high velocity tails of the low velocity peaks lie in the region of the spectrometer which at times loses area (the positive, low velocity region; see section on "Investigation of the Mossbauer Spectrometer). Even when the spectrometer is losing area, the maximum amplitude of a peak is unaffected, because the channel dwell time of the spectrometer remains constant. The correction of the spectrum depends mainly upon the large amplitudes, which have the largest correction factors. One would therefore expect that whether the spectrometer were functioning optimally or not, the correction of the spectrum by Program Mosscorr would be approximately correct.

The uncorrected spectrum shows the low velocity overlapped peak (at 295°K) to be 88.7% the sum of the high velocity peaks (because of the diminishing

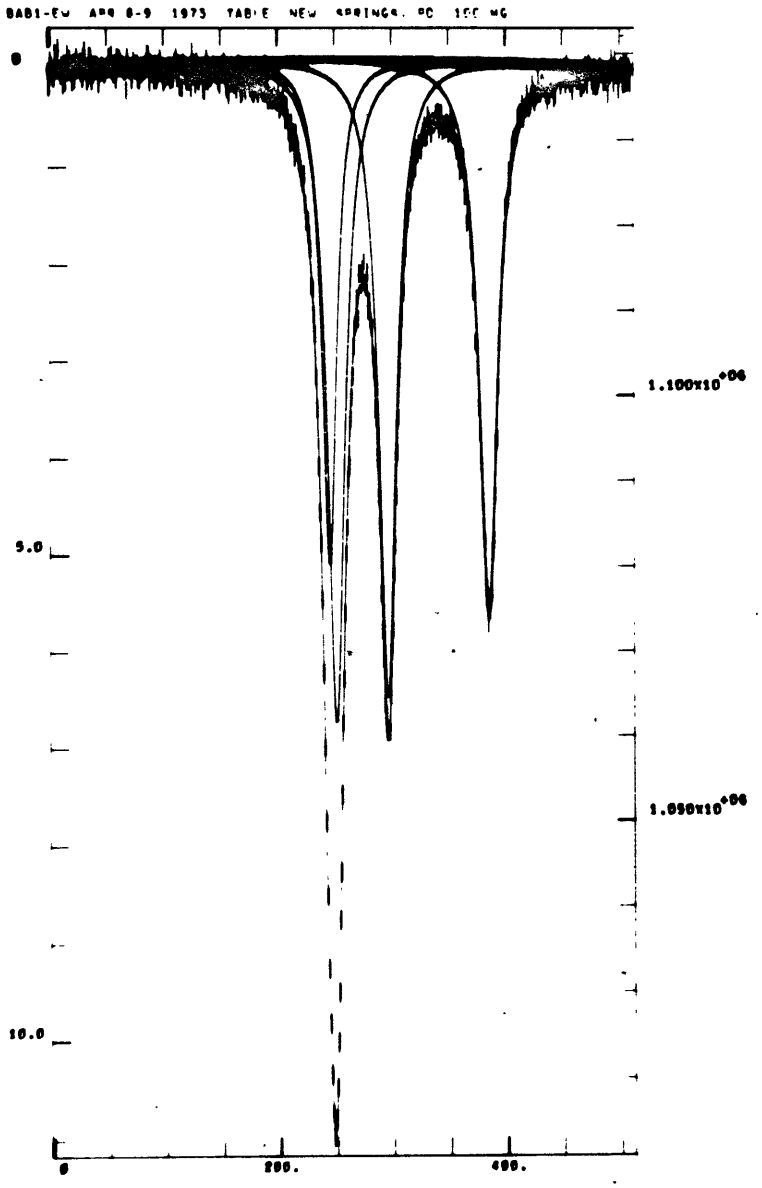

FIG. 12.

Babingtonite BAB1, free fit. Ferric peaks have largest amplitude.

of amplitude due to thickness). After correction, it is 97.3% of this sum. The low velocity peak at 77°K is not as intense, but also increases greatly on correction. Therefore, the low velocity ferrous and ferric peaks are of the same transition type. Whether this type is $\frac{1}{2} \rightarrow \frac{1}{2}$ or $\frac{1}{2} \rightarrow \frac{3}{2}$ is of no matter to the correction of the spectrum. The high velocity has been assumed to be $\frac{1}{2} \rightarrow \frac{1}{2}$ for sake of simplicity in the text.

Pollak et al. (ref. 89) concluded that the high velocity ferrous peaks of biotite were of the $\frac{1}{2} \rightarrow \frac{1}{2}$ type. They assumed that the electric field gradient of the sites was oriented "along the direction of elongation of the octahedron (z-direction)."

In synthetic rare-earth iron garnets, the quadrupole splitting for Fe^{+3} has been measured at 610°K and calculated theoretically by Nicholson and Burns for both the octahedral and tetrahedral sites. Both these authors and Sharma (ref. 45) obtained the negative sign for the quadrupole splitting by calculation. The negative sign of the quadrupole splitting means that the $\frac{1}{2} \rightarrow \frac{1}{2}$ transition is of the higher energy, or velocity.

Ingalls (ref. 42) calculated the Sternheimer (polarization) factors for ferrous iron, and pointed out that the sign of the quadrupole splitting of ferrous iron is negative if the effects of the lattice are neglected, and the unpaired electron is the only source of the electric field gradient. Lattice effects are small for sites of cubic symmetry.

The compound ferrous fluosilicate, $FeSiF_6 \cdot 6H_2O$, contains ferrous iron in a slightly distorted octahedron of oxygen atoms, formed from the water molecules. Johnson et al. (ref. 43) measured the quadrupole splitting of this compound and found that it had the negative sign.

From the results of the above authors, and the experimental result on babingtonite, it appears that the high velocity peaks for octahedral sites in silicates, whether they are ferrous or ferric, are probably both of the same ($\frac{1}{2} \rightarrow \frac{1}{2}$) transition type, and the low velocity peaks are the $\frac{1}{2} \rightarrow \frac{3}{2}$ type. Results for tetrahedral ferric iron in garnet are the same. The only other types of sites common in the silicates of the present work are the low symmetry M2 site of pyroxenes, and the eight-fold site of garnet. Because these are both occupied by ferrous iron, and the sign of the quadrupole splitting for ferrous iron appears to be mainly determined by the unpaired electron, not by its environment (ref.[41]), these two ferrous sites probably have the same sign as the other ferrous sites.

Therefore, the convention followed in the use of Program Mosscorr for the present work (<u>all</u> high velocity peaks of the <u>same</u> transition type, $\frac{1}{2} \rightarrow \frac{1}{2}$) has a high probability of being correct.

REFERENCES

General

1. Burns, R. G., "Mineralogical Applications of Crystal Field Theory" (1970, University Press, Cambridge).
2. Danon, J., "Lectures on the Mossbauer Effect" (1968, Gordon and Breach Science Publ.).
3. Deer, Howie and Zussman, "Rock-Forming Minerals" (1962, Longmans, London).
4. Gruverman, I. J., "Mossbauer Effect Methodology" (1966, Plenum Press; 7 volumes).
5. Maxwell, J. A., "Rock and Mineral Analysis" (1968, Interscience Publ.) P. 207, 419; 416.
6. Wertheim, G. K., "Mossbauer Effect: Principles and Applications" (1968, Academic Press).

Total Iron

7. Graff, P. R., and Langmyhr, F. J., "Studies ---Determination of Silicon in Materials decomposed by Hydrofluoric Acid---." Anal. Chim. Acta 21, 429-31 (1959).
8. Miller, C. C. et al., "A Critical Investigation of the Use of the Silver Reductor---." Analyst 77, 2-7 (1952).
9. Shell, H. R., "Determination of Silica in Fluosilicates without Removal of Fluorine." Anal. Chem. 27, 2006-7 (1955).

10. Durrant, P. J. and Durrant, B., "Advanced Inorganic Chem." (1962, Wiley).

11. Jackson, P. J., "The Determination of Ferrous Iron in P. F. Ash ---." J. Appl. Chem. 7, 605 (1957).

12. Langmyhr, F. S., Kringstad, K., "---Precipitates Formed by the Decomposition of Silicate Rocks in 38-40% Hydrofluoric Acid." Anal. Chim. Acta 35, 131-35 (1966).

13. MacCardle, L. E., and Scheffer, E. R., "Determination of Ti (III) in Titaniferous Slags." Anal. Chem. 23, 1169-70 (1951).

14. Reuter, B., and Siewart, J. "---Verfahren--- der Oxydationsstufe des Vanadins und des Vanadingehalts--." Z. Anal. Chem. 162, 175-80 (1958).

15. Wickham, D. G., and Whipple, E. R., "The Determination of Oxid. and Reducing Cations in-- Oxides--." Talanta 10, 314-15 (1962).

16. Wilson, A. D., "The Microdetermination of Fe^{+2} in Silicate Min.--." Analyst 85, 823-27 (1960).

17. Bancroft, G. M., et al., "Appl. of the Mossbauer---1. Iron silicates of known crystal structure." Geochim. Cosmo. Acta 31, 2219-46 (1967).

18. Bancroft, G. M., et al., "Appl. of the Mossbauer ---2. Iron silicates of unknown and complex crystal structures." ibid 32, 547-59 (1968).

19. Bancroft, G. M., et al., "Mossbauer Spectra of Omphacites," in Pyroxenes and Amphiboles-- Crystal chemistry and phase petrology. Min. Soc. Am. Spec. Paper 2, 59-65 (1969).

20. Bancroft and Burns (1969), see amphiboles.

21. Burns and Greaves (1971), see amphiboles.

22. Bowen, L. H., et al. (1969), see micas.

23. Greaves, C. J., et al. (1971), see amphiboles.

24. Häggstrom, L., "Mossbauer Study of Oxidized Iron Silicate Minerals." Phys. Stat. Solidi 33, 741 (1969).

25. Häggstrom et al. (1969), see micas.

26. Hogarth, D. D., "Biabsorption---Five Phlogopite Samples--." Can. Min. 10, 710 (1970).

27. Hogg, C. S., et al., "The Mossbauer Spectra of Several Micas-- ." Min. Mag. 37, 606 (1970).

28. Bowman, J. D., et al., "Granular Mossbauer Absorbers." Nucl. Instr. Methods 50, 13-21 (1967).

29. Bykov, G. A., and Pham Zuy Hien, "---Resonant Absorption of Gamma Quanta in Crystals." Sov. Phys. JETP 16, 646-51 (1963).

30. Frauenfelder, H., et al. "Elliptical Polarization of Fe^{57} Gamma Rays." Phys. Rev. 126, 1065-75 (1962).

31. Hafemeister, D. W., and Shera, E. G., "Calc. of Mossbauer Abs. Areas for Thick Absorbers." Nucl. Instr. Methods 41, 133 (1966).

32. Margulies, S., and Ehrman, J. R., "Transmission and Line Broadening of Resonance Radiation-- ." Nucl. Instr. Methods 12, 131-37 (1961).

33. Roberts, L. D., and Thompson, J. O., "---Mossbauer-Type Study of Au^{197}." Phys. Rev. 129, 664 (1963).

34. Steyart, W. A., and Taylor, R. D., "--Absolute Measurement of--- Recoil-free Fraction." Phys. Rev. 134, 3A, A716-22 (1964).

35. Stone, A. J., et al., "Mosspec: a Programme Resolving Mossbauer Spectra." (obtained from NTIS). (The computer program used was one specially written for MIT, not the above.)

36. Ure, M. C. D., and Flinn, P. A., "A Technique for the Removal of the "Blackness" Distortion of Mossbauer Spectra." Mossbauer Effect Methodology, Vol. 7 (ed., Gruverman).

Mossbauer Spectra (Debye Theory)

37. Feuchtwang, T. E., "On the Possible Observation of Localized Vibrational Modes---." Reviews of Mod. Phys. 36, 437 (1964).

38. Kaufman, B., and Lipkin, H. J., "Momentum Transfer to Atoms Bound in a Crystal." Annals of Phys. 18, 294-309 (1962).

39. Maradudin, A. A., "The Mossbauer Effect for an Impurity Nucleus." Solid State Physics (#18), 367-88 (1966).

40. Muir, A. H., Atomics International Doc. AI-6692 (1962).

Mossbauer Spectra (Quadrupole Splitting)

41. Ingalls, R., "Electric-field Gradient Tensor in Ferrous Compounds." Phys. Rev. 133, A787-95 (1964).

42. Ingalls, R., "---Sternheimer Factors for the Ferrous Ion." Phys. Rev. 128, 1155 (1962).

43. Johnson, C. E., et al., "Electric Quadrupole Moment of the 14.4 kev State of Fe^{57}." Phys. Rev. 126, 1503 (1962).

44. Nicholson, W. J., and Burns, G., "Quadrupole Coupling Constant eqQ/h of Fe^{+3} in Several Rare-Earth Iron Garnets." Phys. Rev. 133, A1568-70 (1964).

45. Sharma, R. R., "Nuclear Quadrupole Interactions in Several Rare-Earth Iron Garnets." Phys. Rev. B6, 4310-23 (1972).

Ilmenite (Magnetic Properties)

46. Goodenough, J. B., and Stickler, J. J., "Theory of the Magnetic Properties of the Ilmenites $MTiO_3$." Phys. Rev. 164, 768-78 (1967).

47. Ishikawa, Y., and Akimoto, S., "---Ilmenite ($MeTiO_3$) and Hematite (αFe_2O_3) System. I, Crystal Chemistry." J. Phys. Soc. Japan 13, 1110-18 (1958).

48. Ishikawa, Y., and Akimoto, S., "---II, Magnetic Property." ibid 13, 1298-1310.

49. Shirane, G., et al., "Neutron-Diffraction---$FeTiO_3$ and its Solid Solutions with α-Fe_2O_3." J. Phys. Chem. Solids 10, 35-43 (1959).

Garnets

50. Burns, R. G., "Mixed Valencies and Site Occupancies of Iron in Silicate Min.-- Mossbauer--." Canadian J. of Spect. 17 (2), 51-59 (1972).

51. Dowty, E., "Crystal Chemistry of Titanian and Zirconian Garnet: I. Review and Spectral Studies." Am. Min. 56, 1983-2009 (1971).

52. Frondel, C., and Ito, J., "Stilpnomelane and Spessartite-Grossularite from Franklin, N. J." Am. Min. 50, 498-501 (1965).

53. Hartman, P., "Can Ti replace Si in Silicates?" Min. Mag. 37, 366-69 (1969).

54. Howie, R. A., and Wooley, A. R., "The Role of Titanium--Andradite --." Min. Mag. 36, 775-90 (1968).

55. Huckenholz, H. G., "Synth. and Stab. of Ti-Andradite." AJS 267-A, 209-32 (1969).

56. Lyubutin, I. S., et al., "Temp. Depend. of the Mossbauer Effect for Octahedral Iron Atoms in Garnet." Sov. Physics Solid State 12, 1100 (1970).

57. Lyubutin, I. S., et al., "Temp. Depend. of the Mossbauer Effect for Fe^{+2} in Dodeca. Coord. in Garnet." Sov. Phys. Cryst. 15, 1091 (1971).

58. Lyubutin, I. S., et al., "Temp. Depend. of the Mossbauer Effect for Tetrahedral Iron Atoms in Garnets." ibid 15, 936 (1971).

59. Moore, R. K., and White, W. B., "Intervalence electron transfer effects in the spectra of the Melanite Garnets." Am. Min. 56, 826-40 (1971).

60. Novak, G. A., and Gibbs, G. V., "The Crystal Chemistry of the Silicate Garnets." Am. Min. 56, 791-825 (1971).

Amphiboles

61. Bancroft, G. M., and Burns, R. G., "Mossbauer and Absorption Spectral Study of Alkali Amphiboles." Min. Soc. Am. Spec. Pap. 2, 137-48 (1969).

62. Burns, R. G., and Greaves, C. J., "Correlations of Infrared and Mossbauer Site Population--Actinolites." Am. Min. 56, 2010-33 (1971).

63. Greaves, C. J., et al., "Resolution of Actinolite Mossbauer Spectra in Three Ferrous Doublets." Nature 229, 60-61 (1971).

64. Law, A. D., "Critical Evaluation of Statistical Best Fits to Mossbauer Spectra." (Holmquistite) Am. Min. 58, 128-31 (1973).

65. Mason, B., "Kaersutite from San Carlos, Ariz.-----." Min. Mag. 36, 997-1002 (1968).

66. Prinz, M., et al., "Comments on Kaersutite from San Carlos, Ariz.----." Min. Mag. 37, 333-37 (1969).

67. Bancroft, G. M., et al., "Mossbauer---Diopside-Hedenbergite Tie Line." Am. Min. 56, 1617-25 (1971).

68. Burns, R. G., et al., "Titanaugites contain Tetrahedral Fe^{+3} ions---." Geol. Soc. Am. Ann. Meet., Boulder, Colo., Abstr. 4(7), 463-4 (1972).

69. Burns, R. G., and Huggins, F. E., "Visible-Region Spectra of a Ti^{+3} Fassaite from the Allende Meteorite: A Discussion." (to be published).

70. Clarke, R. S., et al., "The Allende, Mexico, Meteorite Shower." Smithsonian Contrib. to the Earth Sciences 1970, No. 5.

71. Dowty, E., and Clark, J. R., "---Properties of a Ti^{+3} Fassaite from the Allende Meteorite." Am. Min. 58, 230-42 (1973).

72. Frondel, C., and Ito, J., "Zincian Aegirine-Augite and Jeffersonite from Franklin, N. J." Am. Min. 51, 1406-13 (1966).

73. Hafner, S. S., and Huckenholz, H. G., "Mossbauer Spectrum of Synth. Ferri-diopside." Nature (Phys. Sci.) 233, 9 (1971).

74. Manning, P. G., and Nickel, E. H., "A Spectral Study--- Titanaugite--Riebeckite---." Can. Min. 10, 71-83 (1969).

75. Peacor, D. R., "Refinement of the Crystal Structure of a Pyroxene of Formula $M_1 M_{11} (Si_{1.5} Al_{0.5}) O_6$." (Oka), Am. Min. 52, 31 (1967).

76. Prewitt, C. T., "Synthesis of a Pyroxene Containing Trivalent Titanium." Contr. Min. and Petr. 35, 77-82 (1972).

77. Virgo, D., and Hafner, S., "Re-evaluation---Orthopyroxene by the Mossbauer Effect." Earth Planet. Sci. Lett. 4, 265-69 (1968).

78. Virgo, D., and Hafner, S., "Fe^{+2}, Mg Order-disorder in Natural Orthopyroxenes." Am. Min. 55, 201-23 (1970).

79. Williams, P., Bancroft, G. M., et al., "Anomalous Mossbauer Spectra of C2/c Clinopyroxenes." Nature (Phys. Sci.) 230, 149-51 (1971).

Babingtonite

80. Araki, T., et al., "The Crystal Structure of a Babingtonite." Am. Min. 57, 323-24 (abstr.) (1972). (Zeit. Krist. 135, 355-73 (1972))

81. Burt, D. M., "Multisystems Analysis of the Relative Stabilities of Babingtonite and Ilvaite." Carnegie Inst., Year Book 70, 189-97.

82. Palache, C., and Gonyer, F. A., "On Babingtonite." Am. Min. 17, 295-303 (1932).

Micas

83. Annersten, H., et al., "Mossbauer Study of Synth. Ferriphlogopite---." Phys. Stat. Solidi (b) 48, K137 (1971).

84. Bowen, L. H., et al., "Mossbauer Study of Micas and Their Potassium Depleted Products," Am. Min. 54, 72-84, (1969).

85. Häggstrom, L., et al., "Mossbauer Study of Iron-rich Biotites." Chem. Phys. Lett. 4, 107-8 (1969).

86. Hayama, Y., "Some Considerations on the Color of Biotite--- Metamorphism." J. Geol. Soc. Japan 65, 21-30 (1959).

87. Hazen, R. M., and Wones, D. R., "The Effect of cation substitutions on the Physical Properties of Trioctahedral Micas." Am. Min. 57, 103-29 (1972).

88. Jakob, J., "Über das auftreten von dreiwertigem Titan in Biotiten." Schweiz. Min. Petr. Mitt. 17, 149-53 (1937).

89. Pollak, H., et al., "Mossbauer Effect in Biotite," Phys. Stat. Solidi 2, 1653-59 (1962).

Neptunite

90. Bancroft, G. M., et al., "Oxidation State of Iron in Neptunite from Mossbauer Spectroscopy." Acta. Cryst. 22, 934-35 (1967).

91. Borisov, S. V., et al., "The Crystal Structure of Neptunite." Sov. Phys. Cryst. 10, 684-89 (1966).

92. Cannillo, E., et al., "The Crystal Structure of Neptunite," Acta. Cryst. 21, 200-208 (1966).

93. Laird, J., and Albee, A. L., "Chemical Composition and---Properties of Benitoite, Neptunite and Joaquinite." Am. Min. 57, 85-102 (1972).

Gillespite

94. Clark, M. G., et al., "Mossbauer Spectrum of Fe^{+2} in a Square-Planar Environment." J. Chem. Phys. 47, 4250 (1967).

Localities

95. Dickey, J. S., "Eclogitic and other Inclusions---Deborah Volc. Fmn., Kakanui, New Zealand." Am. Min. 53, 1304-19 (1968).

96. Gold, D. P., and Vallee, M., "Field Guide to the Oka Area." (1969), Quebec Dept. of Nat. Resources.

97. Gold, D. P., "The Minerals of the Oka Carbonatite---Quebec." Min. Soc. of India, IMA Vol. (1966).

98. Gold, D. P., "---Oka and St. Hilaire." Unpubl. Ph.D. thesis, McGill Univ., Montreal (1963).

99. Miller, R., "The Webster-Addie Ultramafic Ring,---N.C.--- Alter'n of Chromite." Am. Min. 38, 1134-47 (1953).

100. Palache, C., "The Minerals of Franklin and Sterling Hill, Sussex Count y, N.J." U.S.G.S. Prof. Paper 180.

101. Scott, A., "The Crawfordjohn Essexite and Associated Rocks," Geol. Mag. 1915, p. 455-61.

102. Tilley, C. E., "Paragenesis of Anthophyllite and Hornblende from the Bancroft Area, Ontario," Am. Min. 42, 412-16 (1957).

Supplementary References

103. Goldanskii, V. I. and Herber, R. H., "Chemical Applications of Mossbauer Spectroscopy" (1968, Academic Press).

104. Papike, J. J. and Clark, J. R., "The Crystal Structure and Cation Distribution of Glaucophane" Am. Min. 53, 1156-1173 (1968).

105. Papike, J. J., et al. "Crystal-Chemical Characterization of Clinoamphiboles ---" Min. Soc. Am. Spec. Paper 2, 117-136 (1969).

106. Ernst, W. G. and Wai, C. M. "Mossbauer, Infrared, X-Ray ---- Cation Ordering --- Sodic Amphiboles" Am. Min. 55, 1226-1258 (1970).

107. Dowty, E. and Lindsley, D. H., "Mossbauer Spectra of Synthetic Hedenbergite-Ferrosilite Pyroxenes" Am. Min. 58, 850-868 (1973).